

PLANT RESPONSE
TO MODIFIED CONDITIONS OF
LIGHT AND NUTRIENTS

Polzella Antonella

TUTOR:
Prof. Scippa Gabriella Stefania

CO-TUTORS:
Prof. Chiatante Donato
Dr. Montagnoli Antonio

THESIS SUBMITTED FOR THE DEGREE OF
DOCTOR OF PHILOSOPHY
AT THE UNIVERSITY OF MOLISE



DEPARTMENT OF BIOSCIENCES AND TERRITORY

CURRICULUM BIO-ENVIRONMENTAL

CYCLE XXXI

2019

DECLARATION

Except where reference is made to other sources, I declare that the contents in this thesis are my own work and have not been previously submitted, in part or in full, for the award of a higher degree elsewhere.

PUBLICATIONS ARISING FROM THIS WORK

“Toward an understanding of mechanisms regulating plant response to biochar application”

Antonella Polzella, Elena De Zio, Simona Arena, Gabriella Stefania Scippa, Andrea Scaloni, Antonio Montagnoli, Donato Chiatante, Dalila Trupiano

Published online on 25 November 2018 on Plant Biosystems - Vol. 153(1), 2019

DEDICATION

To myself, to my courage and stubbornness.

To pillars of my life: my beloved family and Giovanni.

ACKNOWLEDGEMENTS

I am very grateful for having this opportunity and experience to do my PhD in Pesche, Varese and Lancaster. I really learned a lot during the past three years and I enriched my scientific knowledge and my personality. Today, looking back I know to thank many people, who helped and accompanied me in this long and nice journey.

Firstly, I would like to express my deepest gratitude to my tutor and co-tutors. Prof. Scippa Gabriella Stefania, for her scientific guidance and many constructive suggestions, Prof. Chiatante Donato, it is a big shame he is retiring, only who has met him can say to have been lucky, and Dr. Montagnoli Antonello, for me also a big and dear friend who showed me the solution each time I couldn't find it.

I am very grateful to my Lancaster supervisor, Prof. Toledo-Ortiz Gabriela, for her lovely, infinite and kind support. Without her, it would not have been possible for me to know, study and manipulate Arabidopsis mutants.

I am indebted to several people, which I have collaborated with or have helped me in various ways during all PhD period. My colleagues but mainly “academic friends” in University of Pesche: Dalila, Elena, Melissa, Antonio and Pamela. They have been always ready to give me a scientific comment, a personal suggestion or simply a hug. The great people I met in University of Varese: Mattia, Barbara, Oriana, Federica, Rosy, Daniela and Cristiano, with whom I shared so many beautiful and formative experiences. For one year, they have been my second family and I will bring them in my heart forever. The lovely people in University of Lancaster: Jon, Dennis, Brittany and Phoebe for supporting work in every moment I needed.

Obviously, it cannot miss my infinite thank you to all my big and beautiful family, without them it would have been difficult! Particularly, a special thank you to Giovanni, my lifetime love, my future husband, he always believes in myself, that is why I can do everything.

ABSTRACT

In natural environments plant growth, development, productivity, and distribution are highly dependent on a wide number of different biotic and abiotic factors. Among all water, temperature, light, and nutrients are the most important ones. Understanding mechanisms and adaptive responses of plant growth to changes in the availability of these environmental components is of the fundamental importance. In this framework, the present thesis aimed at widen the knowledge on plant response to modifications of soil nutrient availability and to the alteration in quality and quantity of light spectrum.

To accomplish this aim, the effects of changes in nutrient composition have been investigated by adding biochar amendment to the soil, whereas alterations in quality and quantity of light spectrum have been obtained by using different artificial lighting systems. The response to biochar soil amendment has been analyzed at morpho-physiological and molecular levels in different plant species (i.e. tomato, pea and *Arabidopsis*), alone and in combination with light spectra alterations. Results obtained in this thesis show that although biochar addition misbalances the photosynthetic machinery in tomato plants, it might improve *Pisum* and *Arabidopsis* growth, even at higher magnitude when the light spectrum is characterized by a specific composition. In addition, morpho-physiological plant response leads to hypothesize that photoreceptors such as phyA, phyB, and light signaling components such as pifs, could be involved in processes of growth stimulation in nitrogen and light stress conditions.

As part of the Ph.D project, the effects of a new artificial lighting system named CoeLux[®], on morpho-physiology of several different plant species (i.e. *Anthurium*, *Basilicum*, *Q. ilex*) have been investigated. Experiments with CoeLux[®] lighting system showed a species-specific plant response mechanism and a high plant efficiency to receive and use CoeLux[®] lighting system by performing good photosynthetic and stomatal activities.

SOMMARIO

In natura la crescita, lo sviluppo, la produttività e la distribuzione delle piante sono altamente influenzati da un ampio numero di diversi fattori biotici e abiotici. Tra tutti i fattori biotici, l'acqua, la temperatura, la luce e i nutrienti restano quelli di maggiore rilevanza. Così come resta di fondamentale importanza lo studio dei meccanismi della crescita e delle risposte di adattamento delle piante ai cambiamenti della disponibilità di queste stesse componenti ambientali. In tale contesto, il presente lavoro di tesi mira ad ampliare la conoscenza sulla risposta delle piante alla disponibilità modificata di nutrienti nel suolo e alla manipolazione qualitativa e quantitativa dello spettro di luce.

Per conseguire questo obiettivo sono stati studiati gli effetti dei cambiamenti nella disponibilità di nutrienti nel terreno attraverso l'aggiunta di un ammendante organico quale il biochar, invece le alterazioni sia qualitative che quantitative dello spettro di luce sono state ottenute usando diversi sistemi di illuminazione artificiale. Il biochar è stato utilizzato solo ed in combinazione con diversi spettri di luce, di cui gli effetti sono stati analizzati sia al livello morfo-fisiologico che molecolare in diverse piante (ad es. pomodoro, pisello e *Arabidopsis*).

I risultati ottenuti in questa tesi dimostrano che sebbene il biochar aggiunto nel terreno porta ad uno squilibrio dell'apparato fotosintetico nelle piante di pomodoro, esso potrebbe migliorare la crescita delle piante di *Pisum* e *Arabidopsis*, in maggior misura se si utilizza in combinazione con una luce caratterizzata da una specifica composizione spettrale. Inoltre, la risposta morfo-fisiologica delle piante porta ad ipotizzare che i fotorecettori, come phyA, phyB e fattori coinvolti nella segnalazione luminosa come pifs potrebbero essere coinvolti in processi di stimolazione della crescita in condizioni di stress di luce e di azoto.

Come parte del progetto di dottorato, sono stati studiati gli effetti di un nuovo sistema di illuminazione artificiale chiamato CoeLux[®] sulla morfo-fisiologia di diverse specie di piante (ad es. *Anthurium*, *Basilicum*, *Q. ilex*). Gli esperimenti con il sistema di illuminazione CoeLux[®] hanno dimostrato un meccanismo di risposta specie-specifico ed un'alta efficienza della pianta nel ricevere ed usare la luce CoeLux[®] attraverso lo svolgimento di una buona attività sia fotosintetica che stomatica.

Contents

DECLARATION AND PUBLICATIONS ARISING FROM THIS WORK	i
DEDICATION	ii
ACKNOWLEDGEMENTS	iii
ABSTRACT	iv
SOMMARIO	v
CHAPTER I - General Introduction	1
1.1 The Influence of Endogenous and Exogenous Factors on Plant Growth	2
1.2 The Plant Response to Nutrients and Light Supply Changes	3
1.3 The Aim and Structure of the Thesis	6
1.4 References	8
CHAPTER II - Toward an Understanding of Mechanisms Regulating Plant Response to Biochar Application	15
2.1 Introduction	16
2.2 Material and Methods	18
2.2.1 Experimental Set Up and Biochar Treatment	18
2.2.2 Soil Analysis	19
2.2.3 Plant Growth Analysis	19
2.2.4 Protein Extraction and Two-Dimensional Electrophoresis	19
2.2.5 In-Gel Digestion, Mass Spectrometry Analysis and Identification	20

2.2.6	ACO Expression Measurements	21
2.2.7	PCR-Based Detection of <i>P. infestans</i> in Leaves	21
2.3	Results	22
2.3.1	Biochar Effect on Soil Characteristics	22
2.3.3	Effects of Biochar on Leaf Proteome	24
2.3.4	Analysis of LeACO1 Gene Expression Patterns	29
2.3.5	Detection of the Tomato Late Blight Pathogen: <i>Phytophthora infestans</i>	29
2.4	Discussion and Conclusions	30
2.5	Acknowledgments	34
2.6	References	35
CHAPTER III - The Interplay of LED Spectra and Biochar in <i>Arabidopsis columbia</i> and <i>Pisum sativum</i> L. Morpho-Physiological Traits		41
3.1	Introduction	42
3.2	Materials and Methods	45
3.2.1	Plant Material and Experimental Setup	45
3.2.2	Growth Room Characteristics	46
3.2.3	Biochar Characterization	47
3.2.4	Soil Characterization	48
3.2.5	Morphological Measurements	48
3.2.6	Physiological Measurements	49
3.2.7	Statistical Analysis	50
3.3	Results	50
3.3.1	Biochar and Soil Characteristics	50
3.3.2	Morphological Traits of <i>Arabidopsis</i>	51

3.3.3	Morphological Traits of <i>P. sativum</i>	54
3.3.4	Physiological Traits	56
3.4	Discussion	59
3.5	Conclusions	64
3.6	Acknowledgments	64
3.7	References	65
CHAPTER IV - The Possible Photoreceptor Role in Response to Modified Light and Nitrogen Availability		75
4.1	Introduction	76
4.2	Materials and Methods	78
4.2.1	Hydroponic Growing System	78
4.2.2	Plant Material, Solution Preparation and Growing Conditions	78
4.2.3	N Starvation Treatment	79
4.2.4	Morphological Measurements and Determination of Photosynthetic Pigment Contents	80
4.2.5	Statistical Analysis	80
4.3	Results	81
4.3.1	Morphological Traits	81
4.3.2	Photosynthetic Pigment Contents	84
4.4	Discussion and Conclusions	86
4.5	References	89
CHAPTER V - The Plant Response to CoeLux® Lighting System		95
5.1	Introduction	96
5.2	Materials and Methods	98

5.2.1	The CoeLux [®] Lighting System	98
5.2.2	Plant material and Experimental Design	99
5.2.3	Morpho-physiological measurements	102
5.3	Results	103
5.3.1	Short-Term Experiments	103
5.3.2	Long-Term Experiments	105
5.4	Discussion and Conclusions	111
5.5	References	113
CHAPTER VI - Synthesis and Outlook		119
ORAL/POSTER PRESENTATIONS FROM THIS WORK		123
LIST OF ABBREVIATIONS		125
LIST OF TABLES		127
LIST OF FIGURES		129

Chapter I

General Introduction

1.1 The Influence of Endogenous and Exogenous Factors on Plant Growth

Plant growth and development are finely regulated by the integration of many environmental and endogenous signals. Because they dictate plant characteristics from within the cell, the genetic factors are considered internal factors (i.e. endogenous) and they represent the overall plant genetic material, including genes, chromosomes, genomes and all those that represent gene expression (Johnson and Stinchcombe, 2007; Bailey *et al.*, 2009; Schweitzer *et al.*, 2012b). On the other hand, the environmental factors, external non-genetic factors (i.e. exogenous), are generally divided into two groups: biotic and abiotic. Biotic factors include all living components, such as animals, plants, fungi, and bacteria; abiotic factors are all non-living components (Buchmann, 2000) comprising (i) topography (intended as all earth physical features such as land elevation, slope, terrain, etc.), (ii) soil physical and chemical properties (e.g. soil nutrient availability, texture, structure, pH, and so on) and (iii) climate factors comprising light, temperature, water, aeration, etc. (Dunson and Travis, 1991).

To ensure their living and surviving in a natural environment, plants have evolved mechanisms to rapidly respond to modify conditions produced by the interactions between the above-mentioned biotic and abiotic factors. For instance, excess or deficit of water availability affects plant growth and yield in terms of tissue development, transpiration, stomatal activity, CO₂ assimilation, photosynthetic activity, and flowering (Osakabe *et al.*, 2014; Abdallah *et al.*, 2018). Similarly, plants are able to perform vital activities in certain and optimal temperature range and it is known that high and low temperatures mostly alter the flowering and photosynthetic processes (Allakhverdiev *et al.*, 2008; Ashraf and Harris, 2013; Prasad and Djanaguiraman, 2014). Likewise, gases, pollutants, and wind strongly affect plant biomass, productivity, and evapotranspiration (Zengin and Munzuroglu, 2005). Several studies have shown that low light causes the reduction of plant growth and photosynthetic pigment accumulation (Adelusi and Aileme, 1977), whereas others have reported that the plant root structure is affected by soil texture, structure and nutrient availability (Oke, 1985). Furthermore, it is well established that the influence of the interaction of these factors on plant growth, for example, the interaction between temperature, water and salt stress may be associated with photo-inhibition (Osmond *et al.*, 1987). On the other hand, the close relation between light and temperature can positively affect the plant developmental stages, for instance the optimal plant growth and photosynthesis proved at medium irradiance and high

nutrient levels in Thompson *et al.*'s report (1988). However, plants are able to counteract the changes of the biotic and biotic environmental components. Indeed plants respond to modified water availability by activating a series of signaling pathways (Zhu, 2002) and respond to temperature variations through production of secondary metabolites (Mathur *et al.*, 2014). Furthermore, plants are capable to activate tolerance mechanisms for pollutant detoxification as for instance metal immobilization, sequestration and compartmentalization (Patra *et al.*, 2004; John *et al.*, 2009; Dalvi and Bhalerao, 2013). Finally, plants are able to acclimatize certain irradiance values and nutrient availability by physiological adjustment promoting carbon gains (Thompson *et al.* 1988).

1.2 The Plant Response to Nutrients and Light Supply Changes

Plant growth is highly dependent on mineral nutrient uptake (Clarkson, 1980; Sinclair, 1992). In seeds, roots and leaves, the nutrient content in the growth media affects several activities, including organ function, rate of organ growth and turnover, and plant life-history strategies (Kerkhoff *et al.*, 2006). Generally, the nutrients required for plant growth are classified into three groups. The first group is composed by three basic elements that plants can obtain from water and atmosphere such as carbon (C), hydrogen (H), and oxygen (O). The other two groups comprises the so-called soil-derived nutrients that are the (i) macronutrients such as nitrogen (N), phosphorus (P), potassium (K), sulfur (S), calcium (Ca), and magnesium (Mg) and the (ii) micronutrients like boron (B), chloride (Cl), copper (Cu), iron (Fe), manganese (Mn), molybdenum (Mo), nickel (Ni) and zinc (Zn) (Mahler, 2004). In Table 1.1 these elements are summarized in relation to their specific function in plant biological processes affecting the growth and development. Although plants mainly take up C from the air, they acquire the rest of nutrients almost exclusively from the soil through the root systems. Thus, the nutrient concentrations in plant tissues are dependent on resource availability in the soil which in turn depends on the rate of their uptake as well as on the rate of replacement due to bacterial N fixation, organic matter mineralization, atmospheric deposition or weathering (Lukac *et al.*, 2010). Among all the above-listed elements, N and P remain the most limiting ones in many ecosystems and for many plant biological processes (Wassen *et al.*, 2005; Chapman *et al.*, 2006; Lambers *et al.*, 2008).

Nutrient	Function
N	All enzymatic reactions, photosynthesis and constituent of several vitamins
P	Photosynthesis, respiration, metabolism, cell division, root development, flower initiation, seed and fruit development
K	Metabolism, photosynthesis, protein synthesis, opening and closing of leaf stomata
S	Metabolism and constituent of several amino acids
Ca	Formation and maintaining of the cell wall membrane
Mg	Photosynthesis and other enzymatic reactions
B	RNA formation, cellular activities and pollen germination
Cl	Photosynthesis and water content regulation
Cu	Photosynthesis
Fe	Photosynthesis and respiration
Mn	Metabolism and Photosynthesis
Mo	Metabolism
Ni	Iron Metabolism
Zn	Metabolism and Protein synthesis

Table 1.1. Essential macro- and micro- nutrients for plant growth and their functions within plant tissue (Baligar *et al.*, 2007).

Different plant species respond to changes in soil nutrient availability by modulating organ development. Different levels of nutrient availability in the soil may induce an alteration in leaf dry matter content (Hodgson *et al.*, 2011). The root system morphological and architectural characteristics, tightly associated with nutrient uptake efficiency, as well as the root/shoot biomass allocation might be also modulated in the case of nutrient shortage conditions (Hill *et al.*, 2006). Generally, the P deficiency causes the inhibition of plant primary root growth. On the contrary, plants increase both the growth and density of lateral (i.e. secondary) and hair root growth in response to N, P, Fe and S deficiency (López-Bucio *et al.*, 2003; Britto and Kronzucker, 2008). Furthermore, also high nutrient levels might be toxic for plants causing the production of reactive

oxygen species (ROS), which in turn cause a plant cellular damage (Connolly and Walker, 2008; Morgan and Connolly, 2013).

Light is an essential element for plant life. Plants, as sessile organisms, developed specialized structures to receive, modulate and convert different quality and quantity of light that can reach plant tissue in different directions. The electromagnetic spectrum is composed of different types of radiations such as radio waves, microwaves, infrared, visible light, ultraviolet, X-rays and gamma rays. Among them, only the visible light can be perceived by the human eye, characterized by wavelengths between about 400 nm and 700 nm (DeVany *et al.*, 1969; Fig. 1.1a). Photosynthetic organisms such as plants, algae, and cyanobacteria are able to perform the photosynthetic process in which light is converted to chemical energy. Plants receive and absorb light through light-absorbing molecules called pigments, mainly Chlorophyll a, Chlorophyll b and carotenoids that are three key pigments absorbing light energy in a specific wavelength range (Fig. 1.1b). Beside pigment molecules, in plant tissue, there are also photoreceptor proteins that detect and use the light for important biological processes.

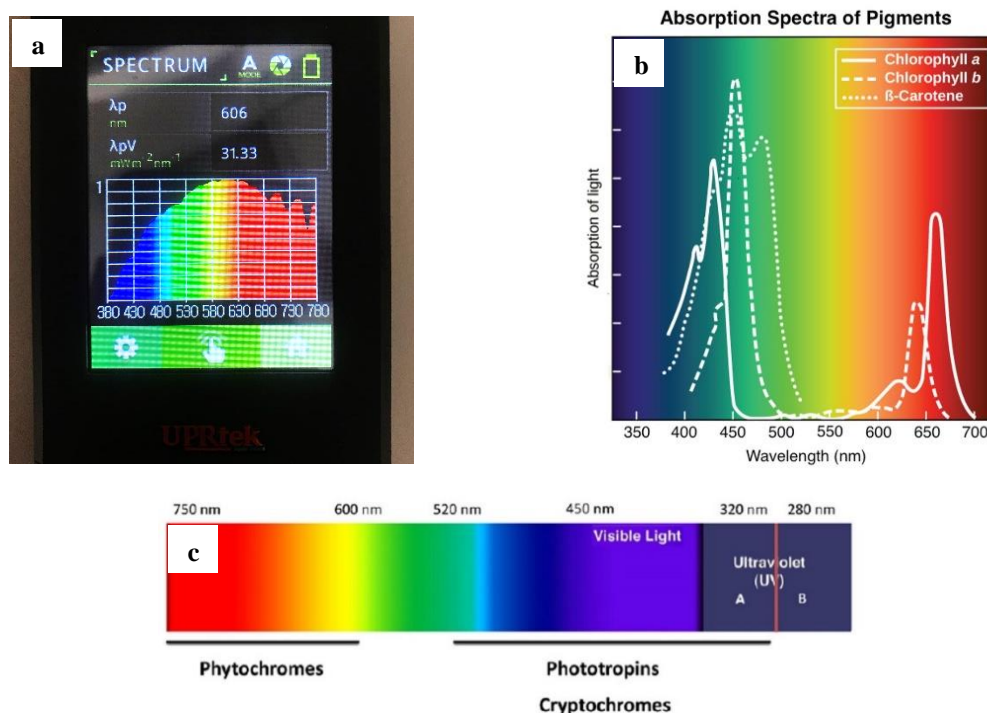


Figure 1.1. (a) Spectrum of visible light detected with Handheld Spectrometer (UPRtek). (b) Absorption spectra of the two key pigments and β -carotene, the representative of the carotenoid group (OpenStax College, Biology). (c) Absorption regions of main photoreceptors (Modified from Parihar *et al.*, 2016).

I There are three classes of plant signal-transducing photoreceptors, namely Phytochromes (Phys), Cryptochromes (Crys) and Phototropins (Phots). Each photoreceptor operates in a specific range of the visible spectrum as shown in the detail in Fig. 1.1c.

The Phys are involved in many important photomorphogenic responses in plant growth and development, e.g. germination, stem elongation, leaf expansion, formation of some pigments, chloroplast development and flowering (Franklin and Quail, 2010). They exist in two photoconvertible forms absorbing in the light spectrum region between 600 and 750 nm, in the red (Pr) and far-red (Pfr) light, which represent the biologically active and inactive form, respectively (Quail, 1997; Reed, 1999; Shinomura *et al.*, 2000). The Crys are blue-light and UV-A sensitive photoreceptors absorbing in the 320-520 nm range of visible spectrum functioning mainly as entrainment of the circadian clock, and in the flowering and photomorphogenic activities. Similarly, the Phots operate in blue, UV-A and green light (320-520 nm range) playing a key role in phototropism, chloroplast movement and stomatal opening (Briggs *et al.*, 2001; Möglich *et al.*, 2010; De Wit *et al.*, 2016; Parihar *et al.*, 2016).

Optimal light irradiance is required for a normal plant growth, however, the possible high or low level of irradiance might affect photosynthetic process and in turn plant yield (Ma *et al.*, 2015). For example, Powles and Critchley (1980) showed that bean plants under a low level of light had a reduced growth due to a lower rate of photosynthetic electron transport and carbon dioxide (CO₂) assimilation. Nevertheless, Guo *et al.* (2006) reported that in the bayberry tree the high irradiance caused the depression of photosynthesis and photosystem II (PSII) efficiency and activated the protective mechanism of photoinhibition. Additionally, other responses to variation in light availability include changes of morphological and physiological features of organs involved in the light acquisition and carbon assimilation processes, such as leaf and shoot (Valladares and Niinemets, 2008).

1.3 The Aim and Structure of the Thesis

How plant responds to the alteration of environmental components affecting their growth and development is of great importance for widening the understanding of biological mechanisms that may allow plants to adapt to important modifications such as “climate change”. Nutrient and light availabilities meaningfully affect plant growth and development, however, the majority of the

studies carried so far on plant response to change of these two environmental components, have manipulated a single parameter. For instance, several studies have investigated the influence of nutrient contents on plant growth (da Silveira Pontes *et al.*, 2010; Kazakou *et al.*, 2014), as well as other reports have studied the effect of light spectra on numerous plant growth parameters (Smirnakou *et al.*, 2017; Montagnoli *et al.*, 2018). Whereas the interplay of these two factors have been rarely investigated (Siebenkäs *et al.*, 2015). In this framework, the present thesis focused on investigating plant response to the combining manipulation of nutrient supply and light irradiation both at qualitative and quantitative levels. In particular, plant morpho-physiological traits were measured in response to the application of biochar amendment, a source of soil nutrient supply, and the modification of light spectra emitted by various LED lighting systems. Particularly, since it is well known that biochar amendment increases soil nitrogen content and availability, the present work aimed to cover the possible role of nitrogen and different lighting conditions on plant growth.

In detail, proteomic and molecular analysis on leaves of tomato plants were carried to investigate the response to changes in soil quality by using biochar amendment (see Chapter II). In chapter III the morpho-physiological traits of *Pisum sativum* and *Arabidopsis thaliana* (Columbia ecotype) were analyzed in relation to biochar application and the alteration of light spectra sourced by the LED. Furthermore, the possible role of photoreceptors was investigated in *Arabidopsis* mutants grown in a hydroponic system and in manipulated availability of nitrogen and artificial lighting (see Chapter IV). Finally, part of the study was focused on the morpho-physiological changes of ornamental, aromatic, forestry and agronomic plant species grown under CoeLux[®] lighting system (see Chapter V).

1.4 References

- I
- Abdallah M. B., Trupiano D., Polzella A., De Zio E., Sassi M., Scaloni A., Zarrouk M., Youssef N. B., Scippa G. S. (2018). Unraveling physiological, biochemical and molecular mechanisms involved in olive (*Olea europaea* L. cv. *Chétoui*) tolerance to drought and salt stresses. *Journal of Plant Physiology*, 220, 83-95.
- Adelusi A. A., Aileme J. D. (1997). Effect of light and mineral nutrient stress on the yield and yield components of cowpea (*Vigna unguiculata*). *Nigerian Journal of Botany*, 10, 1-6.
- Allakhverdiev S. I., Kreslavski V. D., Klimov V. V., Los D. A., Carpentier R., Mohanty P. (2008). Heat stress: an overview of molecular responses in photosynthesis. *Photosynthesis Research*, 98, 541–550.
- Ashraf M., Harris P.J.C. (2013). Photosynthesis under stressful environments: an overview. *Photosynthetica*, 51(2), 163–190.
- Bailey J. K., Schweitzer J. A., Ubeda F., Koricheva J., LeRoy C. J., Madritch M. D., Rehill B. J., Bangert R. K., Fischer D. G., Allan G. J., Whitham T. G. (2009). From genes to ecosystems: a synthesis of the effects of plant genetic factors across levels of organization. *Philosophical Transactions of the Royal Society of London B: Biological Sciences*, 364(1523), 1607-16.
- Baligar V. C., Fageria N. K. (2007). Agronomy and Physiology of Tropical Cover Crops. *Journal of Plant Nutrition*, 30, 1287–1339.
- Briggs W. R., Olney M. A. (2001). Photoreceptors in Plant Photomorphogenesis to Date. Five Phytochromes, Two Cryptochromes, One Phototropin, and One Superchrome. *Plant Physiology*, 125(1), 85-88.
- Britto D. T., Kronzucker H. J. (2008). Cellular mechanisms of potassium transport in plants. *Physiologia Plantarum*, 133, 637-650.
- Buchmann N. (2000). Biotic and abiotic factors controlling soil respiration rate in *Picea abies* stands. *Soil Biology and Biochemistry*, 32, 1625-1635.

- Chapin F. S., Bloom A. J., Field C. B., Waring R. H. (1987). Plant responses to multiple environmental factors. *BioScience*, 37, 49–57.
- Chapman S.K., Langley J. A., Hart S. C., Koch G. W. (2006). Plants actively control nitrogen cycling: uncorking the microbial bottleneck. *The New Phytologist*, 169, 27-34.
- Cheng L., Tang X., Vance C. P., White P. J., Zhang F., Shen J. (2014). Interactions between light intensity and phosphorus nutrition affect the phosphate-mining capacity of white lupin (*Lupinus albus* L.). *Journal of Experimental Botany*, 65(12), 2995-3003.
- Connolly E. L., Walker E. L. (2008). Time to pump iron: iron-deficiency-signaling mechanisms of higher plants. *Current Opinion in Plant Biology*, 11, 530-535.
- da Silveira Pontes L., Louault F., Carrère P., Maire V., Andueza D., Soussana J.-F. (2010). The role of plant traits and their plasticity in the response of pasture grasses to nutrients and cutting frequency. *Annals of Botany*, 105, 957–965.
- Dalvi A. A., Bhalerao S. A. (2013). Response of plants towards heavy metal toxicity: an overview of avoidance, tolerance and uptake mechanism. *Annals of Plant Sciences*, 2(9), 362–368.
- De Vany A. S., Eckert R. D., Meyers C. J., O'Hara D. J., Scott R. C. (1969). A Property System for Market Allocation of the Electromagnetic Spectrum: A Legal-Economic-Engineering Study. *Stanford Law Review*, 21, 1499.
- De Wit M., Galvão V. C., Fankhauser C. (2016). Light-Mediated Hormonal Regulation of Plant Growth and Development. *The Annual Review of Plant Biology*, 67, 513-37. <http://doi.org/10.1146/annurev-arplant-043015-112252>.
- Dunson W. A., Travis J. (1991). The role of abiotic factors in community organization. *The American Naturalist*, 138(5), 1067-1091.
- Franklin K. A., Quail P. H. (2010). Phytochrome functions in Arabidopsis development. *Journal of Experimental Botany*, 61(1), 11-24.
- Guo Y. P., Guo D. P., Zhou H. F., Hu M. J., Shen Y. G. (2006). Photoinhibition and xanthophyll cycle activity in bayberry (*Myrica rubra*) leaves induced by high irradiance. *Photosynthetica*, 44, 439–446.

- Hill J. O., Simpson R. J., Moore A. D., Chapman D. F. (2006). Morphology and response of roots of pasture species to phosphorus and nitrogen nutrition. *Plant and Soil*, 286, 7–19.
- Hodgson J. G., Montserrat-Martí G., Charles M., Jones G., Wilson P., Shipley B., Sharafi M., Cerabolini B. E. L., Cornelissen J. H. C., Band S. R., Bogard A., Castro-Diez P., Guerrero-Campo J., Palmer C., Perez-Rontome M. C., Carter G., Hynd A., Romo-Diez A., de Torres Espuny L., Royo Pla F. (2011). Is leaf dry matter content a better predictor of soil fertility than specific leaf area? *Annals of Botany*, 108, 1337-1345.
- John R., Ahmad P., Gadgil K., Sharma S. (2009). Heavy metal toxicity: effect on plant growth, biochemical parameters and metal accumulation by *Brassica juncea* L. *International Journal of Plant Production*, 3(3), 65–76.
- Johnson M. T., Stinchcombe J. R. (2007). An emerging synthesis between community ecology and evolutionary biology. *Trends in Ecology & Evolution*, 22(5), 250-7.
- Kazakou E., Violle C., Roumet C., Navas M.-L., Vile D., Kattge J., Garnier E. (2014). Are trait-based species rankings consistent across data sets and spatial scales? *Journal of Vegetation Science*, 25, 235–247.
- Kerkhoff A. J., Fagan W. F., Elser J. J. Enquist B. J. (2006) Phylogenetic and growth form variation in the scaling of nitrogen and phosphorus in the seed plants. *The American Naturalist*, 168, 4.
- Lambers H., Chapin III F. S., Pons T. L. (2008) Plant physiological ecology, Springer Verlag.
- López-Bucio J., Cruz-Ramírez A., Herrera-Estrella L. (2003). The role of nutrient availability in regulating root architecture. *Current Opinion of Plant Biology*, 6(3), 280-7.
- MA X., Song L., Yu W., Hu Y., Liu Y., Wu J., Ying Y. (2015). Growth, physiological, and biochemical responses of *Camptotheca acuminata* seedlings to different light environments. *Frontiers in Plant Science*, 6, 321.
- Mathur S., Agrawal D., Jajoo A. (2014). Photosynthesis: response to high temperature stress. *Journal of Photochemistry and Photobiology B: Biology*, 137, 116-126.

- Möglich A., Yang X., Ayers R. A., Moffat K. (2010). Structure and Function of Plant Photoreceptors. *The Annual Review of Plant Biology*, 61, 21-47. <http://doi.org/10.1146/annurev-arplant-042809-112259>.
- Montagnoli A., Dumroese R. K., Terzaghi M., Pinto J. R., Fulgaro N., Scippa G. S., Chiatante D. (2018). Tree seedling response to LED spectra: implications for forest restoration. *Plant Biosystems*, 152, 515-523.
- Morgan J. B., Connolly E. L. (2013). Plant-soil interactions: nutrient uptake. *Nature Education Knowledge*, 4(8), 2.
- Oke S. O. (1985). Effect of soil texture nutrient stress and water stress on yield of *Andropogon gayanus*. knuth and *Schizchyrium sanguineum* (Rertz) alston. M.Sc. Thesis, University of Ife (Now Obafemi Awolowo University), Nigeria.
- Osakabe Y., Osakabe K., Shinozaki K., Tran L.-S. P. (2014). Response of plants to water stress. *Frontiers in Plant Science*, 5, 86.
- Osmond C. B., Austin M. P., Berry J. A., Billings W. D., Winner W. E. (1987). Stress physiology and distribution of plants. *Bioscience*, 37, 33-47.
- Parihar P., Singh R., Singh S., Tripathi D. K., Chauhan D. K., Singh V. P. and Prasad S. M. (2016). Photoreceptors mapping from past history till date. *Journal of Photochemistry and Photobiology, B: Biology*, 162, 223-231.
- Patra M., Bhowmik N., Bandopadhyay B., Sharma A. (2004). Comparison of mercury, lead and arsenic with respect to genotoxic effects on plant systems and the development of genetic tolerance. *Environmental and Experimental Botany*, 52(3), 199–223.
- Poorter H., Niklas K. J., Reich P. B., Oleksyn J., Poot P., Mommer L. (2011). Biomass allocation to leaves, stems and roots: meta-analyses of interspecific variation and environmental control. *New Phytologist*, 193(1), 30-50.
- Powles S. B., Critchley C. (1980). Effect of light intensity during growth on photoinhibition of intact attached bean leaflets. *Plant Physiology*, 65, 1181–1187.

- I
- Prasad P. V. V., Djanaguiraman M. (2014). Response of floret fertility and individual grain weight of wheat to high temperature stress: sensitive stages and thresholds for temperature and duration. *Functional Plant Biology*, 41, 1261-1269.
- Quail P. (1997). An emerging molecular map of the phytochromes. *Plant Cell and Environment*, 20, 657-666.
- Reed J.W. (1999). Phytochromes are Pr-iptetic kinases. *Current Opinion in Plant Biology*, 5, 393-397.
- Schweitzer J. A., Madritch M. D., Felker-Quinn E., Bailey J. K. (2012b). From genes to ecosystems: how plant genetics links above- and below-ground processes. In: Wall D, editor. Soil ecology and ecosystem services. Oxford, U.K: *Oxford University Press*, pp. 82–98.
- Shinomura T., Uchida K., Furuya M. (2000). Elementary processes of photoperception by Phytochrome A for high-irradiance response of hypocotyls elongation in Arabidopsis. *Plant Physiology*, 122, 147-156.
- Siebenkäs A., Schumacher J., Roscjer C. (2015). Phenotypic plasticity to light and nutrient availability alters functional trait ranking across eight perennial grassland species. *AoB Plants*, 7, plv029.
- Smirnakou S., Ouzounis T., Radoglou K. (2017). Continuous spectrum LEDs promote seedling quality traits and performance of *Quercus ithaburensis* var. *macrolepis*. *Frontiers in Plant Science*, 8, 188.
- Stuefer J. F., Huber H. (1998). Differential effects of light quantity and spectral light quality on growth, morphology and development of two stoloniferous *Potentilla* species. *Oecologia*, 117, 1-8.
- Thompson W. A., Stocker G. C., Kriedemann P. E. (1988). Growth and photosynthetic response to light and nutrients of *Flindersia brayleyana* F. Muell., a rainforest tree with broad tolerance to sun and shade. *Australian Journal of Plant Physiology*, 15, 299-315.

- Uchida R. (2000). Essential Nutrients for Plant Growth: Nutrient Functions and Deficiency Symptoms. *Plant Nutrient Management in Hawaii's Soils, Approaches for Tropical and Subtropical Agriculture*, (eds. College of Tropical Agriculture and Human Resources).
- Valladares F., Niinemets Ü. (2008). Shade tolerance, a key plant feature of complex nature and consequences. *Annual Review of Ecology, Evolution, and Systematics*, 39, 237-257.
- Wassen M.J., Venterink H. O., Lapshina E. D., Tanneberger F. (2005) Endangered plants persist under phosphorus limitation. *Nature*, 437, 547-550.
- Zengin F. K., Munzuroglu O. (2005). Effects of some heavy metals on content of chlorophyll, proline and some antioxidant chemicals in bean (*Phaseolus vulgaris* L.) seedlings. *Acta Biologica Cracoviensia Series Botanica*, 47(2), 157–164.
- Zhu J. K. (2002). Salt and drought stress signal transduction in plants. *Annual Review of Plant Biology*, 53, 247-273.

Chapter II

Toward an Understanding of Mechanisms Regulating Plant Response to Biochar Application

Polzella Antonella^a, De Zio Elena^a, Arena Simona^b, Scippa Gabriella Stefania^a,
Scaloni Andrea^b, Montagnoli Antonio^c, Chiatante Donato^c, Trupiano Dalila^a

^a Department of Biosciences and Territory, University of Molise, Pesche, Italy.

^b Proteomics and Mass Spectrometry Laboratory, ISPAAM, National Research
Council, Napoli, Italy.

^c Department of Biotechnology and Life Science, University of Insubria, Varese,
Italy.

This Chapter has been published on Plant Biosystems, Vol. 153(1), 2019

Abstract

Plant growth and development are affected by several environmental factors, among which soil nutrient availability. Biochar addition to soil is recognized to exert beneficial effects on soil fertility and thus plant growth; furthermore, it is a promising option for climate change mitigation. However, multi-species studies and meta-analyses have indicated considerable variations in biochar responses among plant species. To date, information on the biochar effect on plants, especially at molecular level, are still scarce.

Using a multi-target approach with a model plant such as tomato, we demonstrate that biochar has a negligible effect on soil nutrient content and plant growth, even if it misbalances the plant photosynthetic machinery, as well as mechanisms recognizing pathogen-derived molecules. Ethylene could be one of the signal-molecule driving the alteration of tomato-pathogen recognition signaling by inactivation of vesicle trafficking. All these modifications could be at the basis of the increased susceptibility of biochar treated plants to pathogen attack.

Further organ and tissue specific multi-level studies, from high-resolution internal processes towards high-throughput external phenotyping, coupled with powerful biostatistic and informatic analysis, will help to decipher, in a network-type fashion, all the factors and signaling mechanisms related to the complex interaction between different plant, soil and biochar types.

Keywords: leaves, *Lycopersicon esculentum*, ethylene, morphology, *Phytophthora infestans*, proteome, soil amendment.

2.1 Introduction

Biochar application to soil is considered as a promising strategy to sustain soil fertility, thus to promote plant growth, simultaneously sequestering atmospheric CO₂ and reducing greenhouse gases emissions, such as CO₂, CH₄, N₂O (Agegnehu *et al.* 2017). It is a carbonaceous product obtained from the pyrolysis of plant and waste feedstocks occurring at high temperatures (between 350-700 °C) in oxygen-limiting conditions (Lehmann and Joseph, 2009).

The wide variety of both biochar and soil with overall complex physical, chemical and biological interactions between them, induce different effects on plant growth and response (Mukherjee and Lal, 2013). In detail, several reports prove biochar benefits on many soil parameters, including nutrient retention, cation-exchange and water-holding capacity, electric conductivity, pH, microbial and mycorrhizal activity (Glaser *et al.*, 2002), which improve soil

fertility and thereby plant growth (Major *et al.*, 2010; Jeffery *et al.*, 2011; Trupiano *et al.*, 2017). Nevertheless, other reports show conflicting effects. For instance, biochar negatively influences plant NH_4^+ adsorption and uptake, due to its surface properties, determining a lower nitrogen (N) release, and thus negatively affecting leaf N and chlorophyll content in tomato plants (Akhtar *et al.*, 2014). As well as, in saline sodic soil, there is an antagonist interaction between biochar and phosphorus (P), producing a detrimental effect on the P availability and *Suaeda salsa* growth (Xu *et al.*, 2016). Furthermore, in species with indeterminate habit, such as tomato, the growth enhancement using biochar is unlikely to occur (Vaccari *et al.*, 2015). However, multi-species studies and meta-analyses proved considerable variations in biochar responses among plant species (Thomas and Gale, 2015), although molecular mechanisms sustaining these different responses are almost unknown.

Recently, Viger *et al.* (2015) have defined a first model to explain the early response, signaling and altered gene expression in *Arabidopsis thaliana* grown in biochar-amended soil. Although in their work, they have noted a biochar-induced increase of *Arabidopsis* plants rate of growth, contrarily to a previous study (Meller Harel *et al.*, 2012), a down-regulation of a large suite of plant defense genes and related-stress signaling response was also observed. Mechanisms related to plant defense signaling are still not understood, but phytohormones, such as ethylene, jasmonic and salicylic acid, seem to have a key role in the regulation of stress-related genes. This highlights the complex plant-soil-biochar interaction and suggests the importance of future investigations on different biochar types and plant species, determining whenever expression changes in genes related to defense may result in an increased organism susceptibility to pathogen attack.

Tomato plant (*Lycopersicon esculentum*, Mill.) is one of most widely grown vegetable (Tranchida-Lombardo *et al.*, 2018) and it is susceptible to certain fungal diseases, such as the late blight caused by *Phytophthora infestans*, which lead often to localized cell death through a hypersensitive plant response (Rigano *et al.*, 2014).

Thus, tomato is used often as a model plant system, although, to date, information on the effects of biochar on tomato growth and pathogen-resistance are still scarce or completely absent. In the present work, we provide a complete picture of the tomato plant response to biochar application, describing the changes in plant morphological parameters in combination with

corresponding changes in proteome profiles and susceptibility to *P. infestans* attack. Results obtained contribute elucidating molecular mechanisms regulating plant growth-defense response.

2.2 Material and Methods

2.2.1 Experimental Set Up and Biochar Treatment

One-month-old tomato seedlings (*Lycopersicon esculentum*, Mill.) (var. San Marzano; Vivaio Mignogna, Ripalimosani, CB - Italy) were transplanted in plastic pots (10 L) prepared with non-amended (control=C) and biochar-amended (treatment=B) soils. Soil was collected from an uncultivated pasture area, located in Pesche, at a depth of 0–20 cm. It is unlikely that these soils contain charcoal already, since there has not been a tradition of crop residue or other burning on the land. The soil was found to be neutral, relatively low in organic matter and to have a clay soil texture (%clay: 52.7 ± 3.4 , %sand: 15.7 ± 0.6 , %silt: 31.6 ± 2.7). For the experiment, soil was air dried for 72 h, weighed and finely crushed then mixed thoroughly before packing lightly in the pots on top of 100 g of pebbles placed on the base to improve drainage. The weight of each filled pot was 10000 g. The biochar used was a commercial charcoal provided by “Romagna Carbone s.n.c.” (Italy), which was obtained from orchard pruning biomass through a slow pyrolysis process at 500 °C in a transportable ring kiln of 2.2 m in diameter and holding around 2 ton of feedstock. The biochar doses were equivalent to application rates of 65 g for Kg of dry soil. Resulting biochar was crushed into particles smaller than 5 cm of diameter before the soil application. Biochar chemical characteristics are described in Trupiano *et al.* (2017). After mixing, the pots were filled in order to ensure the same soil bulk density. There were ten pots (one plant per pot) for each treatment arranged in a complete randomized block design and rotated each day to a different position within the block for the duration of the trial. The pots were fully irrigated to prevent water stress (twice a day, as required), and a suspended shade cover net was used to reduce exposure to sunlight.

2.2.2 Soil Analysis

Soils were sampled at the end of the experiment and air dried for 72 h. Methods for the characterization of moisture, electrical conductivity (EC), Cation exchange capacity (CEC), total nitrogen (N_{tot}), total phosphorus (P_{tot}), available phosphorus (P_{av}) pH and particle size distribution were determinate following standard procedure, described in Trupiano *et al.* (2017). Organic carbon (C_{org}) was assessed according to Walkley-Black test method (1934).

2.2.3 Plant Growth Analysis

After plants treatment, the main morphometric parameters were measured weekly: LN=leaflets number; CLN=compound leaves; SB=stem branching; SH=stem height. The Image J 1.41 (Wayne Rasbanb, National Institute of Health, Bethesda, MD; <http://rsb.info.nih.gov/ij/>) software was used for analysis. At the end of the experiment, leaf and root biomass allocation was determined before (leaf and root fresh weight=LFW and RFW) and after (leaf and root dry weight=LDW and RDW) two days of drying in an oven at 60 °C.

Chlorophyll (Chl a and b) and carotenoid (Car) contents were determined spectrophotometrically by using N,N'-dimethylformamide (DMF) method, detailed reported in Trupiano *et al.* (2017). The following equations were used: $Chla = 12.70_{A664.5} - 2.79_{A647}$; $Chlb = 20.70_{A647} - 4.62_{A664.5}$; total Chl = $17.90_{A647} + 8.08_{A664.5}$; Carotenoids = $[(1000 * A_{480}) - (1,12 * Chla) - (34,07 * Chlb)] / 245 V/W$, where A = absorbance in 1.00 centimeter cuvettes, V= DMF volume used to dissolves samples and W=mg of fresh tissue. All the measurements were performed on six plants.

2.2.4 Protein Extraction and Two-Dimensional Electrophoresis

Total proteins were extracted from leaves samples following the phenol protocol with minor modifications, as reported in Trupiano *et al.* (2014). For isoelectrofocusing (IEF), 17 cm, linear pH 4–7 isoelectrofocusing pH gradient (IPG) ReadyStrip strips (Bio-Rad, Hercules, CA, USA) were rehydrated and focused as reported in Ialiccio *et al.* (2012). After focusing, proteins were reduced by incubating the IPG strips with 1% w/v dithiothreitol in 2,5 ml of 50 mM Tris–HCl (pH 8.8), 6 M urea, 30% w/v glycerol, 2% w/v SDS for 20 min, and then alkylated with 2.5% w/v

iodoacetamide in 2,5 ml of 50 mM Tris–HCl (pH 8.8), 6 M urea, 30% w/v glycerol, 2% w/v SDS for 20 min.

Electrophoresis in the second dimension was carried out on 12% polyacrylamide gels (17×24cm×1 mm) with a Protean apparatus (Bio-Rad) in 25 mM Tris–HCl, pH 8.3, 1.92 M glycine and 1% w/v SDS, with 90 V applied for 19 h, until the dye front reached the bottom of the gel. 2-DE gels were stained with colloidal Coomassie G250. Each sample was run in biological triplicate. Gel scanning, densitometric and statistical analysis 2-DE gels were scanned using a GS-800 calibrated densitometer (Bio-Rad). Image analysis was performed using the PDQUEST software (Bio-Rad) to identify differentially expressed proteins. Spot detection and matching between gels were performed automatically, followed by manual verification. After normalization of the spot densities against the whole-gel densities, statistical Student's t-test analysis at significance level ($P < 0.01$) was chosen to find out significant changes between samples. An absolute two-fold change in normalized spot densities was then considered indicative of a differentially modified protein; values > 2 or < 0.5 were associated with increased or decreased protein amounts after treatment, respectively.

2.2.5 In-Gel Digestion, Mass Spectrometry Analysis and Identification

Protein spots of interest were excised from gels and triturated. After a washing step with water, proteins were reduced, S-alkylated and digested with trypsin as previously reported (Trupiano *et al.*, 2012a). Briefly, digest aliquots were removed and subjected to a desalting/concentration step on mZipTipC18 (Millipore Corp., Bedford, MA, USA) using 5% formic acid/50% acetonitrile as eluent. Then, peptide mixtures were analyzed by nano-liquid chromatography-electrospray ionization-linear ion trap-tandem mass spectrometry (nanoLC-ESI-LIT-MS/MS) using an LTQ XL mass spectrometer (Thermo Finnigan, San Jose, CA, USA), which was equipped with a Proxeon nanospray source connected to a nanoEasy chromatographer (Proxeon, Odense, Denmark). The Mascot software package (Matrix Science, UK) was used to identify spots unambiguously (Trupiano *et al.*, 2012a).

2.2.6 ACO Expression Measurements

RNA was extracted from 0.1 g of a pooled sample becoming from the fourthly expanded leaves of 10 plants by using the RNeasy Plant Mini kit (Qiagen, Valencia, CA), according to manufacturer's suggestions. RNA concentration, integrity and quality was checked as detailed reported in (Trupiano *et al.*, 2012b). cDNA was synthesized by using 1.0 µg of total RNA, the poly(A) oligonucleotide primer and Superscript III reverse transcriptase (Invitrogen Co., Carlsbad, CA, USA). *LeACO1* specific primers (F5'-ATGGAGAACTTCCCAAT-3'; R 5'-CTAAGCACTTGCAATTG-3') were used for PCR amplification (Barry *et al.*, 1996). To account for small differences in RNA loadings, data were normalized to α -tubulin gene expression (α -*Tub*; F5'-TGACGAAGTCAGGACAGGAA-3'; R5'-CTGCATCTTCTTTGCCACTG-3'; Solyc04g077020.2; Chen *et al.*, 2013).

Conditions for RT-PCR reactions (25 µl of vol) were as follows: 95 °C for 1 min, followed by 35 cycles of 94 °C for 45 s, 55 °C (α -*Tub*) or 52 °C (*LeACO1*) for 1 min, 72 °C for 1 min, then followed by 1 cycle of 72 °C for 5 min. Three independent extractions were performed, each with two technical replications. Images of gels were acquired by Chemidoc (Quantity One software; Bio-rad) and analyzed using Image J 1.41 software. Negative controls devoid of template were used in each experiment to check for contaminated reagents.

2.2.7 PCR-Based Detection of *P. infestans* in Leaves

PCR was applied to determine the growth of *P. infestans* on plants grown on non-amended and biochar-amended soils. DNA was isolated from a pooled sample becoming from the fourthly expanded leaves of 10 plants using the DNeasy Plant Mini Kit (Qiagen). The above reported α -*Tub* primers were used to quantify *L. esculentum* DNA (Chen *et al.*, 2013), while the primers PiO8-3-3F (5'-CAATTCGCCACCTTCTTCGA-3') and PiO8-3-3R (5'-GCCTTCCTGCCCTCAAGAAC-3'), which were designed based on highly repetitive sequences from the *P. infestans* genome (Judelson and Tooley, 2000), were used to quantify *P. infestans* DNA.

Conditions for PCR reactions (25 µl of vol) were as follows: 95 °C for 1 min, followed by 40 cycles of 94 °C for 45 s, 55 °C (α -*Tub*) or 58 °C (PiO8-3-3) for 1 min, 72 °C for 1 min, then followed by 1 cycle of 72 °C for 5 min. Three independent extractions were performed, each with

two technical replications. Images of gels were acquired and analyzed as reported above. Negative controls devoid of template were used in each experiment to check for contaminated reagents.

2.3 Results

2.3.1 Biochar Effect on Soil Characteristics

Soil chemical analysis showed that biochar addition resulted in an increase of pH, EC, P_{tot} and C_{org} values, while moisture, N_{tot} , P_{av} and CEC were unchanged (Table 2.1).

	C	B
pH	6.9 ± 0.2 a	8.0 ± 0.0 b
EC (dS/m)	0.71 ± 0.0 a	1.0 ± 0.0 b
Moisture (g/kg)	48.4 ± 3.5 a	59.0 ± 0.2 a
N_{tot} (g/kg)	0.8 ± 0.0 a	1.0 ± 0.0 a
P_{tot} (mg/kg)	199.9 ± 9.9 a	376.6 ± 86.5 b
P_{av} (mg/kg)	<12.0 ± 0.0 a	<12.0 ± 0.0 a
C_{org} (g/kg)	9.6 ± 0.4 a	18.5 ± 0.8 b
CEC (cmol/kg)	21.0 ± 0.6 a	20.7 ± 0.5 a

Table 2.1. Substrates chemical properties. Data represent the mean (n=4) ± standard error. Mean values marked with the same letter are not statistically different. One-way ANOVA was applied to weigh the effects biochar treatments ($p \leq 0.05$).

2.3.2 Biochar Effect on Plant Growth

No difference in growth parameters were recorded between non-amended and biochar-amended plants. In detail, LN, CLN, SB and SH values were unchanged (Fig. 2.1) producing no variation

in total biomass accumulation, both as LDW and RDW (Fig. 2.2); chlorophyll and carotenoid contents were also unchanged (data not shown).

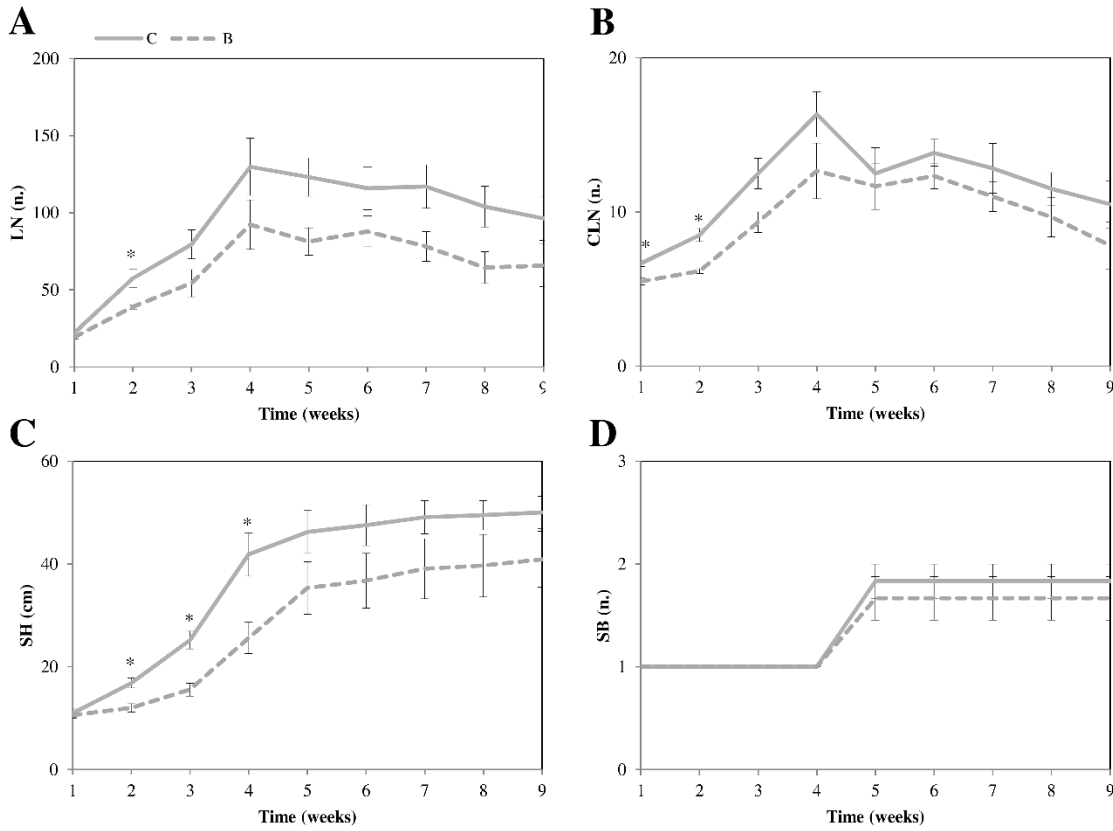


Figure 2.1. Morphological analysis. The main plant parameters were analyzed, i.e. LN=leaflets number; CLN=compound leaves; SB=stem branching; SH=stem height. Data represent the mean ($n = 6$) \pm standard error. Mean values marked with asterisks are statistically different at $*p \leq 0.05$. C= tomato plants grown in non-amended soils (control); B= tomato plants grown in biochar-amended soils.



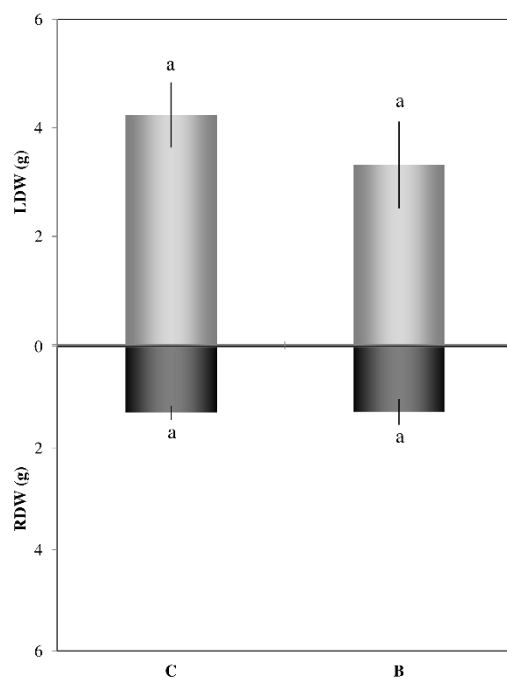


Figure 2.2. Leaf and root biomass (g of dry tissue weight). Data represent the mean ($n = 6$) \pm standard error. Mean values marked with the same letter are not statistically different ($p \leq 0.05$). C= tomato plants grown in non-amended soils (control); B= tomato plants grown in biochar-amended soils.

2.3.3 Effects of Biochar on Leaf Proteome

Leaf proteomic maps of tomato plants grown on non-amended and biochar-amended soils contained an average of 300 well-resolved spots, ranging in Mr from about 76 to 12 kDa. We here provide the first proteomic profile of tomato leaves influenced by presence/absence of biochar. These maps were highly reproducible, most spots detected in 2-DE gels showed analogous positions and intensities, as indicated by the degree of gel similarity between the various samples and the reference map. Computer-assisted comparison of 2-DE maps revealed 15 protein spots as differentially represented ($P < 0.01$) among samples, which were subjected to trypsinolysis and further nanoLC-ESI-LIT-MS/MS analysis for protein identification (Fig. 2.3). The list of all identified proteins together with their information and representation profiles are shown in Table 2.

When compared to plants grown on non-amended soil, those grown on biochar-amended soil presented an over-representation of 7 components, namely two isoforms of ribulose

bisphosphate carboxylase/oxygenase activase (RCA; spots 1 and 2), remorin (spot 3), 2-cysteine peroxiredoxin B (spot 7), soluble inorganic pyrophosphatase (PPA6; spot 9), chitinase (spot 12) and a class I heat shock (spot 15), together with a down-representation of 8 components, namely ATP synthase CF1 alpha subunit (spot 4), ribulose bisphosphate carboxylase large chain (rbcL; spot 5), RAB GTPase homolog E1b (spot 6), two isoforms of subtilisin-like protease (spots 8 and 10), oxygen-evolving enhancer protein 2-1 (OEE2; spot 11), embryo defective protein 1241 (fragment; spot 13), and a photosystem I reaction center subunit II-2 (PSAD2; spot 14) (Table 2.2).

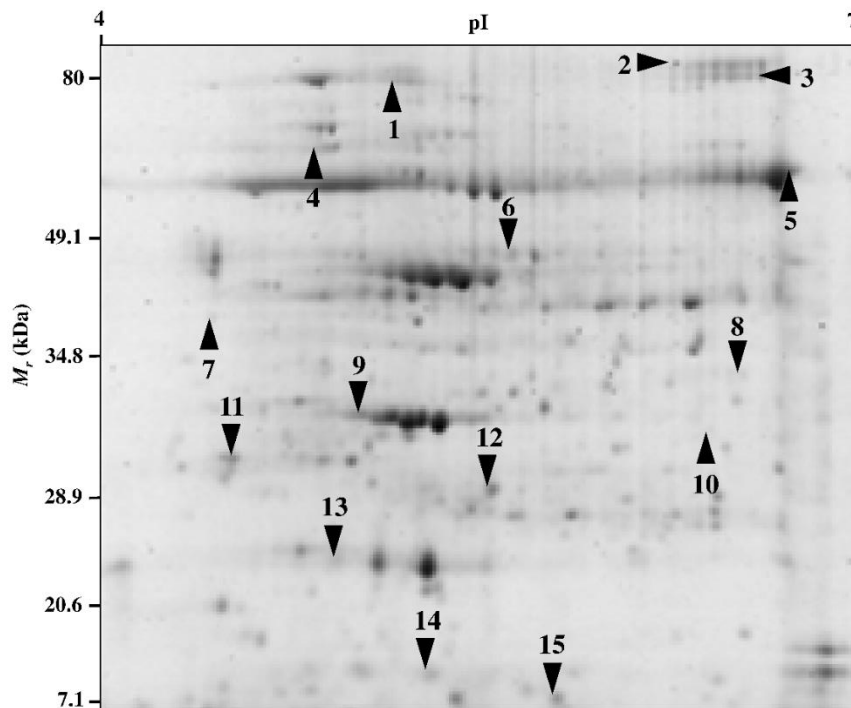
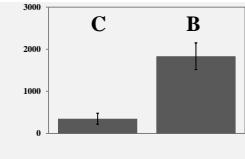
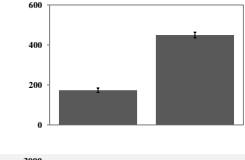
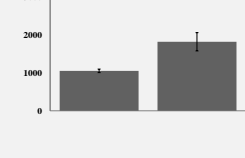
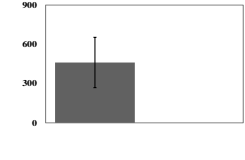
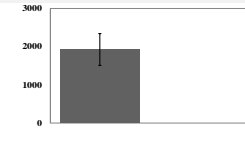
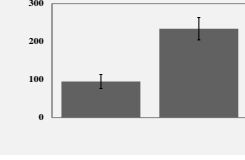
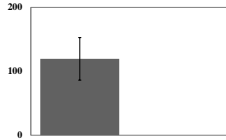
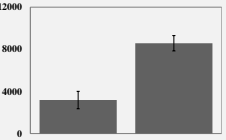
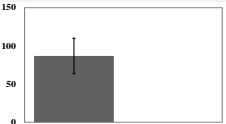
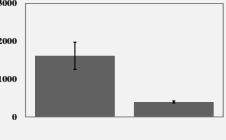
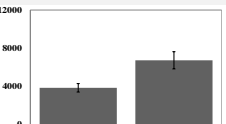
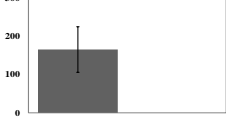


Figure 2.3. Reproducible 2-DE maps of tomato leaves (control) showing 15 differentially represented proteins. Arrows indicate the position of each protein spot; spot identification information is reported in Table 2.2.

Chapter II

Spot	Accession	Gene name	Protein description	Mascot Score	Theor. M_r/pI	Exp. M_r/pI	Peptides matched	Sequences matched	Coverage %	Functional classification	Details classification	Protein representation levels
1	K4D489	RCA	Ribulose biphosphate carboxylase/oxygenase activase	1621	49.2/8.62	77.0/5.16	188	25	51.8	Photosynthesis	'PS.calvin cycle.rubisco interacting'	
2	K4D489	RCA	Ribulose biphosphate carboxylase oxygenase activase	1218	49.2/8.62	81.0/6.40	69	23	50.3	Photosynthesis	'PS.calvin cycle.rubisco interacting'	
3	Q9XEX8	rem-1	Remorin family	280	21.8/5.64	79.0/6.68	12	7	28.7	Transcription	'RNA. regulation of transcription.unclassified'	
4	A0A0C5CHA6	atpA	ATP synthase CF1 alpha subunit	189	55.4/5.14	67.0/4.84	4	4	10.1	Photosynthesis	'PS.lightreaction. ATPsynthase. alpha subunit'	
5	A0A0C5CHE6	rbcL	Ribulose biphosphate carboxylase large chain	573	52.9/6.55	57.5/6.70	16	11	24.7	Photosynthesis	'PS.calvin cycle.rubisco large subunit'	
6	K4C8Q1	TUFA	RAB GTPase homolog E1b	510	48.9/6.17	44.0/5.60	11	10	24.9	Protein synthesis	'protein.synthesis. elongation'	
7	K4D389	BAS1	2-cysteine peroxiredoxin B	157	29.5/6.00	37.0/4.46	5	4	20	Disease/Defense	'redox.peroxiredoxin.BAS1'	

*Toward an Understanding of Mechanisms
Regulating Plant Response to Biochar Application*

8	O04678	SBT1.7	Subtilisin-like protease (fragment)	351	76.4/6.17	34.6/6.60	8	7	12.7	Protein destination and storage	'protein.degrada- tion.subtilases'	
9	K4B2L1	PPA6	Soluble inorganic pyrophosphatase 1	271	32.4/6.01	33.0/4.99	11	5	18.6	Metabolism	'nucleotide metabolism.phos- photransfer and pyrophosphata- ses.misc'	
10	O04678	SBT1.7	Subtilisin-like protease (fragment)	646	76.4/6.17	33.8/6.51	22	12	24.1	Protein destination and storage	'protein.degrada- tion.subtilases'	
11	P29795	PSBP1	Oxygen-evolving enhancer protein 2-1	542	20.2/5.32	30.0/4.52	42	10	43.3	Photosynthesis	'PS.lightreaction.p hotosystem II.PSII polypeptide subunits'	
12	Q05539	T15B16. 5	Chitinase family	352	25.0/5.63	27.5/5.56	32	6	38.5	Disease/Defense	'stress.biotic'	
13	K4D311	-	Embryo defective 1241 (fragment)	297	42.1/4.77	23.6/4.92	6	5	14.3	Protein destination and storage	'protein.folding'	
14	P12372	PSAD2	Photosystem I reaction center subunit II-2	107	17.5/9.14	14.8/5.28	4	2	12	Photosynthesis	'PS.lightreaction.p hotosystem I.PSI polypeptide subunits'	

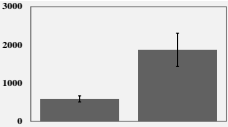
15	Q9SYU 8	HSP17. 8	Class I heat shock	363	17.7/5.84	10.0/5.86	17	8	55.2	Disease/Defense	'stress.abiotic.heat'	
----	------------	-------------	--------------------	-----	-----------	-----------	----	---	------	-----------------	-----------------------	---

Table 2.2. Differentially-represented proteins in leaves from tomato plants grown in non-amended soils (C) and tomato plants grown in biochar-amended soils (B). The list includes: spot number on the reference gel (see Fig. 2.3), hit and accession number, protein description, Mascot Score, theoretical and experimental protein Mr and pI values, peptides and sequences matched, sequence coverage (%), functional and detail classification, and protein representation levels.

2.3.4 Analysis of LeACO1 Gene Expression Patterns

Results of LeACO1 gene expression analysis showed a lower expression level of this gene and, an indirect lesser ethylene hormone amount, in the leaves of plants grown on biochar-treated soil compared to those grown on non-amended soil (Fig. 2.4).

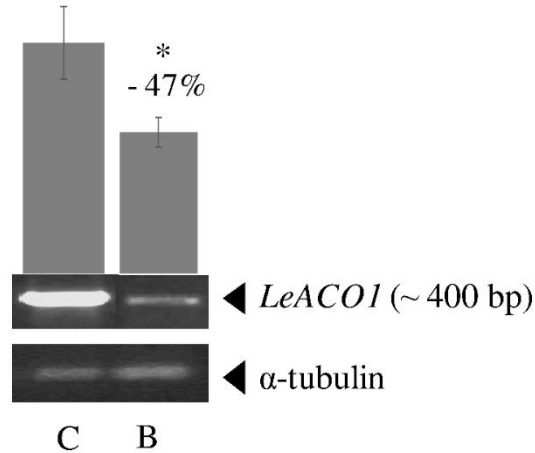


Figure 2.4. LeACO1 gene expression level. The LeACO1 expression level in leaves of tomato plant grown on non-amended (C) and biochar-amended (B) soil. Three independent biological replicates were run for each tissue, each with two technical replications. Data were normalized to α -tubulin as a loading control. Bars represent the standard error of mean values. Asterisk indicates significant differences at ($p \leq 0.05$).

2.3.5 Detection of the Tomato Late Blight Pathogen: *Phytophthora infestans*

Genomic DNA was extracted from tomato leaves to assess the presence/absence of *P. infestans* pathogen. Molecular analysis showed the presence of highly conserved genomic region PiO8-3-3 that highlighted the presence of *P. infestans* pathogen in plants grown on biochar-treated soil (Fig. 2.5).

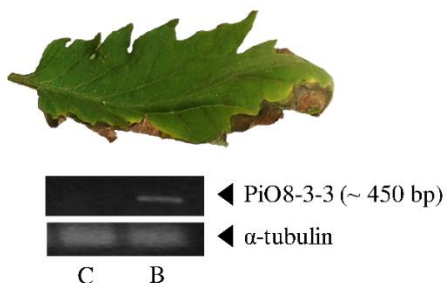


Figure 2.5. Detection of *P. infestans*. Photos in the upper panel shows representative picture of *P. infestans* infected leaves of tomato plant grown on biochar-amended soil. The lower panel shows the detection of *P. infestans* PiO8-3-3 DNA region in leaves of tomato plant grown on non-amended (C) and biochar-amended (B) soil. Three independent biological replicates were run for each tissue, each with two technical replications. Data were normalized to α -tubulin as a loading control. Bars represent the standard error of mean values.

2.4 Discussion and Conclusions

In the present study, we investigated the almost-unknown effects of biochar amendment on tomato plants by using a multi-target approach. Data showed that the application of biochar to nutrient-poor and neutral soil induced an increase of pH, EC, P_{tot} and C_{org} values, leaving unchanged the CEC, N_{tot} and P_{av} counterparts. At the same time, it determined a slight decrease of tomato leaflets number, compound leaves and stem height only in the first phases of plant growth after the transplant, and not over-time.

It is widely known that plant biomass accumulation is highly dependent on N and P concentration, largely due to the key role of these two macronutrients in a variety of biochemical processes, including photosynthesis, energy metabolism, signal transduction, biosynthesis of macromolecules and protein regulation (Wright *et al.*, 2004; Abbasi and Yousra, 2012; Tavarini *et al.*, 2015). Under an adequate N amount, it is expected an increased N allocation toward chloroplast thylakoid membrane proteins and pigment-protein complexes, thus increasing the light-saturated photosynthesis rate. On the other hand, P is essential for plant development and growth, being a major component of nucleic acids, sugar phosphates and phospholipids.

Biochar usually contains N, P and basic cations like Ca^{2+} , Mg^{2+} and K^{+} (Major *et al.*, 2010); thus, directly or indirectly it improves soil nutrients availability and use efficiency (Lehmann and Joseph, 2009). However, depending on feedstock properties, pyrolysis conditions and soil characteristics, biochar has been noted for its ability to retain $\text{NH}_4^{+}\text{-N}$ (Gai *et al.*, 2014), and/or

NO₃-N (Gale *et al.*, 2017). Both biochar and N, as a limiting factor, might be detrimental on P and K soil content (Chan *et al.*, 2008). The effects of biochar on P availability have been positively proved in acidic soils, whereas its impact on alkaline soils is generally negative due to P sorption or precipitation (Parvage *et al.*, 2013). In fact, alkaline pH and large amount of P sorption sites, such as Ca²⁺, Mg²⁺, Al³⁺ and Fe³⁺ oxides, which are contained in biochar, may be responsible for P precipitation and insolubilization (Marks *et al.*, 2014).

A limited availability of P generally activates the plant metabolic and developmental processes to maximize inorganic phosphate (Pi) acquisition transport and use (Yang and Finnegan, 2010). In tomato plants grown on biochar-treated soil, proteomic data, reported in our work, revealed an over-representation of PPA6, a member of a class of enzymes that catalyzes the hydrolysis of PPI to produce two orthophosphates (2Pi) and release energy (Heinonen, 2001). Thus, PPA6, through recycling of the pyrophosphate (PPI) deriving from many biosynthetic reactions, may play a role in the plant adaptation to phosphorus deficiency condition. Hernández-Domínguez *et al.* (2012) demonstrated that, in common bean, Pi deficiency induces an ATP reduction, thereby the PPI hydrolysis rates must increase to compensate the P limitation. Furthermore, transgenic tobacco and potato plants expressing the *E. coli ppal* gene showed a stunted growth mainly due to a decrease in hexose phosphates and PPI content (Sonnewald, 1992). Authors hypothesized that the decrease of cytosolic PPI may reduce the energy gain and, thereby, sugar produced by photosynthesis can be accumulated in source leaves, inhibiting long-distance sucrose transport, and mobile energy source for all plant cells (Gaxiola *et al.*, 2012). Sugar accumulation in leaves determines a reduction in the photosynthetic process probably due to a metabolite feedback regulation, which in turn induces electron transfer and RubisCO amount and activity decrease (Lemoine *et al.*, 2013). This effect was confirmed in tomato biochar-treated plants by down-representation of *rbcL* and ATP synthase CF1 alpha subunit, as well as by the reduction of the embryo defective protein 1241, chloroplast GrpE protein, important for chloroplast protein import and functionality maintenance (Flexas *et al.*, 2006). In these plants, although the chlorophyll and carotenoid contents resulted unchanged, the reduction of PSAD2 and OEE2 may limit the assembly/functionality of the photosystems I and II, altering the electron transport chain and the photosynthetic machinery.

In biochar amended tomato plants, photosynthesis misbalance may dramatically determine ROS production, as demonstrated by the over-representation of 2-cysteine peroxiredoxin B and a

class I heat shock protein, intimately associated with ROS induction. 2-cysteine peroxiredoxins play a dual function in all living cells both as chaperone and as thiol-based peroxidases, accounting for up to 40% of total peroxidase activity of chloroplast (Neumann *et al.*, 2009). However, ROS can also mediate important signal transduction events via redox-sensitive transcription factors, which in turn activate the heat shock proteins expression (Suzuki and Mittler, 2006; Pandey *et al.*, 2017). Class I heat shock proteins are a group of chaperone-like proteins often constitutively expressed in plants and highly induced by different environmental stressors (Wang *et al.*, 2004; De Silva, 2017). Plants synthesize different classes of heat shock proteins or other chaperones that, in concert, play complementary and sometimes overlapping roles in the protection of proteins from stress (Timperio *et al.*, 2008). In tomato plants, the presence of biochar in the poor-nutrient neutral soil may thus represent a cause of stress, inducing the over-expression of several proteins involved in defense machinery.

Above-mentioned protection toward stress can also be mediated by the essential enzyme RCA, which was also found over-represented in tomato biochar-amended plants. RCA is canonically associated with the activation/maintenance of RuBisCo catalytic activity by promoting the ATP-dependent removal of any inhibitors tightly bound (sugar phosphates) from the catalytic site of RuBisCo. However, it has been demonstrated that this enzyme can play also a role as chaperone in protecting functional proteins from several stress-related damages (Chen *et al.*, 2015).

In biochar-treated plants, proteomic data also showed an over-representation of biotic stress-related components, namely chitinase and remorin. Chitinase up-regulation in leaf tissues has already been associated with *P. infestans* oomycete infection; in fact, the role of chitinases in defense response to fungal contagion has widely been documented (Jalil *et al.*, 2015). Similarly, remorins are plant-specific proteins associated with plasma membrane microdomains involved in biotic and abiotic stress, and hormone-mediated responses/signal transduction (Le Febvre *et al.*, 2009). The transient and rapid induction of remorin gene expression upon biotic stimuli, such as powdery mildew infection, suggests possible roles of these proteins in plant-fungi interactions (Le Febvre *et al.*, 2009).

How and by which signaling mechanisms biochar influences plant immunity and defense is still not understood, although it has been previously associated with a defense machinery dysfunction, and a reduction of several stress-related genes in biochar-treated *Arabidopsis* plants

(Viger *et al.*, 2015). In this context, phytohormones, such as ethylene, jasmonic and salicylic acid, seem to have a key role in the regulation of stress-related genes. These hormones are likely to be also dispensable in signaling related to extracellular pathogen recognition by controlling vesicles trafficking machinery (Inada and Ueda, 2014; Song *et al.*, 2014). In our study, the leaf of tomato plant treated with biochar showed a reduction of ethylene (indirectly measured as *LeACO1* amount), and a significant reduction of components involved in pathogen recognition, including a RAB GTPase homolog E1b and two subtilisin-like proteases. Ethylene is known to regulate multiple physiological and developmental processes in plants, including responses to abiotic and biotic stress conditions. Double signaling function of ethylene in disease resistance has been addressed. In some studies, ethylene was shown to promote disease development; in others, it appears to be involved in plant resistance, inducing certain types of pathogenesis-related proteins (Gamalero *et al.*, 2016; Elías *et al.*, 2018). Spanu and Boller (1989) showed that in tomato leaves infected by *P. infestans*, the early and local active response to pathogen attack, mainly associated with plant defense induction, was regulated by a specific ethylene spatial gradient. Furthermore, ethylene acts in cross-communicating signaling pathways with salicylic and jasmonic acid to regulate vesicle trafficking and secretory pathways activated in several plant responses (Inada and Ueda, 2014).

In the regulation of vesicles trafficking, also RABs play a pivotal role. They are a group of small monomeric GTPases that act as molecular switches to vesicle budding from a donor compartment toward a specific target compartment, and, eventually, tethering and fusion of the vesicles with the target membrane. Rivero *et al.* (2017) also discussed the emerging roles of these small GTPases in the regulation of membrane trafficking during plant-pathogen interaction, which is crucial along the different steps of the pathogen recognition, interaction and signal transduction. Other proteins involved in pathogen recognition are subtilisin-like proteases. They are serine proteolytic enzymes that control plant development, physiology, defense and stress responses (Tripathi and Sowdhamini, 2006). The first evidence for the importance of subtilisin-like proteins in plant-pathogen interaction was reported in tomato, where their expression was shown to be induced by pathogen attack and salicylic acid application (Figueiredo *et al.*, 2014). Further to be involved in host-pathogen interaction, recognition and signaling, another interesting feature of subtilisin-like proteins is their involvement in plant programmed cell death localized at the site of attempted pathogen invasion. Based on the above evidences, we hypothesize that the trafficking

dysfunction, probably due to ethylene-related network alteration, may be at the basis of a defective pathogen recognition, and may correlate susceptibility of tomato biochar-treated plants to pathogen attack.

In conclusion, this work provides novel insights regarding the effect of biochar soil amendment upon tomato plant analyzing changes in growth parameters and proteome profiles. Indeed, our results demonstrated that the addition of biochar has negligible effect on tomato growth and soil P and N content. However, our proteomic data suggest that biochar could a) misbalance the photosynthetic machinery, and b) impair the mechanisms recognizing pathogen-derived molecules. Furthermore, ethylene seems to be one of the signal molecules affecting tomato plant susceptibility to *P. infestans* attack.

Results presented highlight the importance of further global gene expression studies and complete hormonal profiling at organ- and tissue-specific scale (De Zio *et al.*, 2016) to decipher, in a network-type fashion, all the factors and mechanisms related to the complex interaction between plant, soil and biochar. In regard of an increase in pathogen susceptibility of biochar-treated plants, cell imaging with fluorescently tagged effector proteins and membrane trafficking components is needed to throw light upon this complex interaction.

2.5 Acknowledgments

The authors thank Dr. Carla Amendola and Dr. Roxana Ginerete (University of Molise) for their technical support during laboratory measurements. Research was supported by grants from Molise Region (PSR Molise 2007/2013-Misura 124) through the ProSEEAA Project (CUP: D95F14000030007).

2.6 References

- Abbasi M. K., Yousra M. (2012). Synergistic effects of biofertilizer with organic and chemical N sources in improving soil nutrient status and increasing growth and yield of wheat grown under greenhouse conditions. *Plant Biosystems*, 146, 181-189.
- Agegnehu G., Srivastava A. K., Bird M. I. (2017). The role of biochar and biochar-compost in improving soil quality and crop performance: a review. *Applied Soil Ecology*, 119, 156-170.
- Akhtar S. S., Li G., Andersen M. N., Liu F. (2014). Biochar enhances yield and quality of tomato under reduced irrigation. *Agriculture Water Management*, 138, 37-44.
- Barry C. S., Blume B., Bouzayen M., Cooper W., Hamilton A. J., Grierson D. (1996). Differential expression of the 1-aminocyclopropane-1-carboxylate oxidase gene family of tomato. *The Plant Journal*, 9, 525-35.
- Chan K. Y., Van Zwieten L., Meszaros I., Downie A., Joseph S. (2008). Using poultry litter biochars as soil amendments. *Soil Research*, 46, 437-444.
- Chen T., Lv Y., Zhao T., Li N., Yang Y., Yu W., He X., Liu T., Zhang B. (2013). Comparative transcriptome profiling of a resistant vs. Susceptible Tomato (*Solanum lycopersicum*) cultivar in response to infection by tomato yellow leaf curl virus. *PLoS ONE*, 8, e80816.
- Chen Y., Wang X. M., Zhou L., He Y., Wang D., Qi Y. H., Jiang D. A. (2015). Rubisco activase is also a multiple responder to abiotic stresses in rice. *PLoS ONE*, 10, e0140934.
- De Silva H. C. C., Asaeda T. (2017). Stress response and tolerance of the submerged macrophyte *Elodea nuttallii* (Planch) St. John to heat stress: a comparative study of shock heat stress and gradual heat stress. *Plant Biosystems*, 152, 787-764.
- De Zio E., Trupiano D., Montagnoli A., Terzaghi M., Chiatante D., Grosso A., Marra M., Scaloni A., Scippa G. S. (2016). Poplar woody taproot under bending stress: the asymmetric response of the convex and concave sides. *Annals of Botany*, 118, 865-883.
- Elías J. M., Guerrero-Molina M. F., Martínez-Zamora M. G., Díaz-Ricci J. C., Pedraza R. O. (2018). Role of ethylene and related gene expression in the interaction between strawberry

plants and the plant growth-promoting bacterium *Azospirillum brasilense*. *Plant Biology*, 20(3), 490–496.

Figueiredo A., Monteiro F., Sebastiana M. (2014). Subtilisin-like proteases in plant–pathogen recognition and immune priming: a perspective. *Frontiers of Plant Science* 5, 739.

Flexas J., Ribas-Carbó M., Bota J., Galmés J., Henkle M., Martínez-Cañellas S., Medrano H. (2006). Decreased Rubisco activity during water stress is not induced by decreased relative water content but related to conditions of low stomatal conductance and chloroplast CO₂ concentration. *New Phytologist*, 172, 73–82.

Gai X., Wang H., Liu J., Zhai L., Liu S., Ren T., Liu H. (2014). Effects of feedstock and pyrolysis temperature on biochar adsorption of ammonium and nitrate. *PLoS ONE*, 9, e113888.

Gale N. V., Halim M. A., Horsburgh M., Thomas S. C. (2017). Comparative responses of early-successional plants to charcoal soil amendments. *Ecosphere*, 8, 10.

Gamalero E., Marzachì C., Galetto L., Veratti F., Massa N., Bona E., Novello G., Glick B. R., Ali S., Cantamessa S., D’Agostino G., Berta G. (2016). An 1-Aminocyclopropane-1-carboxylate (ACC) deaminase-expressing endophyte increases plant resistance to flavesence dorée phytoplasma infection. *Plant Biosystems*, 151, 331–340.

Gaxiola R. A., Sanchez C. A., Paez-Valencia J., Ayre B. G., Elser J. J. (2012). Genetic manipulation of a ‘vacuolar’ H⁺-PPase: from salt tolerance to yield enhancement under phosphorus-deficient soils. *Plant Physiology*, 159, 3–11.

Glaser B., Lehmann J., Zech W. (2002). Ameliorating physical and chemical properties of highly weathered soils in the tropics with charcoal—a review. *Biology and Fertility of Soils*, 35, 219–230.

Heinonen J. K. (2001). *Biological Role of Inorganic Pyrophosphate*. Kluwer Academic Publishers. Boston, MA.

Hernández-Domínguez E. E., Valencia-Turcotte L. G., Rodríguez-Sotres R. (2012). Changes in expression of soluble inorganic pyrophosphatases of *Phaseolus vulgaris* under phosphate starvation. *Plant Science*, 187, 39–48.

- Hoffman R., Roebroek E., Heale J. B. (1988). Effects of ethylene biosynthesis in carrot root slices on 6-methoxymellein accumulation and resistance to *Botrytis cinerea*. *Physiologia Plantarum*, 73, 71–76.
- Iallicicco M., Viscosi V., Arena S., Scaloni A., Trupiano D., Rocco M., Chiatante D., Scippa G. S. (2012). *Lens culinaris* Medik. seed proteome: analysis to identify landrace markers. *Plant Science*, 197, 1-9.
- Inada N., Ueda T. (2014). Membrane trafficking pathways and their roles in plant-microbe interactions. *Plant and Cell Physiology*, 55, 672–86.
- Jalil S. U., Mishra M., Ansari M. I. (2015). Current view on chitinase for plant defence. *BioSciences Trends*, 8, 6733–6743.
- Jeffery S., Verheijen F. G. A., Van der Velde M., Bastos A. C. (2011). A quantitative review of the effects of biochar application to soils on crop productivity using meta-analysis. *Agriculture Ecosystems and Environment*, 144, 175–187.
- Judelson H. S., Tooley P. W. (2000). Enhanced polymerase chain reaction methods for detecting and quantifying *Phytophthora infestans* in plants. *Phytopathology*, 90, 1112–9.
- Lefebvre B., Timmers T., Mbengue M., Moreau S., Hervé C., Tóth K., Bittencourt-Silvestre J., Klaus D., Deslandes L., Godiard L., Murray J. D., Udvardi M. K., Raffaele S., Mongrand S., Cullimore J., Gamas P., Niebel A., Otta T. (2010). A remorin protein interacts with symbiotic receptors and regulates bacterial infection. *Proceedings of the National Academy of Sciences U S A*, 107, 2343–2348.
- Lehmann J., Joseph S. (2009). Biochar for Environmental Management: Science and Technology. *Earthscan Press, London, UK*, pp 1–10.
- Lemoine R., La Camera S., Atanassova R., Dédaldéchamp F., Allario T., Pourtau N., Bonnemain J. L., Laloi M., Coutos-Thévenot P., Maurousset L., Faucher M., Girousse C., Lemonnier P., Parrilla J., Durand M. (2013). Source-to-sink transport of sugar and regulation by environmental factors. *Frontiers of Plant Science*, 4, 272.
- Major J., Rondon M., Molina D., Riha S. J., Lehmann J. (2010). Maize yield and nutrition during 4 years after biochar application to a Colombian savanna oxisol. *Plant Soil*, 333, 117–128.

Marks E. A. N., Alcañiz J. M., Domene X. (2014). Unintended effects of biochars on short-term plant growth in a calcareous soil. *Plant Soil*, 385, 87–105.

Meichtry J., Amrhein N., Schaller A. (1999). Characterization of the subtilase gene family in tomato (*Lycopersicon esculentum* Mill.). *Plant Molecular Biology*, 39, 749–760.

Meller Harel Y., Kolton M., Elad Y., Rav-David D., Cytryn E., Borenshtein M., Shulchani R., Graber E. R. (2012). Biochar impact on plant development and disease resistance in pot trials. Biological Control of Fungal and Bacterial. *Plant Pathogens*, 78, 141–147.

Mukherjee A., Lal R. (2013). Biochar impacts on soil physical properties and greenhouse gas emissions. *Agronomy Journal*, 3, 313–339.

Neumann C. A., Cao J., Manevich Y. (2009). Peroxiredoxin 1 and its role in cell signaling. *Cell Cycle*, 8, 4072–8.

Pandey A., Sekar K. C., Tamta S., Rawal R. S. (2017). Assessment of phytochemicals, antioxidant and antimutagenic activity in micropropagated plants of *Quercus serrata*, a high value tree species of Himalaya. *Plant Biosystems*, 152, 929-936.

Parvage M. M., Ulén B., Eriksson J., Strock J., Kirchmann H. (2013). Phosphorus availability in soils amended with wheat residue char. *Biology and Fertility of Soils*, 49, 245–250.

Rigano M. M., Arena C., Di Matteo A., Sellitto S., Frusciante L., Barone A. (2014). Eco-physiological response to water stress of drought-tolerant and drought-sensitive tomato genotypes. *Plant Biosystems*, 150, 682–691.

Rivero C., Traubenik S., Zanetti M. E., Blanco F. A. (2017). Small GTPases in plant biotic interactions. *Small GTPases*, 1–11.

Song W. Y., Peng S. P., Shao C. Y., Shao H. B., Yang H. C. (2014). Ethylene glycol tetra-acetic acid and salicylic acid improve anti-oxidative ability of maize seedling leaves under heavy-metal and polyethylene glycol 6000-simulated drought stress. *Plant Biosystems*, 148, 96–108.

Sonnewald U. (1992). Expression of *E. coli* inorganic pyrophosphatase in transgenic plants alters photoassimilate partitioning. *The Plant Journal*, 2, 571-81.

- Spanu P., Boller T. (1989). Ethylene Biosynthesis in Tomato Infected by *Phytophthora Infestans*. *Biochemical and Physiological Aspects of Ethylene Production in Lower and Higher Plants*, 255-260.
- Suzuki N., Mittler R. (2006). Reactive oxygen species and temperature stresses: a delicate balance between signaling and destruction. *Physiologia Plantarum*, 126, 45–51.
- Tavarini S., Pagano I., Guidi L., Angelini L. G. (2015). Impact of nitrogen supply on growth, steviol glycosides and photosynthesis in *Stevia rebaudiana* Bertoni. *Plant Biosystems*, 150, 953–962.
- Thomas S. C., Gale N. (2015). Biochar and forest restoration: a review and meta-analysis of tree growth responses. *New Forests*, 46, 931–946.
- Timperio A. M., Egidì M. G., Zolla L. (2008). Proteomics applied on plant abiotic stresses: Role of heat shock proteins (HSP). *Journal of Proteomics*, 71, 391–411.
- Tranchida-Lombardo V., Mercat F., Avino M., Punzo P., Fiore M. C., Poma I., Patanè C., Guarracino M. R., Sunseri F., Tucci M., Grillo S. (2018). Genetic diversity in a collection of Italian long storage tomato landraces as revealed by SNP markers array. *Plant Biosystems*, 3, 1–10.
- Tripathi L. P., Sowdhamini R. (2006). Cross genome comparisons of serine proteases in *Arabidopsis* and rice. *BMC Genomics*, 7, 200.
- Trupiano D., Coccozza C., Baronti S., Amendola C., Vaccari F. P., Lustrato G., Di Lonardo S., Fantasma F., Tognetti R., Scippa G. S. (2017). The effects of biochar and its combination with compost on lettuce (*Lactuca sativa* L.) growth, soil properties, and soil microbial activity and abundance. *International Journal of Agronomy*, 2017, 1–12.
- Trupiano D., Di Iorio A., Montagnoli A., Lasserre B., Rocco M., Grosso A., Scalonì A., Marra M., Chiatante D., Scippa G. S. (2012b). Involvement of lignin and hormones in the response of woody poplar taproots to mechanical stress. *Physiologia Plantarum*, 146, 39–52.
- Trupiano D., Renzoni G., Rocco M., Scalonì A., Viscosi V., Chiatante D., Scippa G. S. (2012). The proteome of *Populus nigra* woody root: response to bending. *Annals of Botany*, 110, 415–432.

- Trupiano D., Rocco M., Renzone G., Scaloni A., Rossi M., Viscosi V., Chiatante D., Scippa G. S. (2014). Temporal analysis of poplar woody root response to bending stress. *Physiologia Plantarum*, 150, 174–193.
- Vaccari F. P., Maienza A., Miglietta F., Baronti S., Di Lonardo S., Giagnoni L., Lagomarsino A., Pozzi A., Pusceddu E., Ranieri R., Valboa G., Genesio L. (2015). Biochar stimulates plant growth but not fruit yield of processing tomato in a fertile soil. *Agriculture Ecosystems and Environment*, 207, 163–170.
- Viger M., Hancock R. D., Miglietta F., Taylor G. (2015). More plant growth but less plant defence? First global gene expression data for plants grown in soil amended with biochar. *GCB Bioenergy*, 7, 658–672.
- Walkley A., Black I. A. (1934). An examination of the Degtjareff method for determining soil organic matter, and a proposed modification of the chromic acid titration method. *Soil Science*, 37, 29–38.
- Wang W., Vinocur B., Shoseyov O., Altman A. (2004). Role of plant heat-shock proteins and molecular chaperones in the abiotic stress response. *Trends of Plant Science*, 9, 244–52.
- Wright I. J., Reich P. B., Westoby M., Ackerly D. D., Baruch Z., Bongers F., Cavender-Bares J., Chapin T., Cornelissen J. H. C., Diemer M., Flexas J., Garnier E., Groom P. K., Gulias J., Hikosaka K., Lamont B. B., Lee T., Lee W., Lusk C., Midgley J. J., Navas M.-L., Niinemets U., Oleksyn J., Osada N., Poorter H., Poot P., Prior L., Pyankov V. I., Roumet C., Thomas S. C., Tjoelker M. G., Veneklaas E. J., Villar R. (2004). The worldwide leaf economics spectrum. *Nature*, 428, 821–827.
- Xu G., Zhang Y., Sun J., Shao H. (2016). Negative interactive effects between biochar and phosphorus fertilization on phosphorus availability and plant yield in saline sodic soil. *Science of the Total Environment*, 568, 910–915.
- Yang X., Finnegan P. M. (2010). Regulation of phosphate starvation responses in higher plants. *Annals of Botany*, 105, 513–26.

Chapter III

The Interplay of LED Spectra and Biochar in *Arabidopsis columbia* and *Pisum sativum* L. Morpho-Physiological Traits

Polzella Antonella^a, Terzaghi Mattia^b, Trupiano Dalila^a, Baronti Silvia^c, Scippa
Gabriella Stefania^a, Chiatante Donato^b, Montagnoli Antonio^b

^aDepartment of Biosciences and Territory, University of Molise, 86090 Pesche, IS,
Italy.

^bDepartment of Biotechnology and Life Science, University of Insubria, 21100
Varese, VA, Italy.

^cInstitute of Biometeorology, National Research Council (IBIMET-CNR), 50145
Firenze, FI, Italy.

A part of this chapter concerning the results of morpho-physiological traits of *Pisum sativum* has been submitted for publication on a peer review journal as follows:

The Interplay of LED Spectra and Biochar in *Pisum sativum* L.
Morpho-Physiological Traits and Fruit Yield

Abstract

Nutrient availability and light are the primary factors for plant growth and development. In a research context of the best indoor cultivation practice, light-emitting diodes (LEDs) lighting systems together with biochar could represent a combined green strategy boosting indoor plant cultivation and contributing to the mitigation of climate change. So far, studies investigating the effect of different spectra on plant morpho-physiology are not exhaustive and none of them analysed the interplay with biochar. In the present study, we investigated the effect of three different light spectra provided by LEDs and a fluorescent reference (control) on the morphological traits of *Arabidopsis columbia* and *Pisum sativum* L. seedlings grown in the presence and in absence of biochar. We also tested the plant photosynthetic machinery efficiency and stomatal activity by the analysis of chlorophyll fluorescence emission and stomatal conductance of pea seedlings. We found that all morpho-physiological traits are sensitive to changes in R:FR ratio which is different for light spectra we used. In particular, seedlings that were grown with AP67 LED lighting type characterized by the lowest R:FR ratio, showed the best plant performance, which in turn was further improved with biochar presence. Our results suggest that although AP67 has a negative impact only on the PSII yield when biochar is added to soil a kind of compensation occurs. Therefore, there is a synergic effect between biochar and AP67 that positively affects the plant growth and development, such that it could be considered as a strategy for plant production within the limits of respect for the environment.

Keywords: Chlorophyll fluorescence, Climate change, Pea seedlings, Photomorphogenesis, Soil Amendment, Stomatal conductance.

3.1 Introduction

In the future, it will be crucial to find new methods and technologies for indoor plant production with lower global environmental impacts. To select optimal plant production systems depending on their purposes and based on the experimental ground, it is increasingly needed to maintain the overall sustainability of society under changing the climate and social conditions (Kozai *et al.*, 2016). Among many requirements for plant growth and development, light plays a key role in

different processes such as photosynthesis, plant defense and phototropism (Ballaré, 2014). To provide the best fitness, plants developed morpho-physiological strategies to use the receipt light. Indeed, thanks to the photoreceptors such as phytochromes, cryptochromes, and phototropins, plants are able to use a light characterized by a different quality, quantity, and direction (Batschauer, 1999). Light sources such as fluorescent, metal halide, high-pressure sodium (HPS), and incandescent lamps are used as conventional light sources for growing plants in indoor cultivation (Jeong *et al.*, 2012; Ouzounis *et al.*, 2014). All these different types of the artificial light source can modify the photosynthetic photon flux (PPF) levels (Chen *et al.*, 2005; Kopsell *et al.*, 2017; Krizek *et al.*, 1998; Mohammed *et al.*, 2014) through the variation in quality and quantity of light. Plants respond to irradiance change through specific photomorphogenic and physiological processes at different scale, leading to a wide range of modifications such as improvement of antioxidant activity in pea (Wu *et al.*, 2007), growth in tomato (Gómez and Mitchell, 2015), and metabolism in mint, basil, lentil, primula and marigold (Mohammed *et al.*, 2014). Higher rates of growth as well as photosynthetic and transpiration activity have been observed in cucumber (Hernández and Kubota, 2016). Moreover, root growth showed significant changes in grape and seedlings of different tree species (Montagnoli *et al.*, 2018; Poudel *et al.*, 2008), anthocyanin content was suppressed in lettuce (Stutte and Edney, 2009), and a delayed or inhibited plant transition to flowering was observed in Indian mustard and basil (Tarakanov *et al.*, 2012). As a result, artificial light sources can provide a strong modification of plant growth in terms of quantity and quality due to the properties of each light type used. The most efficient photosynthetic yield occurs in two distinct broad peaks: in the blue (400–500 nm) and in the red (600–700 nm) ranges (McCree, 1972). In particular, photons in the 500–600 nm range are characterized as having low photosynthetic efficiency, while photons in the 700–800 nm range are considered far-red (FR), which is important for shoot elongation in woody plants modulated by the ratio of red-to-far-red (R:FR) (Apostol *et al.*, 2015; Smirnakou *et al.*, 2017). Although these light sources, especially HPS, are the most commonly used lighting systems, their emissions, both spectrally and energetically, show values far from the optimal ones to perform the photosynthetic process (Darko *et al.*, 2014; Heuvelink *et al.*, 2006). Light-emitting diode (LED) light has the highest PAR efficiency (~ 90%) and it has a monochromatic spectral specificity with possible peak emission wavelengths from ~ 250 (UV) to ~ 1000 nm (infrared). Not surprisingly, in the last decades, solid-state lighting using LED technology has arisen as an alternative source as greenhouse lighting

systems for a series of advantages such as: longer lifetime (about 100 000 h), smaller volume and weigh, solid-state construction, lower heat emission and higher energy-conversion efficiency (Bourget, 2008; Landis *et al.*, 2013). Additionally, specific wavelengths within a narrow spectral range can be set with LEDs with the aim of precisely tuning spectral quality and light intensity (Heuvelink *et al.*, 2006; Ouzounis *et al.*, 2014). In recent years, the use of LEDs as a radiation source for plants has attracted considerable interest because of its vast potential for developmental studies as well as for its commercial applications (Bian *et al.*, 2015; Yeh *et al.* 2015). Thus, the selection of an optimal light source is an essential task in closed plant production systems fully relating to artificial light sources (Kozai *et al.*, 2006).

For closed plant production, it is also crucial to use soil characterized by the highest nutrient availability. Biochar is a natural charcoal obtained by a controlled pyrolysis of organic materials (e.g. agricultural and forest residuals). The process occurs at a very high-temperature range (600-900 °C) and in an oxygen-deficient environment (Hodgson *et al.*, 2016). Biochar considered as a novel and practical approach in the bio-waste treatment and pollution remediation (Fang *et al.*, 2015; Yan *et al.*, 2015). Depending on the process parameters, including primary temperature and feedstock type, biochar shows different physical and structural characteristics (Lehmann *et al.*, 2015). However, the most common physical aspects are a highly porous structure and a large surface area (Atkinson *et al.*, 2010). For many years now, a number of studies have assessed the potential value of the biochar use as a soil amendment able to improve the soil structure and fertility as well as plant growth (Amendola *et al.*, 2017; Trupiano *et al.*, 2017). In particular, biochar showed to increase both soil carbon and soil water content as well as macroaggregates, electrical conductivity (EC), total nitrates/nitrites, ammonia and nitrogen (Amendola *et al.*, 2017; Baronti *et al.*, 2010), extractable phosphorus and cation-exchange capacity (CEC) (Hossain *et al.*, 2010). Furthermore, due to its skeletal-sponge structure, biochar reduces soil leaching of ammonium (Lehmann *et al.*, 2003), improves rhizosphere microbial communities and activities with particular regards to both cellulose degrading and nitrogen-fixing bacteria (Lehmann *et al.*, 2011). At the same time, the use of biochar can be considered as a mean for mitigating greenhouse gas (GHG) emissions enhancing important functions such as soil carbon sequestration and nitrogen soil retention that increasingly contribute to the current global climate change. For these reasons, biochar is becoming a good technological product for a future sustainable plant production (D'Alessandro *et al.*, 2010; Solomon *et al.*, 2007). Unfortunately, the effects of the amendment on

plant production, including crops and forest restoration activities (Dumroese *et al.*, 2018), vary extremely, it depends on type of soil, quantity of used biochar, local conditions and/or plant species. Thus, there is still a need to test the effects of this amendment on plant functional traits to give indications for a future commercial use.

The possible role of the interplay of an optimal light spectrum sourced by LED and a natural amendment product such as biochar could help to boost the development of low environmental impact technologies for indoor plant production system. However, so far, along with the effects on plant performance of LED light spectra and biochar considered separately, also their interplay is still unknown. For these reasons, in the present study, we wanted to investigate the responses of *Arabidopsis columbia* and *Pisum sativum* L. as fast-growing model plants to different light spectra provided by LEDs. We also hypothesized that biochar application will enhance plant performance independently of the light spectra applied. To accomplish this aim, morphological and morpho-physiological traits were measured in *Arabidopsis* and pea seedlings respectively grown in controlled conditions, in pots with commercial soil as control and in other pots with soil plus biochar and with three different LED light spectra and a fluorescent reference (control).

3.2 Materials and Methods

3.2.1 Plant Material and Experimental Setup

Wild-type seeds of *Arabidopsis Columbia* were provided from Institute of Biotechnology of University of Helsinki, Finland. Seeds of *Pisum sativum* L. (medium-late variety, medium-height plant; long, dark green pod with 8-9 seeds; large, wrinkled seed with dark green integument by “Sementi Dotto”) were obtained from a commercial nursery (Varese – Italy). Three and one seeds of *Arabidopsis* and pea respectively were sown in 2 L cylindrical pots (h 15 cm, Ø 11 cm lower and upper Ø 16 cm) filled with 1:2:1 mixture of peat, silica sand, and bark humus and placed in a growth chamber. *Arabidopsis* seedlings after germination were not thinned. In treated pots, the soil was mixed with biochar at a rate of 30 t ha⁻¹ according to Baronti *et al.* (2010). Commercial soil and biochar were mixed in a large box and plastic pots were filled with this mixture. When the leaves of *P. sativum* were fully expanded (from the 27th day after sowing), the emission of

chlorophyll fluorescence and stomatal conductance were measured each 4 days interval until the 43rd day after sowing. Instead of the leaves of Arabidopsis seedlings that were not expanded and detectable by the instruments. Both Arabidopsis and pea seedlings were destructively sampled 49 days after sowing for morphological traits described below (Fig. 3.1). Irrigation frequency was determined gravimetrically: we watered the soil medium until saturation, measured an initial mass, and then irrigated back to saturation when container mass reached 60% of initial mass (Dumroese *et al.*, 2015). No fertilizer was added.

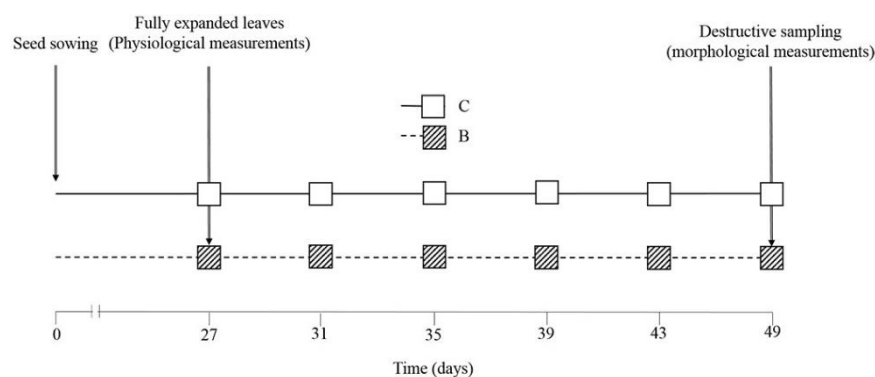


Figure 3.1. The experimental design for physiological and morphological measurements in control (C; solid line □) and biochar treated (B; dashed line ▨) seedlings. Each number corresponds to the sampling date.

3.2.2 Growth Room Characteristics

To perform the experiment a single 4-m wide, 3-m deep and 2.2-m tall growth room at the University of Insubria, Varese (Italy) was used. The room was subdivided into four sections with reflective white panels. Each section was illuminated with either fluorescent light (FLUORA T8 (OSRAM); LEDVANCE GmbH; Garching, Germany) as reference (control) light, or one of three different, commercially available LED light spectra developed specifically for horticultural purpose (Valoya Oy; Helsinki, Finland): NS1, AP67-3L, and AP67 (Table 3.1). Each section had a steel table with 50-mm tall edges. Light intensity yielded approximately $150 \mu\text{mol m}^{-2} \text{s}^{-1}$ (Light Meter sensor – HD2302.0 – Delta Ohm; Caselle di Selvazzano, Italy) at pots height. Temperature and air humidity were maintained at 22 °C and 60–70%, respectively with a photoperiod of 16 h per day.

Light source		Continuous spectrum wave length (nm)				R:FR
		400-500	500-600	600-700	700-800	
		----- (%) -----				
Fluorescent	Fluora T8	34.8	24.1	36.7	4.4	5.7
	NS1	20.2	38.9	35.7	5.2	8.2
LED	AP67-3L	11.9	19.3	60.5	8.3	5.6
	AP67	13.8	15.1	53.0	18.1	2.7

Table 3.1. Spectral distribution and red:far-red of the fluorescent (control) light and the three LED light treatments.

3.2.3 Biochar Characterization

Biochar used in this study was produced by Romagna Carbone s.n.c. (Bagnacavallo, RA, Italy) from orchard pruning biomass through a slow pyrolysis process with an average residence time of 3 h at 500 °C in a kiln of 2.2 m in diameter and holding around 2 ton of feedstock. Measurement of pH was carried out by pH meter (pH 700 pH/mV/°C/°F Bench Meter, Eutech Instruments, Oakton, United States, 2013) according to IBI standards (2014). The electrical conductivity (EC) value was obtained by the direct instrumental determination in 1:20 soil: water (w/v) extracts, according to IBI standards (2014). Cation exchange capacity (CEC) was assessed according to Mehlich (1938) using BaCl₂. Moisture content was calculated according to the Black method (1965) as the difference in sample weight before and after oven drying at 105 °C to constant weight. Several parameters can be used to assess carbon stability in biochar. Calvelo Pereira *et al.* (2011) used the thermo-labile fraction and the oxidation efficiency with potassium permanganate and potassium dichromate, while Enders *et al.* (2012) used a combination of volatile matter and H:C ratios corrected for inorganic C. In the present work, we referred to IBI standards (2014), which define carbon stability as the molar ratio of hydrogen to organic carbon (maximum 0.7). Total nitrogen (N_{tot}), total carbon (C_{tot}), organic carbon (C_{org}) and hydrogen (H) contents were determined by dry combustion (Dumas, 1831) using a CHN elemental analyzer (Carlo Erba Instruments, NA-1500, series 2, Milan, Italy). In the case of C_{org}, combustion was carried out after

the complete removal of inorganic C with acid. Available nitrogen (N_{av}) was determined by a modified Kjeldahl procedure using Devarda's alloy (Liao, 1981) as reducing agent to convert (NO_3) and (NO_2) into (NH_4)⁺ and subsequent Kjeldahl digestion. Total phosphorus (P_{tot}) was detected by spectrophotometry (UV-1601 Shimadzu, Japan) according to the test method described by Bowman (1988). Available phosphorus (P_{av}) was extracted by a $NaHCO_3$ solution at pH 8.5 and evaluated by spectrophotometry according to the Olsen test method (1954). The alkalinity of samples with a pH value greater than 7.0 was determined by titrimetry according to the Higginson and Rayment method (1992).

3.2.4 Soil Characterization

To assess soil chemical-physical properties and the effects of biochar on these characteristics, four soil samples were collected and analyzed before and after biochar application. Methods for the characterization of CEC, P_{tot} and P_{av} , N_{tot} and N_{av} , C_{tot} were described in the previous paragraph of the biochar characterization. The pH was determined by potentiometry (pH meter Eutech Instruments pH 700, 2013) according to Conyers and Davey (1988). EC was measured by direct instrumental determination according to Rhoades (1996). The different forms of available mineral nitrogen were determined by ion selective electrodes (Greenberg *et al.*, 1982) on soil samples dissolved in deionized water.

3.2.5 Morphological Measurements

The stem length (SL; cm) and lateral branches length (LBL; cm) of both plant species were measured dissecting stem and branches and scanning them with a portable scanner (model). Images were then analyzed by Image J software. The number of lateral branches (LBN; no.) of both Arabidopsis and pea seedlings was counted. Leaf area for each Arabidopsis and pea seedling was measured by scanning and analysis using WinRHIZO software (Pro V. 2007d; Regent Instruments Inc.; Ville de Québec, Québec, Canada) and summed to obtain total leaf area (TLA; cm^2). The number of leaves per each rosette (LRN; no.) and flowers (FN; no) of each Arabidopsis seedlings was counted. After gently removing each seedling from the medium, roots were rinsed repeatedly with running tap water and scanned (400 dpi) with a calibrated flatbed scanner coupled

to a lighting system for image acquisition (Expression 10000 XL; Epson America Inc.; Long Beach, California, USA). Total fine root length (FRL; cm) of both plant species and fine root mean diameter (FRD; cm) of only pea seedlings were obtained measuring only lateral roots by WinRHIZO and excluding the taproot. Afterward, biomass (g) of leaves (LDM), fruit (FDM) of only pea seedlings and fine roots (FRDM) of both Arabidopsis and pea seedlings were calculated as dry mass after oven drying 52 h at 75 °C. Finally, we calculated the specific fine root length (length to mass ratio; SFRL) and the fine root tissue density (mass to volume ratio; FRTD) of both Arabidopsis and pea.

3.2.6 Physiological Measurements

Chlorophyll fluorescence was measured with a portable pulse-modulated fluorometer (OS1-FL, Opti-sciences, inc. USA) on one fully expanded leaf randomly selected from each pea seedling. The maximum quantum efficiency of PSII photochemistry for chlorophyll fluorescence in dark-adapted $[(F_v/F_m) = (F_m - F_0) / F_m]$ was detected in the forenoon (10-11 AM) pre-darkening the upper layer of the leaf with a leaf clip for 45 min to ensure complete relaxation of all reaction centers. The maximum efficiency of PSII photochemistry in the light $[\Phi_{PSII} = (F_{ms} - F_s) / F_{ms}]$ was detected in the afternoon (3-4 PM). Finally, non-photochemical quenching $[NPQ = (F_m - F_{ms}) / F_{ms}]$ was calculated (Maxwell and Johnson, 2000). Stomatal conductance (g_s ; $\text{mmol m}^{-2} \text{sec}^{-1}$) was measured using a steady state porometer (PMR 3, PPSsystem, MA, USA) between 2 and 3 PM. When seedlings were harvested for destructive measurements, 2.5 g of fresh weigh leaf tissues were sampled for control and biochar-treated seedlings and for each of the light spectra and then stored at -80 °C. Pigments measurement was performed according to Arnon's method (1949). In particular, Chlorophylls (Chl *a*; Chl *b*; Chl *a + b*) and carotenoids (*Car*) were extracted from 0.25 g leaf tissue using 80% acetone as a solvent. The pigment concentrations were determined by spectrophotometer (BioRad) and using the following equations (1-4):

$$\text{Chl } a = 12.70_{A663} - 2.69_{A645} \quad (1)$$

$$\text{Chl } b = 22.90_{A645} - 4.68_{A663} \quad (2)$$

$$\text{Chl } a + b = 20.20_{A645} + 8.02_{A663} \quad (3)$$

$$\text{Car} = (1000_{A470} - 1.82_{[\text{Chl } a]} - 85.02_{[\text{Chl } b]}) / 198 \quad (4)$$

where A is absorbance in 1.00 cm cuvettes and Chl is $\mu\text{g mL}^{-1}$.

3.2.7 Statistical Analysis

To evaluate significant differences between the influence of biochar and light type, three comparisons for each morphological and physiological measured parameter were performed: (a) control and biochar-treated plants grown with same lighting treatment, (b) control plants grown with different lighting treatment, (c) biochar-treated plants grown with different lighting treatment. Data were analyzed with a two-tailed T-test with a significance level of 95% ($p < 0.05$).

3.3 Results

3.3.1 Biochar and Soil Characteristics

Parameter	Unit	Value
pH	-	9.7 ± 0.1
EC	dS m^{-1}	7.5 ± 0.4
CEC	Cmol kg^{-1}	21.3 ± 0.3
N_{tot}	g kg^{-1}	9.1 ± 0.2
N_{av}	mg kg^{-1}	30 ± 0.4
P_{tot}	mg kg^{-1}	1221.9 ± 21.3
P_{av}	mg kg^{-1}	217 ± 3.0
C_{tot}	g kg^{-1}	778.1 ± 0.1
C_{org}	g kg^{-1}	705.6 ± 0.1
H	g kg^{-1}	45.3 ± 0.2
H/C_{org}	-	0.76

Table 3.2. Biochar chemical-physical characteristics. Each value represents the mean ($n = 8$) \pm SE.

The biochar tested was found to meet the European Biochar Certificate (EBC, 2012) and IBI-Standard (2014) requirements with regard to C_{tot} and C_{org} content, respectively. Its C : H value, close to 0.7, ensures a good stability to the organic carbon. With regard to the conductivity value, the biochar used showed a higher salt content compared to soil. Moreover, available phosphorus and nitrogen represented 17.7% and 0.3% of total phosphorus and nitrogen, respectively (Table 3.2). Soil chemical analysis showed that biochar addition resulted in an increase of N_{av} and C_{tot} values, while pH, EC, CEC, N_{tot} , P_{tot} , and P_{av} were unchanged (Table 3.3).

Parameter	Unit	Soil	Soil+Biochar
pH	-	6.6 ± 0.07a	6.69 ± 0.07a
EC	dS m ⁻¹	0.9 ± 0.3a	0.9 ± 0.3a
CEC	Cmol kg ⁻¹	18 ± 0.87a	19 ± 0.92a
N_{tot}	g kg ⁻¹	13 ± 1.23a	15 ± 1.42a
N_{av}	mg kg ⁻¹	120 ± 4.8a	140 ± 5.6b
P_{tot}	mg kg ⁻¹	456.6 ± 16.7a	484.1 ± 18a
P_{av}	mg kg ⁻¹	40.41 ± 2.22a	42.44 ± 2.33a
C_{tot}	g kg ⁻¹	23 ± 0.55a	26 ± 0.63b

Table 3.3. Chemical-physical analysis performed on soil samples of control and biochar-treated pots. Each value represents the mean of (n=6) ±SE. Different letters within sampling time for each species indicate significant differences among light treatments at $p < 0.05$.

3.3.2 Morphological Traits of *Arabidopsis*

Seedlings of *Arabidopsis* grown in control media with AP67 were taller (stem length; SL) than those grown with AP67-3L while with the other spectra there were not significant differences among themselves and among biochar-treated seedlings. Biochar alone did not affect SL (Table 3.4). Control seedlings did not show significant differences of lateral branches length (LBL) among light treatments, biochar-treated seedlings grown with fluorescent lamp had LBL

significantly higher than those grown with NS1 and AP67-3L. Biochar application did not affect LBL (Table 3.4). Seedlings grown in control media with NS1 and AP67 showed higher lateral branches number (LBN) than those grown with fluorescent lamp, while biochar-treated seedlings grown with AP67 showed higher LBN than those grown with fluorescent lamp. Biochar application increased LBN in seedlings grown with fluorescent lamp (Table 3.4). Leaf rosette number (LRN) was higher in seedlings grown with AP67-3L than those grown with fluorescent lamp and NS1 in control and biochar-amended media respectively. Biochar application decreased LRN in seedlings grown with NS1 and AP67-3L (Table 3.4). Total leaf area (TLA) was higher in control seedlings grown with NS1 than those grown with fluorescent lamp and AP67, which were not significantly different among themselves, both control and biochar-treated seedlings grown with AP67-3L showed the lowest TLA value. Biochar application decreased TLA in seedlings grown with fluorescent lamp, NS1 and AP67 (Table 3.4). Control seedlings grown with AP67 had more flowers (flower number; FN) than those grown with fluorescent lamp which in turn had more flowers than those grown with NS1 and AP67-3L which were not significantly different among themselves. While seedlings grown in biochar-amended media with AP67 had more flowers than those grown with AP67-3L. FN decreased in seedlings grown with fluorescent lamp and AP67 by biochar application (Table 3.4). Fine root length (FRL) for seedlings grown with control media was the lowest value with NS1, while biochar-treated seedlings had higher FRL value with AP67 than those grown with fluorescent lamp and NS1 which were not significant differences among themselves. Biochar application significantly decreased FRL in seedlings grown with all light spectra except for NS1 (Table 3.4). Fine root volume (FRV) had the lowest value in control seedlings grown with NS1 while FRV had higher value in biochar-treated seedlings grown with AP67 than those grown with fluorescent lamp. Biochar application increased and decreased FRV in seedlings grown with NS1 and fluorescent lamp and AP67 together (Table 3.4). Fine root dry mass (FRDM) was higher in control seedlings grown with fluorescent lamp and AP67 than those grown with NS1, while biochar-treated seedlings grown with AP67-3L showed the lowest FRDM value (Table 3.4). Specific fine root length (SFRL) measured in seedlings grown in control and in biochar-amended media showed the greatest and the lowest values with AP67-3L and NS1, fluorescent lamp and NS1, respectively. Biochar application increased and decreased SFRL of seedlings grown with fluorescent lamp and AP67-3L respectively (Table 3.4). Seedlings grown in control media with NS1 showed higher fine root tissue density (FRTD) value than those grown

with fluorescent lamp and AP67 which were not significantly different among themselves. There were no significant differences among biochar-treated seedlings with light spectra and by biochar application (Table 3.4).

Parameter	Units	Light Source				
		Control (C)	Fluorescent		LED	
			Biochar (B)	Fluora T8	NS1	AP67-3L
SL	cm	C	14.9 (1.36) ab	14.6 (1.95) ab	12.7 (0.65) b	15.7 (0.52) a
		B	15.0 (0.93) x	13.5 (0.19) x	13.8 (0.43) x	15.4 (2.23) x
LBL	cm	C	13.2 (0.75) a	5.91 (0.58) b	5.04 (0.63) b	11.7 (1.15) a
		B	9.89 (1.09) x	5.28 (0.53) y	5.47 (1.16) y	7.84 (1.27) xy
LBN	no.	C	0.90 (0.05) b	2.67 (0.33) a	1.94 (0.43) ab	2.08 (0.42) a
		B	1.89 (0.11) y	2.22 (0.36) xy	2.44 (0.29) xy	2.57 (0.10) x
LRN	no.	C	41.0 (3.79) b	51.0 (4.04) ab	60.3 (4.81) a	46.0 (3.61) ab
		B	37.3 (4.48) xy	36.0 (1.53) y	43.7 (1.67) x	39.0 (1.00) xy
TLA	cm ²	C	36.5 (0.89) b	59.7 (2.65) a	15.5 (2.53) c	44.22 (3.38) b
		B	32.3 (0.97) x	36.4 (3.83) x	14.0 (1.32) y	31.24 (0.67) x
FN	no.	C	12.3 (0.33) b	8.67 (0.33) c	7.33 (0.88) c	21.3 (2.33) a
		B	9.00 (0.58) xy	7.33 (1.45) xy	7.00 (0.58) y	10.7 (0.33) x
FRL	m	C	14.2 (0.75) a	5.26 (0.74) b	11.4 (1.23) a	14.1 (0.27) a
		B	5.49 (0.60) y	4.69 (0.68) y	6.69 (0.68) xy	7.80 (0.40) x
FRV	cm ³	C	0.39 (0.03) a	0.06 (0.02) b	0.24 (0.04) a	0.32 (0.01) a
		B	0.12 (0.01) y	0.14 (0.01) xy	0.19 (0.03) xy	0.17 (0.005) x
FRDM	g	C	0.03 (0.003) a	0.01 (0.001) b	0.02 (0.01) ab	0.02 (0.005) a
		B	0.01 (0.001) y	0.004 (0.002) y	0.02 (0.003) x	0.01 (0.002) y
SFRL	m g ⁻¹	C	2996 (69.6) b	937 (79.1) c	7100 (902) a	2943 (358) b
		B	4780 (565) x	1038 (53.9) z	1876 (283) y	2475 (26.1) y
FRTD	g cm ⁻³	C	0.23 (0.05) b	0.54 (0.04) a	0.29 (0.08) ab	0.33 (0.03) b
		B	0.18 (0.03) x	0.35 (0.08) x	0.30 (0.05) x	0.24 (0.05) x

Table 3.4. Morphological measurements (means ± SE) on control (n=6) and biochar treated (n=6) seedlings of *Arabidopsis columbia* grown under one fluorescent (control) and three LED spectra.

Bold values indicate statistically significant differences between control and biochar-treated plants in the same lighting treatment ($p < 0.05$). a, b, c indicate statistically significant differences among lighting type within control plants ($p < 0.05$). x, y, z indicate statistically significant differences among lighting type within biochar-treated plants ($p < 0.05$). SL stem length, LBL lateral branches length, LBN lateral branches number, LRN leaf rosette number, TLA total leaf area, FN flower number, FRL total fine roots length, FRV total fine root volume, FRDM fine root dry mass, SFRL specific fine roots length, FRTD fine roots tissue density.

3.3.3 Morphological Traits of *P. sativum*

Seedlings of *P. sativum* grown in control media were taller (stem length; SL) with NS1 than those grown with a fluorescent lamp (control), while they had the same value with AP67-3L and AP67 which were not significantly different among themselves. For seedlings grown in biochar-amended soil, SL was greater with AP67-3L and AP67, than control and NS1. Biochar application increased and decreased SL in seedlings grown with AP67-3L and AP67, and NS1, respectively (Table 3.5). For lateral branches length (LBL), seedlings grown in control media had the greatest and lowest value with AP67 and NS1 respectively. Seedlings grown with AP67-3L had not lateral branches as well as those grown with a fluorescent lamp and in biochar-amended media (Table 3.5). Lateral branches number (LBN) was the same among light treatments and independently on biochar application (Table 3.5). Total leaf area (TLA) was the greatest for seedlings grown with AP67-3L and AP67 and the lowest for both fluorescent and NS1. In biochar-amended media, seedlings did not show significant differences among the light treatments. Biochar application increased and decreased TLA in seedlings grown with NS1 and AP67, respectively (Table 3.5). Fine root length (FRL) for seedlings grown with control media was the greatest and the lowest value with fluorescent and both NS1 and AP67, respectively, while seedlings grown with AP67-3L showed intermediate values. Biochar-treated seedlings had the greatest FRL value with AP67 while with the other spectra there were not significant differences among themselves. Biochar application significantly increased FRL only in the case of AP67 (Table 3.5). Fine root diameter (FRD) was not affected by both light spectra and biochar application (Table 3.5). Leaf dry mass (LDM) was the greatest and the lowest value in seedlings grown with AP67 and NS1, respectively. Seedlings grown with fluorescent and AP67-3L had intermediate values. Biochar application did not affect LDM among different spectra (Table 3.5). Fruit dry mass (FDM) was the greatest and the lowest value with AP67-3L and NS1, respectively. Both fluorescent and AP67 had intermediate values. Biochar application significantly increased FDM value in the case of control and AP67 (Table 3.5). Fine root dry mass (FRDM) was the greatest value for both control and AP67, while it was an intermediate value with NS1 and AP67-3L. Seedlings grown in biochar-amended media showed similar values among light spectra except for AP67-3L, which had the lowest value. Biochar application did not affect FRDM value among light spectra (Table 3.5). Specific fine root length

(SFRL) measured in seedlings grown in control media showed the greatest and the lowest values with AP67-3L and NS1, respectively. Seedlings grown in biochar-amended media showed the same values among light spectra except for NS1, which had the lowest value. Similarly, seedlings grown in biochar-amended media showed the same pattern. Biochar application did not affect SFRL values within each light spectrum (Table 3.5). Fine root tissue density (FRTD) had the same value among spectra in the case of seedlings grown in control media. Biochar-treated seedlings had similar values among light spectra except for AP67, which had the lowest value. Biochar application significantly increased FRTD only in the case of NS1 (Table 3.5).

Parameter	Units	Control (C) Biochar (B)	Light Source			
			Fluorescent	LED		
			Fluora T8	NS1	AP67-3L	AP67
SL	cm	C	110 (7.01) b	154 (8.84) a	138 (13.3) ab	123 (9.31) ab
		B	127 (12.3) yz	122 (6.06) z	180 (5.40) x	159 (7.26) xy
LBL	cm	C	42.9 (7.57) ab	27.2 (1.12) b	-	69.2 (8.14) a
		B	-	52.5 (6.63) x	-	60.2 (8.02) x
LBN	no.	C	2.25 (0.48) a	2.25 (0.75) a	-	1.50 (0.50) a
		B	-	1.75 (0.48) x	-	1.50 (0.29) x
TLA	cm ²	C	431 (51.3) b	398 (51.5) c	542 (12.2) ab	587 (26.3) a
		B	460 (41.7) x	608 (63.0) x	523 (48.0) x	457 (19.6) x
FRL	m	C	69.9 (4.90) a	42.7 (5.38) b	50.3 (6.62) ab	52.6 (4.57) b
		B	56.0 (3.31) y	55.5 (4.15) y	42.2 (8.88) y	83.7 (4.56) x
FRD	cm	C	1.21 (0.03) a	1.29 (0.02) a	1.24 (0.03) a	1.29 (0.02) a
		B	1.24 (0.03) x	1.28 (0.03) x	1.23 (0.06) x	1.31 (0.01) x
LDM	g	C	2.12 (0.32) bc	2.03 (0.23) c	2.86 (0.25) ab	3.30 (0.12) a
		B	2.63 (0.33) x	2.36 (0.35) x	3.31 (0.31) x	2.90 (0.46) x
FDM	g	C	0.34 (0.06) b	0.05 (0.03) c	1.15 (0.03) a	0.50 (0.06) b
		B	0.91 (0.15) x	-	1.09 (0.22) x	1.05 (0.21) x
FRDM	g	C	0.19 (0.02) a	0.12 (0.01) b	0.12 (0.02) b	0.17 (0.03) ab
		B	0.17 (0.01) xy	0.16 (0.02) xy	0.12 (0.02) y	0.22 (0.02) x
SFRL	m g ⁻¹	C	1531 (11.3) b	1417 (39.7) c	1667 (14.0) a	1474 (46.3) abc
		B	1483 (40.1) x	1362 (22.2) y	1539 (60.2) xy	1469 (12.0) x
FRTD	g cm ⁻³	C	0.15 (0.01) a	0.13 (0.005) a	0.15 (0.01) a	0.13 (0.003) a
		B	0.16 (0.01) x	0.15 (0.004) x	0.14 (0.01) xy	0.13 (0.002) y

Table 3.5. Morphological measurements (means ± SE) on control (n=6) and biochar treated (n=6) seedlings of *Pisum sativum* grown under one fluorescent (control) and three LED spectra.

Bold values indicate statistically significant differences between control and biochar-treated plants in the same lighting treatment ($p < 0.05$). a, b, c indicate statistically significant differences among lighting type within control plants ($p < 0.05$). x, y, z indicate statistically significant differences among lighting type within biochar-treated plants ($p < 0.05$). SL stem length, LBL lateral branches length, LBN lateral branches number, TLA total leaf area, FRL total fine roots length, FRD fine root diameter, LDM leaf dry mass, FDM fruit dry mass, FRDM fine root dry mass, SFRL specific fine roots length, FRTD fine roots tissue density.

3.3.4 Physiological Traits

The maximum quantum efficiency of PSII photochemistry in dark-adapted conditions (F_v/F_m) measured at the first day after sowing (das; 27th), was not significantly different between seedlings grown in biochar and light treatments (Fig. 3.2a). At 31st das, control seedlings grown with NS1 showed the lowest F_v/F_m value compared to other light spectra. Biochar-treated seedlings grown with AP67 had the greatest F_v/F_m value than those grown with NS1 and AP67-3L (Fig. 3.2b). At 35th das, the only significant difference was for F_v/F_m greater in biochar-treated seedlings grown with AP67 than in seedlings grown with NS1 (Fig. 3.2c). F_v/F_m measured at 39th das was significantly greater in seedlings grown in biochar-amended soil with fluorescent lamp than those grown with NS1 (Fig. 3.2d). Biochar application did not affect the F_v/F_m pattern among different light spectra in all das (Fig. 3.2a, 3.2b, 3.2c, 3.2d) except for 43rd das when biochar application increased F_v/F_m value in seedlings grown with both control and AP67 (Fig. 3.2e). For the maximum efficiency of PSII photochemistry in light conditions (Φ_{PSII}), at 27th das, control seedlings grown with AP67 showed lower Φ_{PSII} values than those grown with other light spectra, which were not significantly different among themselves. Biochar-treated seedlings grown with control and NS1 showed greater Φ_{PSII} values than those grown with AP67-3L and AP67, which in turn had the greatest and the lowest Φ_{PSII} value respectively. Both control and biochar-treated seedlings within the same light spectrum did not show significant differences (Fig. 3.2f). At 31st das, both control and biochar-treated seedlings grown with AP67 showed the lowest Φ_{PSII} value compared to all other light spectra and independent on biochar application (Fig. 3.2g). Similarly, at 35th das, control seedlings grown with AP67 had the lowest Φ_{PSII} value compared to those grown with control and AP67-3L. While biochar-treated seedlings grown with AP67 had the lowest Φ_{PSII} value compared to all other light spectra (Fig. 3.2h). At 39th das, control seedlings grown with AP67 had the lowest Φ_{PSII} value compared to those grown with control and NS1. Biochar-treated seedlings grown with AP67 had the lowest Φ_{PSII} value compared to all other light spectra (Fig. 3.2i). Similarly to the

second das (31st; Fig. 3.2g), at the 43rd das both control and biochar-treated seedlings grown with AP67 showed the lowest Φ_{PSII} value compared to all other light spectra and independent on biochar application (Fig. 3.2j). Concerning the non-photochemical quenching pattern (NPQ), at 27th das, control seedlings did not show significant differences among light spectra. Biochar-treated seedlings grown with AP67-3L and AP67 showed greater NPQ values than those grown with control and NS1. Biochar application increased NPQ value only in seedlings grown with AP67-3L (Fig. 3.2k). At 31st das, no significant differences in both biochar and light treatments were detected. Similarly, at 35th das, no significant differences were detected except for control seedlings grown with AP67, which had the lowest NPQ value in comparison to control seedlings grown with other light spectra (Fig. 3.2l). At both 39th and 43rd das, no significant differences were detected for NPQ values in both biochar and light treatments (Fig. 3.2m and 3.2n). In terms of stomatal conductance (g_s ; Fig. 3.3), at 27th das, although control seedlings did not show significant differences, biochar-treated seedlings grown with AP67 showed higher g_s values only than to those grown with a fluorescent lamp (Fig. 3.3a). At 31st das, both control and biochar-treated seedlings did not show significant differences of g_s pattern among light spectra (Fig. 3.3b). g_s measured at 35th das had intermediate values, which were not significantly different in both control seedlings and light spectra. Biochar-treated seedlings grown with AP67 showed higher g_s values only than those grown with a fluorescent lamp (Fig. 3.3c). Similarly, at 39th das, control seedlings did not show significant differences among light spectra, while biochar-treated seedlings grown with AP67 and NS1 had greater g_s values only than those grown with a fluorescent lamp (Fig. 3.3d). At the 43rd das, only biochar-treated seedlings grown with AP67 showed significant higher g_s values than all other light spectra. Biochar application decreased the g_s value in seedlings grown with fluorescent and NS1 (Fig. 3.3e). From the analysis of chlorophyll extraction, no significant differences in Chl_a, Chl_b, Chl_{a+b}, and Car contents were detected (data not shown).

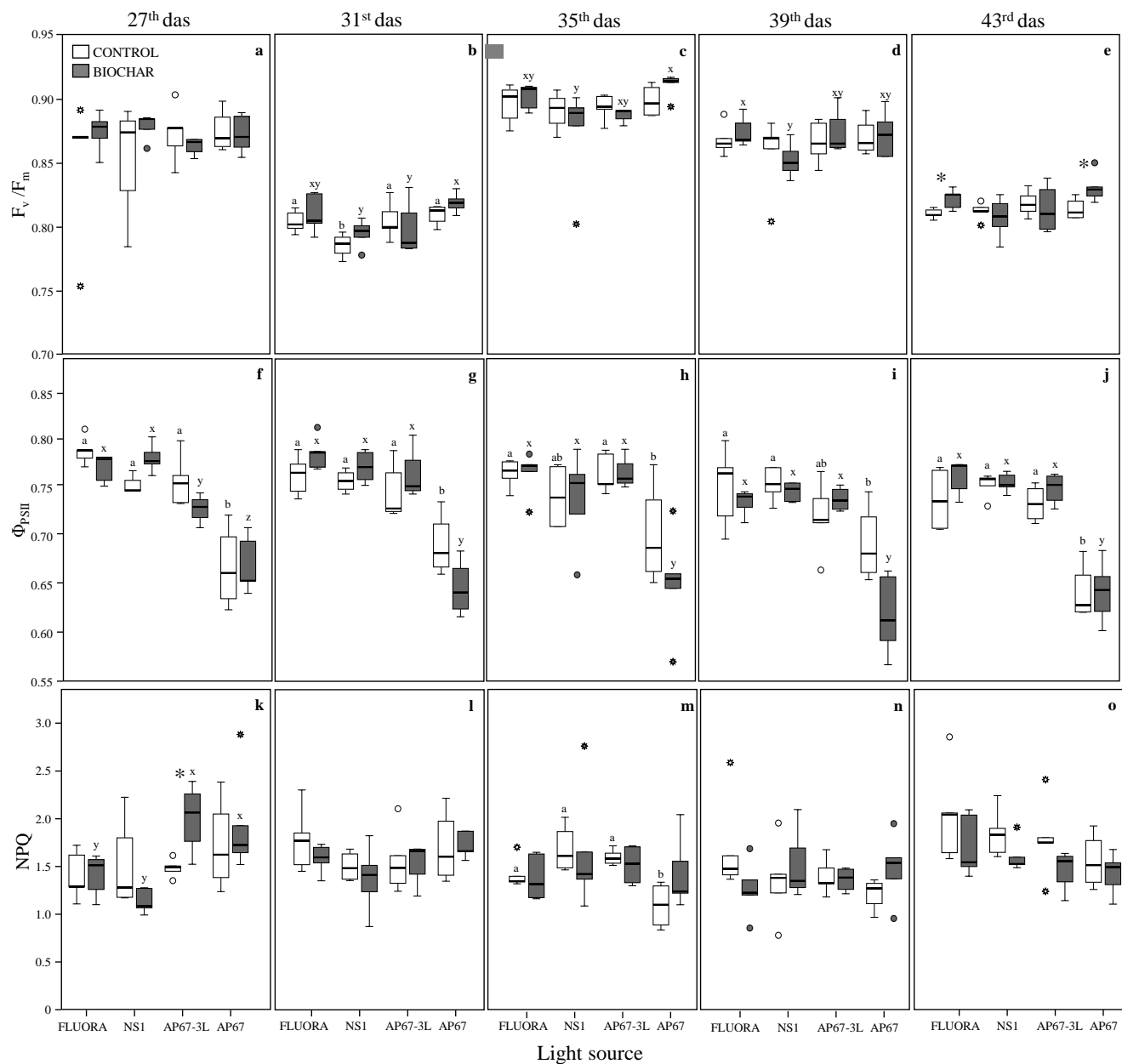


Figure 3.2. Trends of F_v/F_m , Φ_{PSII} and NPQ (rows) measured in five different days after sowing (das; columns) for seedlings grown in non- (*) and biochar-amended (■) soil and with the fluorescent (control) light and the three LED light spectra. Vertical boxes represent approximately 50% of the observations and lines extending from each box are the upper and lower 25% of the distribution. Outliers are represented as solid dots (•) and extremes are represented as stars. The solid, horizontal line in the center of each box is the median value, whereas the dotted horizontal line is the mean ($n=4$). The asterisk indicates statistically significant differences between control and biochar-treated plants in the same lighting treatment ($p < 0.05$). a, b, c indicate statistically significant differences among lighting type within control plants ($p < 0.05$). x, y, z indicate statistically significant differences among lighting type within biochar-treated plants ($p < 0.05$).

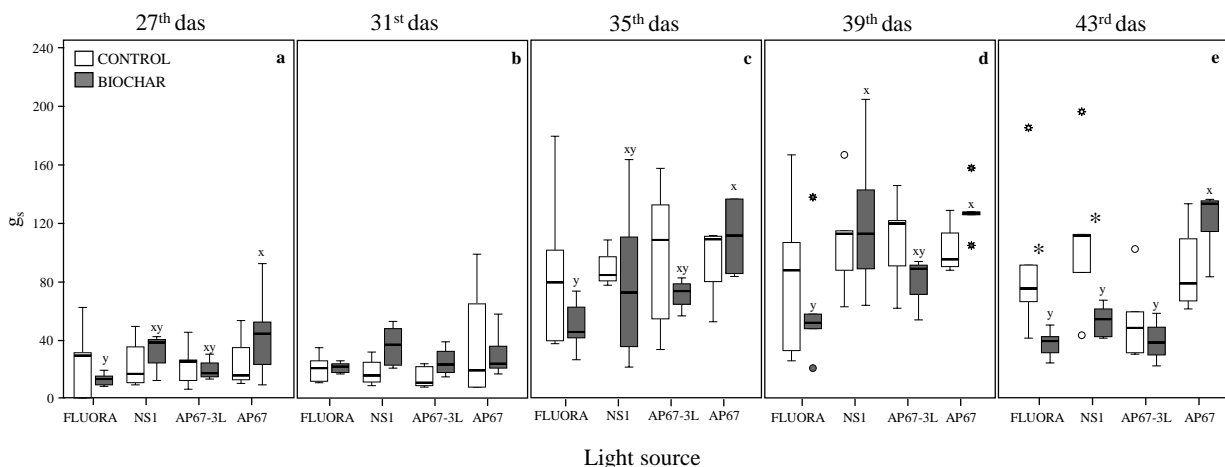


Figure 3.3. g_s pattern (row) detected in five different days after sowing (das; columns) for seedlings grown in non- (*) and biochar-amended (■) soil and with the fluorescent (control) light and the three LED light spectra. Vertical boxes represent approximately 50% of the observations and lines extending from each box are the upper and lower 25% of the distribution. Outliers are represented as solid dots (•) and extremes are represented as stars (*). The solid, horizontal line in the center of each box is the median value, whereas the dotted horizontal line is the mean (n=4). The asterisk indicates statistically significant differences between control and biochar-treated plants in the same lighting treatment ($p < 0.05$). a, b, c indicate statistically significant differences among lighting type within control plants ($p < 0.05$). x, y, z indicate statistically significant differences among lighting type within biochar-treated plants ($p < 0.05$).

3.4 Discussion

In the present work, we assessed morpho-physiological traits of *Arabidopsis columbia* and *P. sativum* seedlings in response to the interplay between biochar amendment and different light spectra provided by LED lighting systems. The two plant species showed different specific responses in relation to the biochar presence, as well as to the LED light spectra. We observed a general negative and positive effect on morphological traits of *Arabidopsis* and pea seedlings respectively grown with the presence of biochar. The negative biochar influence on *Arabidopsis* morphological traits could be attributable to the seedling efficiency in the element use. Although Akhatar *et al.* (2014) demonstrate the low N availability in soil, due to the biochar negative influence on plant NH_4^+ adsorption and uptake, we observed a higher N availability in soil that did not promote *Arabidopsis* growth. Additionally, the negative effect could be due to the modified soil availability of P, thus negatively affecting plant growth (Xu *et al.*, 2016). On the contrary the positive responses of pea seedlings are in accordance with Berihun *et al.* (2017), which related such variations in plant morphology to the improved soil characteristics once biochar was applied. Indeed, among many factors, organic matter (total carbon) and nitrogen content could have a

beneficial impact on soil quality (Bünemann *et al.*, 2018). In our study, together with a significant increase in total carbon and nitrogen availability measured in the biochar-amended soil, a higher fruit dry mass was detected. These findings are in line with previous studies that highlighted an indirect promotion of fruit productivity in relation to the biochar application (Berihun *et al.*, 2017; Eyles *et al.*, 2015; Olmo and Villar, 2018; Reganold *et al.*, 2010). Alternatively, Solaiman *et al.* (2012) ascribed the enhancement in the growth of beans by biochar application due to the increase of soil pH and nutrient availability. Beside soil characteristics, although not measured in this study, these results could be attributable to a different regulation of some genes involved in leaf expansion and the flowering process by the amendment presence (Viger *et al.*, 2015). Concerning the influence of LED light spectra, the analysis of morphological traits of both plant species highlighted different responses depending on the plant sector considered. In *Arabidopsis* seedlings we detected the general positive influence of AP67 similarly to the fluorescent lamp. While we noted a general stimulation of the above-ground part of the pea seedlings grown with AP67 and to a lesser extent with AP67-3L, which are characterized by the lowest R:FR ratio values. Many reports studied the effect of low R:FR values on several plant species, showing a more plant growth independently of the successional status (i.e. early or late) (Mølmann *et al.*, 2006; Montagnoli *et al.*, 2018; Smirnakou *et al.*, 2015). Moreover in nature, the low R:FR is an indication of shading by other plants, therefore it stimulates the elongation growth as a shade avoidance response and an adaptive advantage for competition (Casal, 2012; Franklin and Whitelam, 2005; Pedmale *et al.*, 2016). Additionally, we noted that biochar application reduced the stem length and promoted the elongation of lateral branches as well as the leaf area of pea seedlings grown with NS1, probably due to the highest content in green-blue region and R:FR. At the root scale, although many studies (Brennan *et al.*, 2014; Olmo and Villar, 2018, Xiang *et al.*, 2017;) showed the positive influence of biochar application on the most of root traits due to the improved water and nutrient availability, we observed the biochar positive effect only on fine root both length and tissue density in both plant species. In particular, unlike Amendola *et al.*'s (2017) work, in which roots of grapevine plants in response to biochar application increased root diameter and unchanged root length, herein we detected an opposite trend. Probably the different result could be attributable to the seedling growth in presence of different LED spectra. Indeed, the below-ground part of seedlings responded with a higher variability to differences in light spectra than did shoots. However, since roots are covered by soil, how light could influence root morphology seems still unclear. Many studies

demonstrated the direct contribution of light signals perceived from above ground part to the regulation of growth and development of below-ground part through several internal light-conducting systems from stem to roots (Sun *et al.*, 2003). For instance, stem and root vascular tissues can axially conduct light (Sun *et al.*, 2005), or light is transmitted to specific depths thus performing light-sensitive positive geotropism responses (Kasperbauer and Hunt, 1988; Tester and Morris, 1987). In our study, both the fluorescent light and AP67 had the strongest effect on root morphology in untreated and biochar-treated seedlings respectively. These findings suggest that control seedlings grown with a control light had longer and thinner root traits than biochar-treated seedlings grown with AP67. The AP67 promoting effect on some root traits could be attributable to the spectrum composition (the lowest R:FR value and the highest red content) in accordance to that reported in other studies in which the same LED light types (Montagnoli *et al.*, 2018; Smirnakou *et al.*, 2017) or with the same spectrum characteristics (Li *et al.*, 2018; Poudel *et al.*, 2008; Rabara *et al.*, 2017) were used.

Concerning the physiological traits, although biochar amendment did not significantly affect fluorescence emission in light conditions (Φ_{PSII}) it improved the activity of PSII in dark conditions (F_v/F_m) only at the last sampling date. In a study on *Malus hupehensis* seedlings, Wang *et al.* (2014) found that biochar noticeably increased the photosynthetic rate of three months old seedlings. It is reasonable to assert that the influence of biochar treatment could be evident only when seedlings are well developed and in particular at the fruit stage. This result could be also attributable to the timing of exhausting of seed stored reserves on plant development, mainly at early developmental stages (Montagnoli *et al.*, 2016, 2018). In our study, the test of the fluorescence in dark-adapted conditions throughout the whole experiment showed a kind of bimodal pattern with the highest activity of the PSII at both initial and later stages of the seedlings' development. Lowest values were measured at the second sampling date and at the latest growth stage when seedlings started the fruit stage. The general transient decline of F_v/F_m during the second sampling date by all LED spectra could be a sign of a transient photoinhibition (Krause, 1988) due to a temporary loss of functional Q_B protein synthesis and then recovered in the next sampling date. We also noted the increase of F_v/F_m in the third sampling date by biochar-treated seedlings grown with AP67 which, although herein not measured, could be due to a decrease of F_0 (initial fluorescence at the dark state) as well as an index of antenna pigments activity of the PSII reaction center (Maxwell and Johnson, 2000). Therefore, we suppose that this kind of oscillations

in F_v/F_m trend is independent on both biochar and LED types treatments, but it could be due to the PSII activity following the suturing light provided by the fluorimeter instrument. However, during the whole experiment and for all the considered spectra, F_v/F_m remained around and above the optimal value of 0.83 (Maxwell and Johnson, 2000; Murchie and Lawson, 2013; Ritchie, 2006) confirming that PSII efficiency was not affected by light spectra variation and biochar application during the time. Dark-adapted values of F_v/F_m reflect the potential quantum efficiency of PSII and they could be considered as sensitive indicators of plant photosynthetic performance (Maxwell and Johnson, 2000). The actual Φ_{PSII} , related to the achieved PSII efficiency, was similar among all different spectra with the only exception of seedlings grown with AP67, which showed the lowest values throughout the experiment. According to Schansker *et al.* (2004), the decrease of Φ_{PSII} could indicate an inhibition of the redox reaction after primary acceptor quinone (Q_A) with a slowdown in electron transfer between Q_A^- and the secondary acceptor (Q_B). Besides that, although biochar-treated seedlings grown with AP67 showed an increase of F_v/F_m , in comparison with untreated seedlings, they did not show a positive effect in the Φ_{PSII} . Some reports have defined that low R:FR ratio might act as a shade avoidance signal improving photosynthetic capacity of plants (Valladares and Niinemets, 2008; Gommers *et al.*, 2013). Hence, we suppose that AP67, for its spectrum characteristics (the lowest R:FR ratio value), although it might improve the photosynthetic efficiency, it could have a negative impact on photosynthetic yield. Nevertheless, biochar application could be compensate the AP67 negative effect. Indeed, Huang *et al.* (2004) demonstrated that N-deficiency conditions could cause a loss of photosynthetic pigments. However, in our case, an increase of nitrogen availability and organic carbon following the biochar application in soil was noted, which could have an effect on photosynthetic performance. Furthermore, Viger *et al.* (2015) in their work on gene expression of biochar-treated plants proved that biochar application promoted plant growth through the auxin up-regulation. As well as Salisbury *et al.* (2007) have found a possible cross-talking between plant phytochromes photoreceptors and auxin content. Although phytochromes were able to promote plant development through phytochromes-auxin signaling, in presence of biochar amendment that promoted auxin expression, we suppose that the presence of a kind of positive synergic effect between soil characteristics following biochar application and AP67 spectrum characteristics promoting plant growth and development.

NPQ is one of the consequences of the fluorescence-quenching phenomenon, during which the energy is converted to heat with increased efficiency and the heat dissipation occurs (Maxwell and Johnson, 2000). We noted a similar trend throughout the five sampling points, with the absence of significant differences except for the first sampling date, in which biochar-treated seedlings grown with AP67-3L showed an increased NPQ value in relation to the untreated seedlings. However, we detected a lack of relation between NPQ and the other parameters, mainly due to the high sensitivity of NPQ such as the plant development, the light incidence and/or the leaf stage (Maxwell and Johnson, 2000).

The stomatal conductance showed an increasing trend among the five sampling points, except for the last one in which the biochar application negatively affected g_s in seedlings grown with fluorescent and NS1. Although many studies have reported a positive effect of biochar application on stomatal density and conductance (Akhtar *et al.*, 2015; Yeboah *et al.*, 2017), in our case the addition of biochar induced a reduction of stomatal conductance. This response might be attributable to a kind of drought stress in accordance with previous reports by Abel *et al.* (2013) and Paneque *et al.* (2016). Indeed, given the major water retention capacity of biochar, it may cause the reduction of root water availability, inducing a water deficit and determining the plant stomatal closure. Furthermore, it is widely reported that specific mechanisms of several photoreceptors might promote stomatal opening and density depending on the wavelength of incident light (Shimazaki *et al.*, 2007). In our case, whereas seedlings grown with AP67 showed the highest g_s values getting more sharply when biochar was added, a great decrease of g_s was measured at the last sampling point in biochar treated seedlings grown with the other light spectra. Thus, our findings support the hypothesis that the stomatal opening is related to the spectrum composition in relation to the growth stage. Indeed, Jensen *et al.* (2018) studying stomatal activity depending on stomata density, found both an increase and a decrease of stomata density in response to increasing ratios of blue light and decreasing ratios of green light respectively. Likewise, it has been seen that green-light exposure reversibly decreases stomatal conductance in lettuce (Kim *et al.*, 2004) and it has an unfavorable effect on plants, including decreased chlorophyll content and inhibited stomatal opening (Son *et al.*, 2012). In our case, fluorescent light as well as NS1 and to a lesser extent AP67-3L were characterized by the highest percentage of green-blue thus negatively affecting the stomatal activity.

3.5 Conclusions

The morpho-physiological traits here reported represent a first attempt to unveiling plant growth mechanisms in response to the interplay modification of light spectrum and soil characteristics. Once again the high species-specificity of biochar is demonstrate. Indeed, the present work showed that biochar application had a negative and positive effect on Arabidopsis and pea growth and development respectively, particularly doubling the positive fruit yield of *P. sativum* seedlings. The best performance in terms of seedling morphology was also related to the light spectrum, mainly by seedlings grown with AP67 characterized by the lowest value of R:FR. This might be due to the adaptive advantage for competition as shade avoidance response. Although biochar application increased also the potential PSII efficiency for all spectra, the optimal yield was dramatically reduced only in the case of AP67 and independently of biochar presence. These findings showed an interdependence of seedlings growing with higher soil N availability from the photosynthetic machinery. So far, it is remarkable to assert the existence of a kind of synergism between AP67 and biochar. Indeed, the decreased photosynthetic efficiency due to the spectral characteristics of AP67 does not completely affect the plant conditions since biochar improving the soil characteristics can compensate for the negative impact provided by light.

3.6 Acknowledgments

We are grateful to Dr. Barbara Baesso for her valuable help in the laboratory work. This work was supported by University of Insubria [FAR 2013-2016; Research grant ‘Junior’ 2016-2017]; the EC FP7 [ZEPHYR, grant number 308313, 2012-2015].

3.7 References

- Abel S., Peters A., Trinks S., Schonsky H., Facklam M., Wessolek G. (2013). Impact of biochar and hydrochar addition on water retention and water repellency of sandy soil. *Geoderma*, 202-203, 183-191.
- Akhtar S. S., Li G., Andersen M. N., Liu F. (2014). Biochar enhances yield and quality of tomato under reduced irrigation. *Agriculture Water Management*, 138, 37–44.
- Akhtar S. S., Andersen M. N., Liu F. (2015). Residual effects of biochar on improving growth, physiology and yield of wheat under salt stress. *Agriculture Water Management*, 158, 61-68.
- Amendola C., Montagnoli A., Terzaghi M., Trupiano D., Oliva F., Baronti S., Miglietta F., Chiatante D., Scippa G. S. (2017). Short-term effects of biochar on grapevine fine root dynamics and arbuscular mycorrhizae production. *Agriculture Ecosystems and Environment*, 239, 236-245.
- Apostol K. G., Dumroese R. K., Pinto J. R., Davis A. S. (2015). Response of conifer species from three latitudinal populations to light spectra generated by light-emitting diodes and high-pressure sodium lamps. *Canadian Journal of Forest Research*, 45, 1711-1719.
- Arnon D. I. (1949). Copper enzymes in isolated chloroplasts. Polyphenoloxidase in *beta vulgaris*. *Plant Physiology*, 24, 1-15.
- Atkinson C. J., Fitzgerald J. D., Hips N. A. (2010). Potential mechanisms for achieving agricultural benefits from biochar application to temperate soils: a review. *Plant Soil*, 337, 1-18.
- Ballaré C. L. (2014). Light regulation of plant defense. *Annual Review of Plant Biology*, 65, 335-63.
- Baronti S., Alberti G., Delle Vedove G., Di Gennaro F., Fellet G., Genesio L., Miglietta F., Peressotti A., Vaccari F. P. (2010). The biochar option to improve plant yields: first results from some field and pot experiments in Italy. *Italian Journal of Agronomy*, 5, 3-11.

- Batschauer A. (1999). Light perception in higher plants. *Cell and Molecular Life Sciences*, 55, 153-66.
- Berihun T., Tolosa S., Tadele M., Kebede F. (2017). Effect of biochar application on growth of garden pea (*Pisum sativum* L.) in acidic soils of Bule Woreda Gedeo zone southern Ethiopia. *Journal of Agriculture and Food Chemistry*, 2017(6827323), 1-8.
- Bian Z. H., Yang Q. C., Liu W. K. (2015). Effects of light quality on the accumulation of phytochemicals in vegetables produced in controlled environments: a review. *Journal of the Science of Food and Agriculture*, 95, 869-877.
- Black C. A. (1965). Method of Soil Analysis, Part 2, Chemical and Microbiological Properties, American Society of Agronomy. Inc. Publisher, Madison, Wisconsin USA.
- Bourget C. M. (2008). An introduction to light-emitting diodes. *HortScience*, 43, 1944-1946.
- Bowman J. T., Allen B. R. (1988). Moral development and counselor trainee empathy. *Counseling and Values*, 32.
- Brennan A., Jiménez E. M., Puschenreiter M., Albuquerque J. A., Switzer C. (2014). Effects of biochar amendment on root traits and contaminant availability of maize plants in a copper and arsenic impacted soil. *Plant and Soil*, 379, 351-360.
- Bünemann E. K., Bongiorno G., Bai Z., Creamer R. E., Deyn G. D., de Goede R., Fleskens L., Geissen V., Kuyper T. W., Mäder P., Pulleman M., Sukkel W., van Groenigen J. W., Brussaard L. (2018). Soil quality – A critical review. *Soil Biology and Biochemistry*, 120, 105-125.
- Calvelo Pereira R., Kaal J., Camps Arbestain M., Pardo Lorenzo R., Aitkenhead W., Hedley M., Macías F., Hindmarsh J., Maciá-Agulló J. J. (2011). Contribution to characterisation of biochar to estimate the labile fraction of carbon. *Organic Geochemistry*, 42, 1331-1342.
- Casal J. J. (2012). Shade avoidance. *Arabidopsis Book*, 10, e0157.
- Chen M., Tao Y., Lim J., Shaw A., Chory J. (2005). Regulation of phytochrome B nuclear localization through light-dependent unmasking of nuclear-localization signals. *Current Biology*, 15, 637-42.

- Conyers M. K., Davey B. G. (1988). Observations on some routine methods for soil pH determination. *Soil Science*, 145.
- D'Alessandro D. M., Smit B., Long J. R. (2010). Carbon dioxide capture: prospects for new materials. *Angewandte Chemie International*, 49, 6058-6082.
- Darko E., Heydarizadeh P., Schoefs B., Sabzalian M. R. (2014). Photosynthesis under artificial light: the shift in primary and secondary metabolism. *Philosophical Transactions of The Royal Society B Biological Sciences*, 369, 20130243.
- Dumas J. B. A. (1831). Procédes de l'analyse organique. *Annales de Chimie et de Physique*, 247, 198-213.
- Dumroese R. K., Pinto J. R., Heiskanen J., Tervahauta A., McBurney K. G., Page-Dumroese D. S., Englund K. (2018). Biochar can be a suitable replacement for Sphagnum peat in nursery production of *Pinus ponderosa* seedlings. *Forests*, 9, 232.
- Dumroese R. K., Williams M. I., Stanturf J. A., St. Clair J. B. (2015). Considerations for restoring temperate forests of tomorrow: forest restoration, assisted migration, and bioengineering. *New Forest*, 46, 947-964.
- Enders A., Hanley K., Whitman T., Joseph S., Lehmann J. (2012). Characterization of biochars to evaluate recalcitrance and agronomic performance. *Bioresource Technology*, 114, 644-53.
- Eyles A., Bound S. A., Oliver G., Corkrey R., Hardie M., Green S., Close D. C. (2015). Impact of biochar amendment on the growth, physiology and fruit of a young commercial apple orchard. *Trees*, 29, 1817-1826.
- Fang G., Zhu C., Dionysiou D. D., Gao J., Zhou D. (2015). Mechanism of hydroxyl radical generation from biochar suspensions: implications to diethyl phthalate degradation. *Bioresource Technology*, 176, 210-217.
- Gómez C., Mitchell C. A. (2015). Growth responses of tomato seedlings to different spectra of supplemental lighting. *HortScience*, 50, 112-118.
- Gommers C. M. M., Visser E. J. V., St Onge K. R., Voeselek L. A. C. J., Pierik R. (2013). Shade tolerance: when growing tall is not an option. *Trends in Plant Science*, 18, 65-71.

- Greenberg J. A., Meyerhoff M. E. (1982). Response properties, applications and limitations of carbonate-selective polymer membrane electrodes. *Analytica Chimica Acta*, 141, 57-64
- Hernández R., Kubota C. (2016). Physiological responses of cucumber seedlings under different blue and red photon flux ratios using LEDs. *Environmental and Experimental Botany*, 121, 66-74.
- Heuvelink E., Bakker M. J., Hogendonk L., Janse J., Kaarsemaker R., Maaswinkel R. (2006). Horticultural lighting in the Netherlands: new developments. *Acta Horticulturae*, 711, 25-33.
- Hodgson E., Lewys-James A., Rao Ravella S., Thomas-Jones S., Perkins W., Gallagher J. (2016). Optimisation of slow-pyrolysis process conditions to maximise char yield and heavy metal adsorption of biochar produced from different feedstocks. *Bioresource Technology*, 214, 574-581.
- Hossain M. K., Strezov V., Chan K. Y., Nelson P. F. (2010). Agronomic properties of wastewater sludge biochar and bioavailability of metals in production of cherry tomato (*Lycopersicon esculentum*). *Chemosphere*, 78, 1167-71.
- Huang Z. A., Jiang D. A., Yang Y., Sun J. W., Jin S. H. (2004). Effects of nitrogen deficiency on gas exchange, chlorophyll fluorescence, and antioxidant enzymes in leaves of rice plants. *Photosynthetica*, 42, 357-364.
- Jensen N. B., Clausen M. R., Kjaer K. H. (2018). Spectral quality of supplemental LED grow light permanently alters stomatal functioning and chilling tolerance in basil (*Ocimum basilicum* L.). *Scientia Horticulturae*, 227, 38-47.
- Jeong S. W., Park S., Jin J. S., Seo O. N., Kim G. S., Kim Y. H., Bae H., Lee G., Kim S. T., Lee W. S., Shin S. C. (2012). Influences of four different light-emitting diode lights on flowering and polyphenol variations in the leaves of Chrysanthemum (*Chrysanthemum morifolium*). *Journal of Agricultural and Food Chemistry*, 60, 9793-9800.
- Kasperbauer M., Hunt P. (1988). Biological and photometric measurement of light transmission through soils of various colors. *Botanical Gazette*, 149, 361-364.

- Kim S. J., Hahn E. J., Heo J. W., Paek K. Y. (2004). Effects of LEDs on net photosynthetic rate, growth and leaf stomata of chrysanthemum plantlets in vitro. *Scientia Horticulturae*, 101, 143-151.
- Kopsell D. A., Sams C. E., Morrow R. C. (2017). Interaction of light quality and fertility on biomass, shoot pigmentation and xanthophyll cycle flux in Chinese kale. *Journal of the Science of Food and Agriculture*, 97, 911-917.
- Kozai T., Niu G., Takagaki M. (2016). Plant Factory: an indoor vertical farming system for efficient quality food production. Elsevier, London.
- Kozai T., Ohyama K., Chun C. (2006). Commercialized closed systems with artificial lighting for plant production. *Acta Horticulturae*, 711, 61-70.
- Krause G. H. (1988). Photoinhibition of photosynthesis. An evaluation of damaging and protective mechanisms. *Physiologia Plantarum*, 74.
- Krizek D. T., Mirecki R. M., Bailey W. A. (1998). Uniformity of photosynthetic photon flux and growth of 'poinsett' cucumber plants under metal halide and microwave-powered sulfur lamps. *Biotronic*, 27, 81-92.
- Landis T. D., Pinto J. R., Dumroese R. K. (2013). Light emitting diodes (LED): applications in forest and native plant nurseries. *Forest Nursery Notes*, 33, 5-13.
- Lehmann J., Kuzyakov Y., Pan G., Ok Y. S. (2015). Biochars and the plant-soil interface. *Plant Soil*, 395, 1-5.
- Lehmann J., Rillig M. C., Thiesa J., Masiello C. A., Hockaday W. C., Crowley D. (2011). Biochar effects on soil biota – A review. *Soil Biology and Biochemistry*, 43, 1812-1836.
- Lehmann J., Silva J. P., Steiner C., Nehls T., Zech W., Glaser B. (2003). Nutrient availability and leaching in an archaeo-logical anthrosol and a ferralsol of the central amazon basin: fertilizer, manure and charcoal amendments. *Plant Soil*, 249, 343-357.
- Li C., Liu D., Li L., Hu S., Xu Z., Tang C. (2018). Effects of light-emitting diodes on the growth of peanut plants. *Agronomy Journal*, 110, 1-9.

- Liao P. B., Lin Kramer S. S. (1981). Ion exchange systems for water recirculation. *Journal of the World Aquaculture Society*, 12.
- Maxwell K., Johnson G. N. (2000). Chlorophyll fluorescence – a practical guide. *Journal of Experimental Botany*, 51, 659-668.
- McCree K. J. (1972). Action spectrum, absorptance and quantum yield of photosynthesis in crop plants. *Agriculture and Forest Meteorology*, 9, 191-216.
- Mehlich A. (1938). Use of triethanolamine acetate-barium hydroxide buffer for the determination of some base exchange properties and lime requirement of soil. *Soil Science Society of America, Proceedings*, 29, 374-378.
- Mohammad S., Parisa H., Morteza Z., Amin B., Mehran A., Mohammad S., Benoît S. (2014). High performance of vegetables, flowers, and medicinal plants in a red-blue LED incubator for indoor plant production. *Agronomy for Sustainable Development*, 34, 879-886.
- Montagnoli A., Terzaghi M., Fulgaro N., Stoew B., Wipenmyr J., Ilver D., Rusu C., Scippa G. S., Chiatante D. (2016). Non-destructive phenotypic analysis of early stage tree seedling growth using an automated stereovision imaging method. *Frontiers of Plant Science*, 7, 1644.
- Montagnoli A., Dumroese R. K., Terzaghi M., Pinto J. R., Fulgaro N., Scippa G. S., Chiatante D. (2018). Tree seedling response to LED spectra: implications for forest restoration. *Plant Biosystems*, 152, 515-523.
- Murchie E. H., Lawson T. (2013). Chlorophyll fluorescence analysis: a guide to good practice and understanding some new applications. *Journal of Experimental Botany*, 64, 3983-98.
- Olmo M., Villar R. (2018). Changes in root traits explain the variability of biochar effects on fruit production in eight agronomic species. *Organic Agriculture*, 2018, 1-15.
- Olsen S. R., Cole C. V., Watanabe F. S., Dean L. A. (1954). Estimation of available phosphorus in soils by extraction with sodium bicarbonate. U. S. Department of Agriculture Circular No. 939. Banderis, A. D., D. H. Barter and K. Anderson. Agricultural and Advisor.

- Ouzounis T., Fretté X., Rosenqvist E., Ottosen C. O. (2014). Spectral effects of supplementary lighting on the secondary metabolites in roses, chrysanthemums, and campanulas. *Journal of Plant Physiology*, 171, 1491-9.
- Paneque M., De la Rosa J., Franco-Navarro J. D., Colmenero-Flores J. M., Knicker H. (2016). Effect of biochar amendment on morphology, productivity and water relations of sunflower plants under non-irrigation conditions. *Catena*, 147, 208-287.
- Pedmale U. V., Huang S. C., Zander M., Cole B. J., Hetzel J., Ljung K., Reis P. A. B., Sridevi P., Nito K., Nery J. R., Ecker J. R., Chory J. (2016). Cryptochromes interact directly with PIFs to control plant growth in limiting blue light. *Cell*, 164, 233-245.
- Poudel P. R., Kataoka I., Mochioka R. (2008). Effect of red- and blue-light-emitting diodes on growth and morphogenesis of grapes. *Plant Cell, Tissue and Organ Culture*, 92, 147-153.
- Rabara R. C., Behrman G., Timbol T., Rushton P. (2017). Effect of Spectral Quality of Monochromatic LED lights on the growth of Artichoke seedlings. *Frontiers in Plant Science*, 8, 190.
- Rayment G. E., Higginson F. R. (1992). Australian laboratory handbook of soil and water chemical method. Reed International Books Australia P/L, Trading as Inkata Press, Port Melbourne, 330.
- Rhoades J. D. (1996). Salinity: electrical conductivity and total dissolved solids. In methods of soil analysis: chemical methods. Part 3 DL Sparks, editor. Soil Science Society of America, Madison WI.
- Ritchie G. A. (2006). Chlorophyll fluorescence: what is it and what do the numbers mean? USDA Forest Service Proceedings RMRS-P-43.
- Salisbury F. J., Hall A., Grierson C. S., Halliday K. J. (2007). Phytochrome coordinates Arabidopsis shoot and root development. *Plant Journal*, 50.
- Schansker G., Tóth S. Z., Holzwarth A. R., Garab G. (2014). Chlorophyll *a* fluorescence: beyond the limits of the Q_A model. *Photosynthesis Research*, 120, 43-58.

- Shimazaki K. I., Dio M., Assmann S. M., Kinoshita T. (2007). Light regulation of stomatal movement. *Annual Review of Plant Biology*, 58, 219-247.
- Smirnakou S., Ouzounis T., Radoglou K. (2015). Effects of continuous spectrum LEDs used in indoor cultivation of two coniferous species *Pinus sylvestris* L. and *Abies borisii-regis* Mattf. *Scandinavian Journal of Forest Research*, 32, 115-122.
- Smirnakou, S., Ouzounis, T., Radoglou, K., 2017. Continuous spectrum LEDs promote seedling quality traits and performance of *Quercus ithaburensis* var. *macrolepis*. *Frontiers in Plant Science*, 8, 188.
- Solaiman Z. M., Murphy D. V., Abbott L. K. (2012). Biochars influence seed germination and early growth of seedlings. *Plant Soil*, 353, 273-287.
- Solomon D., Lehmann J., Thies J., Schafer T., Liang B. Q. Kinyangi J., Neves E., Petersen J., Luizao F., Skjemstad J. (2007). Molecular signature and sources of biochemical recalcitrance of organic C in Amazonian Dark Earths. *Geochimica et Cosmochimica Acta*, 71, 2285e2298.
- Stutte G. W., Edney S. (2009). Photoregulation of bioprotectant content of red leaf lettuce with light-emitting diodes. *HortScience*, 44, 79-82.
- Sun Q., Yoda K., Suzuki M., Suzuki H. (2003). Vascular tissue in the stem and roots of woody plants can conduct light. *Journal of Experimental Botany*, 54, 1627-1635.
- Sun Q., Yoda K., Suzuki H. (2005). Internal axial light conduction in the stems and roots of herbaceous plants. *Journal of Experimental Botany*, 56, 191-203.
- Tarakanov I., Yakovleva O., Konovalova I., Anisimov A. (2012). Light-emitting diodes: on the way to combinatorial lighting technologies for basic research and crop production. *Acta Horticulturae*, 956, 171-178.
- Tester M., Morris C. (1987). The penetration of light through soil. *Plant, Cell and Environment*, 10, 281-286.
- Trupiano D., Cocozza C., Baronti S., Amendola C., Vaccari F. P., Lustrato G., Di Lonardo S., Fantasma F., Tognetti R., Scippa G. S. (2017). The effects of biochar and its combination

- with compost on lettuce (*Lactuca sativa* L.) growth, soil properties, and soil microbial activity and abundance. *Journal of Agricultural and Food Chemistry*, 2017, 1-12.
- Valladares F., Niinemets Ü. (2008). Shade tolerance, a key plant feature of complex nature and consequences. *Annual Review of Ecology, Evolution, and Systematics*, 39, 237-257.
- Viger M., Hancock R. D., Miglietta F., Taylor G. (2015). More plant growth but less plant defence? First global gene expression data for plants grown in soil amended with biochar. *GCB Bioenergy*, 7.
- Wang Y., Pan F., Wang G., Zhang G., Wang Y., Chen X., Mao Z. (2014). Effects of biochar on photosynthesis and antioxidative system of *Malus hupehensis* Rehd. seedlings under replant conditions. *Science Horticulturae*, 175, 9-15.
- Wu M. C., Hou C. Y., Jiang C. M., Wang Y. T., Wang C. Y., Chen H. H., Chang H. M. (2007). A novel approach of LED light radiation improves the antioxidant activity of pea seedling. *Food Chemistry*, 101, 1753-1758.
- Xiang Y., Deng Q., Duan H., Guo Y. (2017). Effects of biochar application on root traits: a meta-analysis. *GCB Bioenergy*, 9, 1563-1572.
- Xu G., Zhang Y., Sun J., Shao H. (2016). Negative interactive effects between biochar and phosphorus fertilization on phosphorus availability and plant yield in saline sodic soil. *Science of the Total Environment*, 568, 910-915.
- Yeboah S., Zhang R., Cai L., Li L., Xie J., Luo Z., Wu J., Antille D. L. (2017). Soil water content and photosynthetic capacity of spring wheat as affected by soil application of nitrogen-enriched biochar in a semiarid environment. *Photosynthetica*, 55, 532-542.
- Yan J., Han L., Gao W., Xue S., Chen M. (2015). Biochar supported nanoscale zerovalent iron composite used as persulfate activator for removing trichloroethylene. *Bioresource Technology*, 175, 269-274.
- Yeh N., Ding T. J., Yeh P. (2015). Light-emitting diodes' light qualities and their corresponding scientific applications. *Renewable and Sustainable Energy Reviews*, 51, 55-61.

Chapter IV

The Possible Photoreceptor Role in Response to Modified Light and Nitrogen Availability

4.1 Introduction

Plants are sessile living organisms and to ensure their survival, fitness and productivity they have developed sophisticated mechanisms in reaction to several environmental cues. For instance, it is widely studied the plant ability to plastically change their morphological traits in response to variables related to light and nitrogen (N) availability (Sugiura and Tateno, 2013, 2014; Sugiura *et al.*, 2015).

N is considered a limiting mineral macronutrient required for plant growth and development, given its key role in the constitution of nucleic acid, proteins, enzymes, cell wall and pigment system, (Lezhneva *et al.*, 2014; Khan *et al.*, 2015). The high, intermediate and low N supply levels differently affect plant metabolism, hence the concern on plant response in relation to N availability is always raised (Iqbal *et al.*, 2015). It is reported that plants are able to deal with reduced N availability by promoting the root/shoot ratio or anthocyanin accumulation in leaves to increase the capacity for nutrient acquisition (Rubio *et al.*, 2009). Alternatively, to ensure the nutrient detection there are developmental adaptive mechanisms to stimulate the organ growth, such as primary roots (Walch-Liu and Forde, 2008).

Apart from the N availability, the changes in quality and quantity of light source also significantly affect the plant fitness. Likewise, light is considered a vital environmental factor, not only as an energy source necessary for the photosynthetic process, but also for the regulation of plant growth and development (Jiao *et al.*, 2007). Thereby plants have developed several classes of photoreceptors to perceive light in different conditions, thus characterized from different wavelength (Piao *et al.*, 2015). A class of photoreceptors, namely phytochromes (phys), plays an important role in the plant acclimation to light changes regulating the expression of genes involved in red (R) and far-red (FR) light absorption processes (Chen *et al.*, 2004; Quail *et al.*, 1995). In detail, Phys are dimeric chromoproteins existing in two conformations, the biologically inactive Pr and the active Pfr forms, which in turn absorb in R and FR respectively (Quail *et al.*, 1995; Borthwick *et al.*, 1952). In the widely studied genome of the model plant *Arabidopsis thaliana*, a phytochrome gene family characterized by five members (phyA-phyE) was defined, among which phyA and phyB have main roles in several light-dependent processes (Franklin and Quail, 2010). Specifically, both phyA and phyB are involved in seed germination (Heschel *et al.*, 2007), seedling de-etiolation (Nagatani *et al.*, 1993), regulation of hypocotyl randomization (Poppe *et al.*, 1996)

and leaf architecture (Devlin *et al.*, 2003), internode elongation (Devlin *et al.*, 1998) and entrainment of the circadian clock (Somers *et al.*, 1998). Nevertheless, dark-grown plants show high levels of phyA that is rapidly degraded in light (Li *et al.*, 2011), indeed another important role of phyA alone is in antagonism of shade avoidance (Salter *et al.*, 2003). Furthermore, phyA is necessary for seedling establishment of plant growth in environments characterized by FR light, such as the undergrowth of forests (Yanovsky *et al.*, 1995). On the contrary, light environments characterized by R light and adult plants require phyB (Li *et al.*, 2011), which alone has a role in suppression of shade avoidance (Devlin *et al.*, 1998). Additionally, in response to light conditions, plants are able to activate different developmental programs after germination, which are skotomorphogenesis and photomorphogenesis in the dark and in light respectively. In detail, the regulation of these two processes occurs thanks to specific transcription factors named Phytochrome-Interacting Factors (PIFs) during which the inactive Pr form localizes in the cytosol and the active Pfr form translocates into the nucleus to activate or repress its target genes (Bae *et al.*, 2008; Castillon *et al.*, 2007).

The multiple changes in root and leaf morphology and in photosynthetic pigment contents of a model plant as *Arabidopsis thaliana* that occur upon the deprivation of N and the low light efficiency have been reported in several studies (Givnish, 1988; Poorter *et al.*, 2000; Valladares *et al.*, 2000; Sugiura and Tateno, 2013, 2014). Similarly, many reports have defined the phytochrome roles in different types of plant activities such as photomorphogenesis (Fankhauser and Casal, 2004; Sheerin *et al.*, 2015), biotechnology enhancement for crop improving (Ganesan *et al.*, 2016), gene regulation mediated by light-temperature combination (Toledo-Ortiz *et al.*, 2014; Jung *et al.*, 2016; Lorenzo *et al.*, 2016) or phototropic responses (Whippo and Hangarter, 2004). However, the response and the possible roles of some classes of photoreceptors in these two conditions are still unknown. Although *Arabidopsis thaliana* is not a crop plant, it is used as a model plant in a big variety of studies for many reasons, including a brief life cycle, a small and well-annotated genome, an amenability to tissue culture, the limited cell-layers per cell type (for developing roots), the availability of natural diversity sets and targeted mutants and the ease at which it can be genetically transformed (AGI, 2000). Therefore, by using mutant lines of *Arabidopsis thaliana* (ecotype *Columbia*) in hydroponic growth conditions, we obtained preliminary results to define a possible connection between factors involved in the light perception and modulation and that involved in N transport and metabolism.

4.2 Materials and Methods

4.2.1 Hydroponic Growing System

To perform the experiments an experimental hydroponic growing system was set-up (Fig. 4.1). Plastic boxes (14 x 9 x 7.5 cm) were used as pots filled by full nutrition and/or N starvation solution, 0.5 ml Eppendorf tubes were modified by cutting their base and cap and they were filled by agar (Fig. 4.1a). Once agar was solidified, tubes were inserted in a support that was positioned on the top of each box (Fig. 4.1b, c).

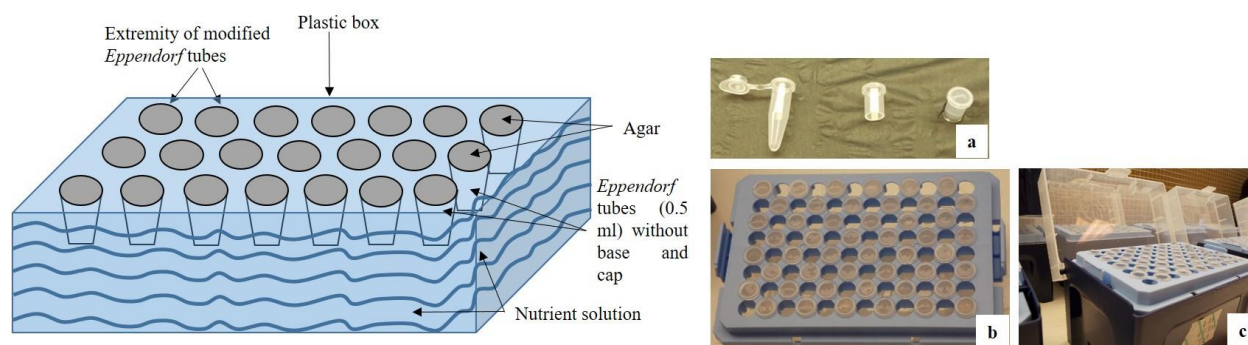


Figure 4.1. Experimental hydroponic growing system. The experimental design (left) and the real experimental system (right). Modified Eppendorf tubes (a) and a support in which to insert the tubes (b) compose the complete growth system (c).

4.2.2 Plant Material, Solution Preparation and Growing Conditions

Experiments were performed at Lancaster Environment Centre (Lancaster University, Lancaster, UK). The wild type *Arabidopsis thaliana* used in this study was Columbia-0 (Col-0). The mutants used were *phyB*, *phyAB* double mutant and *pifs* quadruple mutant (Reed *et al.*, 1994, 1998; Leivar *et al.*, 2009). The solution prepared for the experiment was based on Hoagland's formula (Hoagland and Arnon, 1950) that was modified for the N starvation as reported in Yan *et al.* (2015) at the low N supply level. In detail, the solution was composed of 0.75 mM K_2SO_4 , 0.65 mM $MgSO_4$, 1 μ M $MnSO_4$, 0.1 μ M $CuSO_4$, 1 μ M $ZnSO_4$, 0.035 μ M Na_2MoO_4 , 0.1 mM Fe-EDTA, 0.01 mM H_3BO_3 , 2 mM $CaCl_2$, 0.6 mM KH_2PO_4 , 0.6 mM NaH_2PO_4 except for NH_4NO_3 that in

full nutrition and in N starvation was concentrated 4 mM and 1 mM respectively. The pH of each solution was adjusted to 5.8. The experiment was performed as illustrated in Fig. 4.2. Seeds were surface sterilized in 10% bleach (v/v) for 10 min. After washing twice in sterile water, one seed was sown on tube filled by MS-Medium containing 1.2% agar (w/v) and no sucrose (pH 5.8). In the support of each box 48 tubes were used, for a total of 48 seeds per box. Tubes were placed in the box filled by full nutrition solution. For the following stratification phase, seeds were cold treated for 3 days at 4 °C in the dark. To induce the germination they were exposed to light for 3 hours and incubated in the dark at room temperature overnight. Thereafter, they were transferred in the plant growth chamber (Panasonic MLR-352-PR, Gunma, Japan) where light irradiance was obtained with light-emitting diode lamps. The photon flux density was modified by using a neutral density (ND) light filter (LEE Filters USA and Latin America 210 0.6 ND reducing light 2 stops) obtaining two light conditions: one of 86 (without light filter, normal light, NL) and another of 22 $\mu\text{mol m}^{-2} \text{s}^{-1}$ (with light filter, low light, LL) PAR. Fluence rates were determined by using a PAR meter (Irradian Q201 PAR radiometer, Scotland, United Kingdom). Seedlings were grown in 16-h light/8-h dark with a mean temperature of 20 °C for 15 days.

4.2.3 N Starvation Treatment

For nitrogen deprivation, the full nutrition solution was replaced with the N starvation solution characterized by a modified N content as above-mentioned. 15-day-old seedlings were grown for 7 days in the conditions as above (Fig. 4.2).

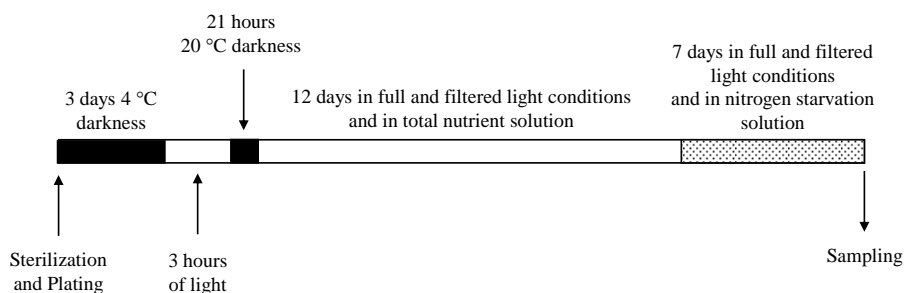


Figure 4.2. Schematic representation of the experimental plan. Sterilized seeds are plated and kept in the dark for 3 days at 4 °C (seed stratification phase). Germination is induced by 3 hours of light treatment and the plates are returned into the darkness at 20–22 °C for 21 hours. The plates are placed into light conditions (full and filtered light) for 12 days. Finally, the solution is changed applying the N starvation treatment unchanging the light conditions for 7 days before the seedlings are sampled.

4.2.4 Morphological Measurements and Determination of Photosynthetic Pigment Contents

22-days-old seedlings were harvested and weighed immediately. Hypocotyl and primary root length and leaf area were documented using a digital camera (Nikon Coolpix L830) and measured by the ImageJ software. Total carotenoid and chlorophylls in 500 μ L of the homogenate (prior to centrifugation) were extracted in 80% acetone for 30 min in darkness (Lichtenthaler, 1983). After clarifying the acetone-extracted samples by centrifugation at 14000g for 15 min, the absorbance of chlorophyll a (Chl_a), b (Chl_b) and carotenoids (Car) in acetone was measured at 644.8, 661.6 and 470 nm respectively by using the microplate reader (SPECTROstar Nano, BMG LABTECH). Chlorophyll and carotenoid contents were estimated using the formulas $\text{Chl}_a = (12.21 \cdot A_{661}) - (2.81 \cdot A_{644})$, $\text{Chl}_b = (20.13 \cdot A_{644}) - (5.03 \cdot A_{661})$ and $\text{Car} = (1000 \cdot A_{470}) - (3.27 \cdot \text{Chl}_a) - (104 \cdot \text{Chl}_b)$. Concentration was expressed per sample fresh weight and measured in biological triplicates.

4.2.5 Statistical Analysis

To evaluate significant differences between the influence of the N and low light availability among mutants, four comparisons for each morphological and physiological measured parameter were performed: (a) seedlings in full nutrition and in N starvation solutions for the same genotype and in the same lighting treatment, (b) seedlings grown in full nutrition solution between different genotypes in each light condition, (c) seedlings grown in N starvation solution between different genotypes in each light condition, (d) seedlings grown in full nutrition and in N starvation solution for the same genotype and between different lighting treatment. Data were analysed with a two-tailed T-test with a significance level of 95% ($p < 0.05$).

4.3 Results

4.3.1 Morphological Traits

The changes of *Arabidopsis* morphological traits in response to modified conditions of light and nutrient were assessed by measuring the hypocotyl and primary root length, leaf area and fresh weight.

Hypocotyl Length

All genotypes maintained their expected growth parameters. Both full nutrition and N starvation conditions had a significant effect on hypocotyl length. Particularly, in NL, N starvation negatively affected hypocotyl length of Col-0, *phyB* and *pifs*, whereas in *phyAB* it was promoted. In the same light condition, as expected, *phyAB* showed the longest hypocotyl followed consecutively decreasing by *phyB*, Col-0 and *pifs* in both full nutrition and N starvation (Fig. 4.3a). Similarly, in LL, the low N availability reduced the hypocotyl length of Col-0 and *pifs* only, also showing, as expected for *pifs*, the shortest hypocotyl than *phyB* and *phyAB* in both full nutrition and N starvation (Fig. 4.3b). Thus, this elongation response is probably PIFs dependent. Moreover, as expected, all genotypes, except for N starved *phyAB*, showed the longest hypocotyl in LL in relation to those grown in NL (Fig. 4.3a, b). Therefore, the changes in light and nutrient supply did not affect the hypocotyl growth of all genotypes tested.

Primary Root Length

The N starvation treatment did not affect the primary root length of all genotypes. The primary root length of Col-0 and *phyAB* grown in NL was negatively affected by the N starvation. *pifs* showed the longest primary root followed decreasing by Col-0 and *phyB* which were not significantly different among themselves and followed decreasing by *phyAB* in both full nutrition and N starvation (Fig. 4.3c). Contrarily, in LL the N starvation positively affected the primary root length of Col-0, *phyB* and *pifs*. While in full nutrition Col-0 showed the longest primary root followed consecutively decreasing by *pifs*, *phyB* and *phyAB*, in N starvation Col-0 and *pifs* showed the longest primary root followed by *phyB* and *phyAB* (Fig. 4.3d). Interestingly, the low light condition negatively affected the primary root length of all genotypes (Fig. 4.3c, d).

Leaf Area

In NL, while N starvation reduced the leaf area of Col-0 and *pifs*, it was promoted in *phyB*. As expected, in normal light condition and in full nutrition Col-0 showed the highest leaf area followed by *phyB* and *pifs*, which were not significantly different among themselves and *phyAB* showed the lowest leaf area value. Similarly, in N starvation *phyB* showed the greatest leaf area followed consecutively decreasing by Col-0, *pifs* and *phyAB* (Fig. 4.3e). Similarly, in LL, N starvation reduced and promoted leaf area of Col-0 and *phyB* respectively. Among genotypes, in full nutrition Col-0 showed the greatest leaf area followed consecutively decreasing by *pifs*, *phyB* and *phyAB*, the similar trend was detected in N starvation except for *phyB* and *phyAB* that were not significantly different among themselves (Fig. 4.3f). As expected, the reduction of light availability decreased the leaf area of all genotypes (Fig. 4.3e, f). Interestingly, leaf area was related to the leaf architecture. Mainly *phyB* leaves of seedlings grown in LL and in N starvation had the highest area value that was confirmed in the observed leaf elongation (Fig. 4.4). Thus, *phyB* mutants seemed to respond to low light and low N supply by promoting their leaf growth.

Fresh Weight

As expected, in NL N starvation reduced the fresh weight of Col-0 and *pifs* together, whereas it was promoted in *phyB*, as it was also noted in leaf structure changes (Fig. 4.4). In full nutrition while Col-0 and *phyAB* showed the highest and lowest fresh weight value respectively than *phyB* and *pifs* had intermediate fresh weight values. On the contrary, in N starvation *phyB* had the highest fresh weight value followed consecutively increasing by Col-0, *pifs* and *phyAB* (Fig. 4.3g). Unexpectedly, in LL N starvation positively affected the fresh weight of *phyB* only. Col-0 showed the highest fresh weight followed consecutively decreasing by *phyB*, *pifs* and *phyAB* in both full nutrition and N starvation (Fig. 4.3h). As expected, all genotypes were negatively affected by the low light availability (Fig. 4.3g, h). Hence, beside the increased fresh weight due to the major leaf expansion of *phyB* grown in LL and in N starvation conditions, the two treatments did not affect fresh weight of the other genotypes.

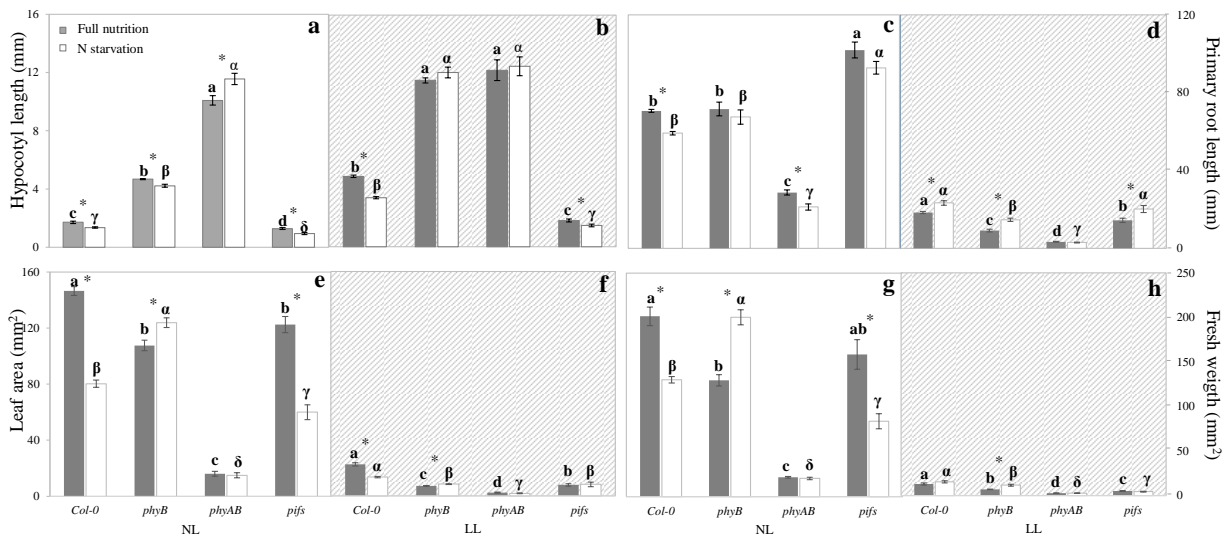


Figure 4.3. Results of morphological measurements (means \pm SE) of Col-0, *phyB*, *phyAB* and *pifs* (n=12) genotype grown in full nutrition (■) and in N starvation solutions (□). Each measured parameter are reported in two graphs in relation to the light condition: Normal Light (NL, white background) and Low Light (LL, line background). a, b, c, d indicate significant differences between different genotypes in Full nutrition solution and in NL and LL separately ($p < 0.05$). α , β , γ , δ indicate significant differences between different genotypes in N starvation solution and in NL and LL separately ($p < 0.05$). Asterisk (*) indicates significant differences between Full nutrition and N starvation solutions in the same genotype and light conditions ($p < 0.05$). Letters in bold indicate significant differences between NL and LL in the same genotype ($p < 0.05$).

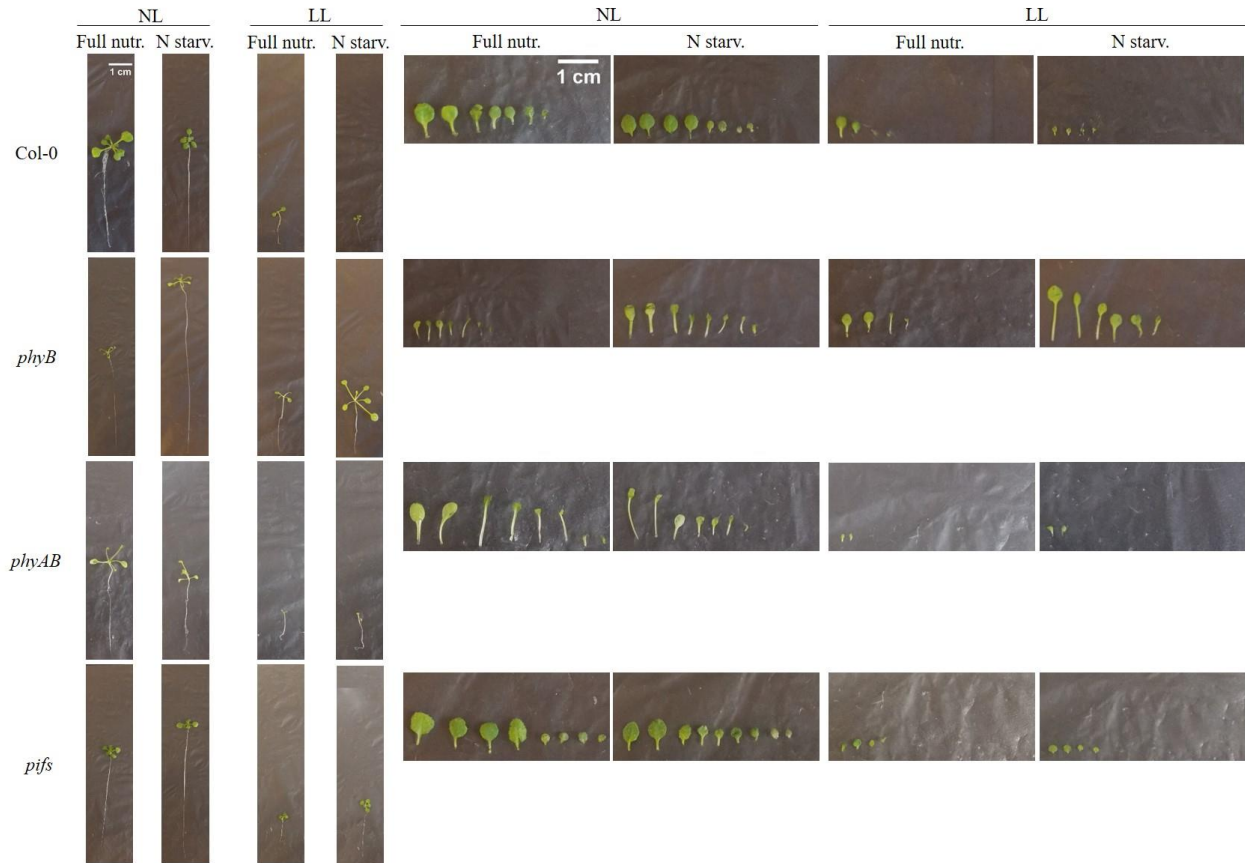


Figure 4.4. Overview of the phenotypes of wild-type (Col-0) and mutant (*phyB*, *phyAB*, *pifs*) seedlings. The group of pictures on left and right highlight the comparisons of leaf morphology and emergence respectively. 22-days-old whole seedlings (left) and leaves (right) grown in normal light (NL) and in low light (LL) in each of them in Full nutrition (Full nutr.) and in N starvation (N starv.) conditions. Scale bars are 1 cm.

4.3.2 Photosynthetic Pigment Contents

To assess a potential influence of modified light and nutrient availability on the photosynthetic efficiency, the extraction and quantification of photosynthetic pigments, such as Chl_a, Chl_b and Car, were performed.

Unexpectedly, in NL the low N availability positively and negatively affected the chl_a of Col-0, *pifs* and *phyB*, *phyAB* respectively. While as expected, in full nutrition Col-0 and *phyAB* had the lowest and highest chl_a levels respectively. Surprisingly, nevertheless they act antagonistically, *pifs* and *phyB* had the same intermediate chl_a values and in N starvation *phyB* and *pifs* had the lowest and highest chl_a levels. Col-0 and *phyAB* had intermediate values (Fig. 4.5a). Surprisingly, in LL and in full nutrition *phyB* showed the lowest chl_a levels, similarly, in N

starvation Col-0 and *phyAB* had higher chl_a levels than *phyB* (Fig. 4.5b). Among two light conditions, as expected, while Col-0 in NL showed lower chl_a levels than those grown in LL in both full nutrition and N starvation, unexpectedly *phyB* in full nutrition and *phyAB* in N starvation in LL had lower and higher chl_a contents respectively than those grown in NL (Fig. 4.5a, b). In NL N starvation negatively affected the chl_b levels of *phyB* and *phyAB*, similarly the low N availability reduced the chl_b levels of *phyB* and *phyAB*, which were not significantly different among themselves (Fig. 4.5c). Whereas in LL and in full nutrition Col-0 has higher chl_b levels than *phyAB* and *pifs*, which were not significantly different among themselves, probably due to a light intensity dependent PIFs response. In N starvation Col-0 and *phyB* showed the highest and the lowest chl_b content respectively (Fig. 4.5d). With light reduction the chl_b levels of Col-0 in both full nutrition and N starvation and of N starved *phyAB* were increased (Fig. 4.5c, d). As expected, in NL *phyB* and *phyAB* together and *pifs* had lower and higher chl_{a+b} levels in response to N starvation respectively. In full nutrition *phyB* and *phyAB* showed higher chl_{a+b} levels than Col-0. Contrarily, as expected, in N starvation *pifs* had the highest chl_{a+b} levels followed by Col-0 and then *phyB* and *phyAB*, which were not significantly different among themselves (Fig. 4.5e). In LL *phyB* showed the lowest chl_{a+b} levels in both full nutrition and N starvation (Fig. 4.5f). While Col-0 and N starved *phyAB* grown in LL showed higher chl_{a+b} levels than those grown in NL in both full nutrition and N starvation, *phyB* in full nutrition grown in LL had lower chl_{a+b} contents than those grown in NL, response surprisingly due to a possible dual role for phyA and phyB (Fig. 4.5e, f). Similarly to previous results, in NL *phyB* and *phyAB* together and *pifs* had lower and higher chl_{a+b} levels in response to N starvation respectively. In in full nutrition, Phys could be defined as positive activators of carotenogenesis, indeed, *phyB* and *phyAB* had higher car levels than Col-0, whereas in N starvation *pifs* unexpectedly showed the highest car levels followed by Col-0 and *phyB*, (Fig. 4.5g). In LL and in full nutrition, Col-0 and *phyAB* had higher car levels than *phyB* and they were not significantly different among themselves. Similarly, in N starvation *phyAB* had the highest car levels followed consecutively decreasing by Col-0 and *phyB* (Fig. 4.5h). However, the lower levels of carotenoids in NL compared to LL is an unexpected result. Unexpectedly, while the low light availability increased the car levels of Col-0 in both full nutrition and N starvation and N starved *phyAB*, in *phyB* in full nutrition they were decreased (Fig. 4.5g, h).

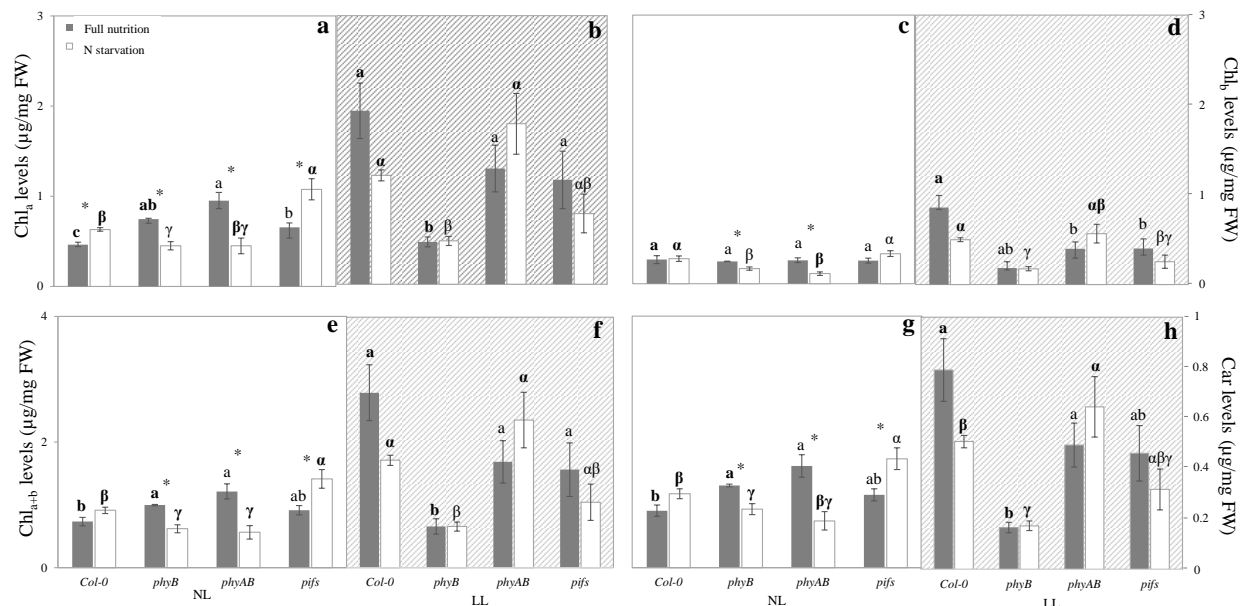


Figure 4.5. Results of photosynthetic pigment level measurements (means \pm SE) of Col-0, *phyB*, *phyAB* and *pifs* ($n=3$) genotype grown in full nutrition (■) and in N starvation solutions (□). Each measured parameter are reported in two graphs in relation to the light condition: Normal Light (NL, white background) and Low Light (LL, line background). a, b, c, d indicate significant differences between different genotypes in Full nutrition solution and in NL and LL separately ($p < 0.05$). α , β , γ , δ indicate significant differences between different genotypes in N starvation solution and in NL and LL separately ($p < 0.05$). Asterisk (*) indicates significant differences between Full nutrition and N starvation solutions in the same genotype and light conditions ($p < 0.05$). Letters in bold indicate significant differences between NL and LL in the same genotype ($p < 0.05$).

4.4 Discussion and Conclusions

The plant photoreceptors are normally involved in light-signalling pathways and they are widely studied in different light quality and quantity conditions. In this study, for the first time, we have demonstrated the further possible role of some photoreceptors, such as *phyB*, *phyAB* and *pifs* in plant changes in response to modified N and light availability. By measuring morphological traits and photosynthetic pigment content of *Arabidopsis* mutants, the influence of N starvation and different light conditions is investigated.

Although there are no reports on photoreceptor responses in N starvation condition, they are widely reported the changes of *Arabidopsis* morphological traits. For instance, the stimulation of the primary root length in response to low N availability, at least in the early stage of post-germinative *Arabidopsis* growth decreasing the shoot to root biomass ratio is fully explained (Smolders and Merckx, 1992; Scheible *et al.*, 1997; Anandacoomaraswamy *et al.*, 2002; Walker

et al., 2001; Richard-Molard *et al.*, 2008). The N starvation causes a root promotion at the expense of shoot that decreases (Krapp *et al.*, 2011). Nevertheless, Martin *et al.* (2002) demonstrate that changes in N availability caused a significant alteration in overall size, including the reduction of root length and fresh weight. Additionally, Wang *et al.* (2014) confirm the stimulation by N starvation of the expression of related genes to anthocyanin biosynthesis, which in turn promotes the root formation. From our results, a general promotion and decrease of root and shoot respectively was reported. In all genotypes this same root:shoot ratio was detected, except for *phyAB* and mainly in normal light condition. Contrarily to the reports mentioned above, the only promotion of root length due to the N starvation condition was observed in low light availability. Indeed, when light irradiance was reduced all genotypes increased and decreased their hypocotyl and primary root length respectively, except for *phyAB*, which responded with an opposite trend. Probably, in response to the low light condition and in low N availability Col-0 and mutants prefer to use the stored N to increase the root length ensuring the nutrition. Moreover, it is known that in normal light conditions phytochromes promote the hypocotyl shortening to activate the photomorphogenesis (Reed *et al.*, 1994; McCormac and Terry, 2002; Franklin and Quail, 2010), hence in our study, *phyB* and *phyAB* mutants, lacking phyB and more sharply phyA, showed longer hypocotyl than wild-type. Nevertheless, the N stress induces the reduction of both hypocotyl and root length, except for *phyAB* mutant. Therefore, we suppose that, although PIFs and Phys have an opposite role in elongation process, in both light and N stress, *phyB* and *pifs*, similarly to Col-0 induce the primary root length to detect more nutrients saving energy to increase the hypocotyl length, instead of *phyAB* that prefers to elongate the hypocotyl. In normal light condition, the lack of phyA could enhance the tolerance of N stress promoting the different growth response.

The decrease of leaf area and fresh biomass in response to low nitrogen and light conditions demonstrated in wild-type (Richard-Molard *et al.*, 2008; Tian *et al.*, 2017), also in our study was observed. Among mutants, while *pifs* had the same trend of wild-type and *phyAB* seemed to be unresponsiveness, *phyB* mutants showed the most interest response. Indeed, although *phyB* mutants are generally characterized by a reduced cotyledon expansion (Franklin and Quail, 2010), in our study, contrarily to wild-type and other mutants, they showed an increased leaf area and consequently fresh weight, in both full nutrition and in N starvation. While in low light availability and in N starvation all genotypes reduced both leaf area and fresh weight, *phyB* responded to low N supply increasing cotyledon expansion and by modifying the leaf architecture. Therefore,

because seedlings lacking phyB overcome the N starvation promoting the growth, we hypothesize that there could be a negative relation between phyB and factors involved in N transport and metabolism to promote the leaf growth.

Additionally, we could explain the singular promotion of pigment accumulation, mainly of Chl_a, in Col-0 due to the decrease of light irradiance through a plant acclimation to low light. Indeed it is known that low light condition has a negative impact on accumulation of plant pigment (Fu *et al.*, 2017). However, from our results, also considering the morphological responses, we can hypothesize that Col-0 in low light irradiance prefers to use the energy to perform photosynthetic process by a more pigment accumulation and independent on N deprivation. As well as, *pifs* mutants showed higher photosynthetic pigment contents but in N starvation. Although it is reported the key role of PIFs in regulating and coordinating the biosynthesis of the functionally related carotenoid and chlorophyll molecules (Meier *et al.*, 2011), we found that seedlings lacking PIFs in low N and in normal light availability are able to accumulate pigments, similarly to Col-0. On the contrary, in normal light condition, because N deprivation reduced the photosynthetic pigment accumulation in *phyB* and *phyAB* mutants, the lack of these photoreceptors did not affect them. Moreover, the reduction of light irradiance seemed to promote the pigment accumulation in *phyAB*, significantly in N starvation. Probably in response to the two stress conditions, such as the low N and light availability, the lack of phyA could enhance pigment accumulation to ensure the photosynthetic process.

Therefore, with our findings, we have demonstrate the involvement of some plant photoreceptors for activating responses to low N supply and light irradiance. We can hypothesize that phyA could have a negative role in plant growth phase and in pigment accumulation in response to N deprivation and in light reduction. As well as, there could be a relation between phyB and factors involved in N transport and metabolism to promote leaf expansion. Thus, even if seedlings are lacking of phyB, they can positively respond to the N starvation conditions by increasing cotyledon growth. Finally, the trends of Col-0 and *pifs* almost always the same, leads to argue the absence of PIFs role in response to these two stress condition. Obviously, our first observations need to further analysis to confirm our hypothesis and to better understand the mechanisms characterizing the responses here detected.

4.5 References

- AGI (The Arabidopsis Genome Initiative) 2000. Analysis of the genome sequence of the flowering plant *Arabidopsis thaliana*. *Nature*, 408, 796-815.
- Anandacoomaraswamy A., DeCosta W. A. J. M., Tennakoon P. L. K., VanDerWerf A. (2002). The physiological basis of increased biomass partitioning to roots upon nitrogen deprivation in young clonal tea (*Camellia sinensis* (L.) O. Kuntz). *Plant and Soil*, 238, 1-9.
- Bae G., Choi G. (2008). Decoding of light signals by plant phytochromes and their interacting proteins. *Annual Review of Plant Biology*, 59, 281-311.
- Borthwick H. A., Hendricks S. B., Parker M. W., Toole E. H., Toole V. K. (1952). A reversible photoreaction controlling seed germination. *Proceedings of the National Academy of Science USA*, 38, 662-666.
- Castillon A., Shen H., Huq E. (2007). Phytochrome interacting factors: Central players in phytochrome-mediated light signaling networks. *Trends of Plant Science*, 12, 514-521.
- Chen M., Chory J., Fankhauser C. (2004). Light signal transduction in higher plants. *Annual Review of Genetics*, 38, 87-117.
- Devlin P. F., Patel S. R., Whitelam G. C. (1998). Phytochrome E influences internode elongation and flowering time in *Arabidopsis*. *The Plant Cell*, 10, 1479-1487.
- Devlin P. F., Yanovsky M. J., Kay S. A. (2003). A genomic analysis of the shade avoidance response in *Arabidopsis*. *Plant Physiology*, 133, 1617-1629.
- Fankhauser C., Casal J. J. (2004). Phenotypic characterization of a photomorphogenic mutant. *The Plant Journal*, 39, 747-760.
- Franklin K. A., Quail P. H. (2010). Phytochrome functions in *Arabidopsis* development. *Journal of Experimental Botany*, 61(1), 11-24.

- Fu Y., Li H., Yu J., Liu H., Cao Z., Manukovsky N. S., Liu H. (2017). Interaction effects of light intensity and nitrogen concentration on growth, photosynthetic characteristics and quality of lettuce (*Lactuca sativa* L. Var. youmaicai). *Scientia Horticulturae*, 214, 51-57.
- Ganesan M., Lee H. Y., Kim J. I., Song P. S. (2016). Development of transgenic crops based on photobiotechnology. *Plant, Cell and Environment*, 40(11), 2469-2486.
- Givnish T. J. (1988). Adaptation to sun and shade: a whole-plant perspective. *Australian Journal of Plant Physiology*, 15, 63-92.
- Heschel M. S., Selby J., Butler C., Whitelam G. C., Sharrock R. A., Donohue K. (2007). A new role for phytochromes in temperature dependent germination. *New Phytologist*, 174, 735-741.
- Hoagland D. R., Arnon D. I. (1950). The water-culture method for growing plants without soil. Berkeley: Circular 347, California Agricultural Experiment Station, College of Agriculture, University of California.
- Iqbal N., Umar S., Khan N. A. (2015). Nitrogen availability regulates proline and ethylene production and alleviates salinity stress in mustard (*Brassica juncea*). *Journal of Plant Physiology*, 178, 84-91.
- Jiao Y., Lau O. S., Deng X. W. (2007). Light-regulated transcriptional networks in higher plants. *Nature Reviews Genetics*, 8(3), 217-230.
- Jung J. H., Domjan M., Klose C., Biswas S., Ezer D., Gao M., Khattak A. K., Box M. S., Charoensawan V., Cortijo S., Kumar M., Grant A., Locke J. C. W., Schäfer E., Jaeger K. E., Wigge P. A. (2016). Phytochromes function as thermosensors in *Arabidopsis*. *Science*, 354(6314), 886-889.
- Khan M. I. R., Trivellini A., Fatma M., Masood A., Francini A., Iqbal N., Ferrante A., Khan N. A. (2015). Role of ethylene in response of plants to nitrogen availability. *Frontiers in Plant Science*, 6, 927.
- Krapp A., Berthomé R., Orsel M., Mercey-Boutet S., Yu A., Castaings L., Elftieh S., Major H., Renou J. - P., Daniel-Vedele F. (2011). *Arabidopsis* roots and shoots show distinct

- temporal adaptation patterns toward nitrogen starvation. *Plant Physiology*, 157, 1255-1282.
- Leivar P., Tepperman J. M., Monte E., Calderon R. H., Liu T. L., Quail P. H. (2009). Definition of early transcriptional circuitry involved in light-induced reversal of PIF-imposed repression of photomorphogenesis in young *Arabidopsis* seedlings. *Plant Cell*, 21(11), 3535-53.
- Lezhneva L., Kiba T., Feria-Bourrellier A. - B., Lafouge F., Boutet-Mercey S., Zoufan P., Sakakibara H., Daniel-Vedele F., Krapp A. (2014). The *Arabidopsis* nitrate transporter NRT2.5 plays a role in nitrate acquisition and remobilization in nitrogen-starved plants. *The Plant Journal*, 80(2), 230-241.
- Li J., Li G., Wang H., Wang Deng X. (2011). Phytochrome signaling mechanisms. *The Arabidopsis Book*, 9, e0148.
- Lichtenthaler H. K., Wellburn A. R. (1983). Determinations of total carotenoids and chlorophylls *a* and *b* of leaf extracts in different solvents. *Biochemical Society Transactions*, 11(5), 591-592.
- Lorenzo C. D., Sanchez-Lamas M., Antonietti M. S., Cerdán P. D. (2016). Emerging hubs in plant light and temperature signaling. *Photochemistry and Photobiology*, 92, 3-13.
- Martin T., Oliver O., Graham I. A. (2002). *Arabidopsis* seedling growth, storage lipid mobilization, and photosynthetic gene expression are regulated by carbon:nitrogen availability. *Plant Physiology*, 128(2), 472-481.
- McCormac A. C., Terry M. J. (2002). Light-signalling pathways leading to the co-ordinated expression of HEMA1 and Lhcb during chloroplast development in *Arabidopsis thaliana*. *The Plant Journal*, 32, 549-559.
- Meier S., Tzfadia O., Vallabhaneni R., Gehring C., Wurtzel E. T. (2011). Transcriptional analysis of carotenoid, chlorophyll and plastidial isoprenoid biosynthesis genes during development and osmotic stress responses in *Arabidopsis thaliana*. *BMC Systems Biology* 5, 77.
- Nagatani A., Reed J. W., Chory J. (1993). Isolation and initial characterization of *Arabidopsis* mutants that are deficient in functional phytochrome A. *Plant Physiology*, 102, 269-277.

- Piao W., Kim E. Y., Han S. H., Sakuraba Y., Paek N. C. (2015). Rice Phytochrome B (osPhyB) negatively regulates dark- and starvation-induced leaf senescence. *Plants*, 4, 644-663.
- Poorter H., Nagel O., Anderson J. M., van Bel A. J. E., Knoblauch M., Ghannoum O., Conroy J. P., Lin G. H., Marino B. D. V., Wei Y. D. (2000). The role of biomass allocation in the growth response of plants to different levels of light, CO₂, nutrients and water: a quantitative review. *Australian Journal of Plant Physiology*, 27, 595–607.
- Poppe C., Hangarter R. P., Sarrock R. A., Nagy F., Schäfer E. (1996). The light-induced reduction of the gravitropic growth-orientation of seedlings of *Arabidopsis thaliana* (L.) Heynh. is a photomorphogenic response mediated synergistically by the far-red absorbing forms of phytochromes A and B. *Planta*, 119, 511-514.
- Quail P. H., Boylan M. T., Parks B. M., Short T. W., Xu Y., Wagner D. (1995). Phytochromes: Photosensory perception and signal transduction. *Science*, 268, 675-680.
- Reed J. W., Nagpal P., Poole D. S., Furuya M., Chory J. (1993). Mutations in the gene for red/far-red light receptor phytochrome B alter cell elongation and physiological responses throughout *Arabidopsis* development. *The Plant Cell*, 5, 147-157.
- Reed J. W., Elumalai R. P., Chory J. (1998). Suppressors of an *Arabidopsis thaliana* phyB mutation identify genes that control light signaling and hypocotyl elongation. *Genetics*, 148(3), 1295-1310.
- Reed J. W., Nagatani A., Elich T., Fagan M., Chory J. (1994). Phytochrome A and phytochrome B have overlapping but distinct functions in *Arabidopsis* development. *Plant Physiology*, 104, 1139-1149.
- Richard-Molard C., Krapp A., Brun F., Ney B., Daniel-Vedele F., Chaillou S. (2008). Plant response to nitrate starvation is determined by N storage capacity matched by nitrate uptake capacity in two *Arabidopsis* genotypes. *Journal of Experimental Botany*, 59(4), 779-791.
- Rubio V., Bustos R., Irigoyen M., Cardone-López X., Rojas-Triana M., Paz-Ares J. (2009). Plant hormones and nutrient signaling. *The Plant Journal*, 69, 361-373.
- Salter M. G., Franklin K. A., Whitelam G. C. (2003). Gating of the rapid shade avoidance response by the circadian clock in plants. *Nature*, 426, 680-683.

- Scheible W.-R., Lauerer M., Schulze E.-D., Caboche M., Stitt M. (1997). Accumulation of nitrate in the shoot acts as a signal to regulate shoot–root allocation in tobacco. *The Plant Journal*, *11*, 671-691.
- Sheerin D. J., Menon C., zur Oven-Krockhaus S., Enderle B., Zhu L., Johnen P., Schleifenbaum F., Stierhof Y. – D., Huq E., Hiltbrunner A. (2015). Phytochrome A and B interact with members of the spa family to promote photomorphogenesis in Arabidopsis by reorganizing the COP1/SPA complex. *The Plant Cell*, *27*, 189-201.
- Smolders E., Merckx R. (1992). Growth and shoot:root partitioning of spinach plants as affected by nitrogen supply. *Plant, Cell and Environment*, *15*, 795-807.
- Somers D. E., Devlin P. F., Kay S. A. (1998). Phytochromes and cryptochromes in the entrainment of the Arabidopsis circadian clock. *Science*, *282*, 1488-1490.
- Sugiura D., Koichiro S., Mikiko K., Hitoshi S., Ichiro T., Masaki T. (2015). Roles of gibberellins and cytokinins in regulation of morphological and physiological traits in *Polygonum cuspidatum* responding to light and nitrogen availabilities. *Functional Plant Biology*, *42*, 397-409.
- Sugiura D., Tateno M. (2013). Concentrative nitrogen allocation to sun-lit branches and the effects on whole-plant growth under heterogeneous light environments. *Oecologia*, *172*, 949-960.
- Sugiura D., Tateno M. (2014). Effects of the experimental alteration of fine roots on stomatal conductance and photosynthesis: case study of devil maple (*Acer diabolicum*) in a cool temperate region. *Environmental and Experimental Botany*. *100*, 105-113.
- Tian Y., Sacharz J., Ware Maxwell A., Zhang H., Ruban A. V. (2017). Effects of periodic photoinhibitory light exposure on physiology and productivity of Arabidopsis plants grown under low light. *Journal of Experimental Botany*, *68*(15), 4249-4262.
- Toledo-Ortiz G., Johansson H., Lee K. P., Bou-Torrent J., Stewart K., Steel G., Rodríguez-Concepción M., Halliday K. J. (2014). The HY5-PIF regulatory module coordinates light and temperature control of photosynthetic gene transcription. *PLoS Genetics*, *10*(6), e1004416.

- Valladares F., Wright S. J., Lasso E., Kitajima K., Pearcy R. W. (2000). Plastic phenotypic response to light of 16 congeneric shrubs from a Panamanian rainforest. *Ecology*, 81, 1925-1936.
- Walch-Liu P., Forde B. G. (2008). Nitrate signaling mediated by the NRT1.1 nitrate transporter antagonizes L-glutamate-induced changes in root architecture. *The Plant Journal*, 54, 820-828.
- Walker R. L., Burns I. G., Moorby J. (2001). Responses of plant growth rate to nitrogen supply: a comparison of relative addition and N interruption treatments. *Journal of Experimental Botany*, 52, 309-317.
- Wang J., Wang Y., Yang J., Ma C., Zhang Y., Ge T., Qi Z., Kang Y. (2014). *Arabidopsis* *ROOT HAIR DEFECTIVE3* is involved in nitrogen starvation-induced anthocyanin accumulation. *Journal of Integrative Plant Biology*, 57(8), 708-721.
- Whippo C. W., Hangarter R. P. (2004). Phytochrome modulation of blue-light-induced phototropism. *Plant, Cell and Environment*, 27, 1223-1228.
- Yan Z., Kim N., Han W., Guo Y., Han T., Du E., Fang J. (2015). Effects of nitrogen and phosphorus supply on growth rate, leaf stoichiometry, and nutrient resorption of *Arabidopsis thaliana*. *Plant Soil*, 388, 147-155.
- Yanovsky M. J., Casal J. J., Whitelam G. C. (1995). Phytochrome A, phytochrome B and HY4 are involved in hypocotyl growth responses to natural radiation in *Arabidopsis*: weak de-etiolation of the phyA mutant under dense canopies. *Plant, Cell and Environment*, 18, 788-794.

Chapter V

The Plant Response to CoeLux[®] Lighting System

5.1 Introduction

In recent years among several artificial indoor lighting systems, a completely new system has been designed. The brand of this innovative technology is CoeLux[®] (CoeLux[®] s.r.l. Lomazzo, Italy) and it was born intending to light up indoors, creating the perception of wide space through a physical reproduction of optical atmospheric phenomena. Thanks to high-tech physical features, this singular lighting system gives a real image of the sky with indefinite depth and artificial sun (Fig. 5.1a). Besides that, an observer is able to perceive a series of other important details that reproduce the natural ones. For example, the penumbra color and dimension, the change in shadow color including the distance of the shadowing objects, the apparent movement of the sun across the sky and the brightness ratio (Fig. 5.1b).

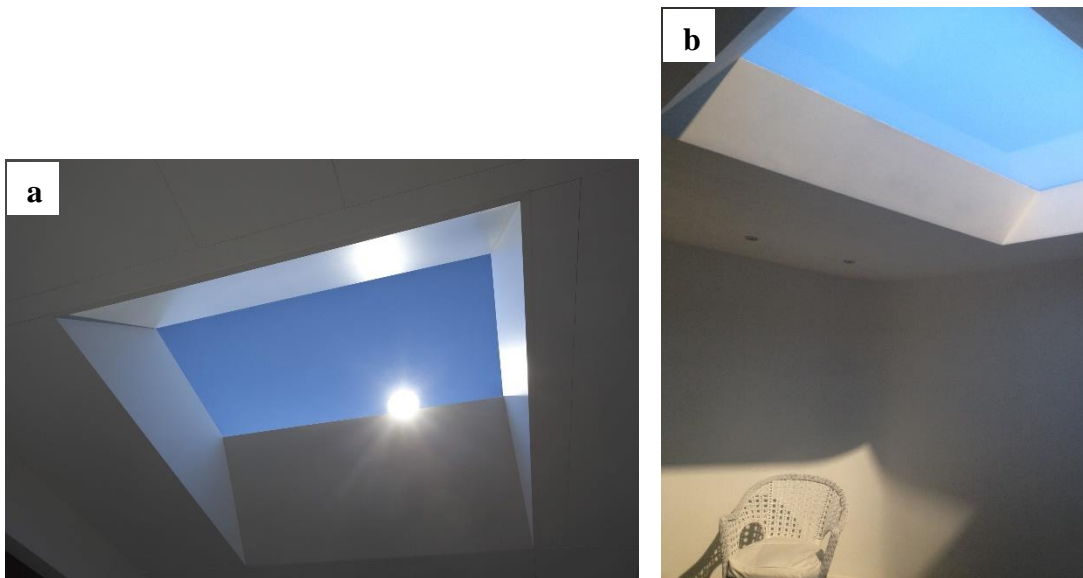


Figure 5.1. Pictures of CoeLux[®] system. A view (a) of the sun and (b) of shadows and sky.

Thus, the key difference between CoeLux[®] and other artificial lighting systems is that CoeLux[®] provides a real impression of skylight together with all their properties. So far, the numerous applications of CoeLux[®] system include the lighting of close space, hospital wards or underground room not naturally illuminated. There are increasingly interests on possible effects of CoeLux[®] lighting systems on human health and plant surviving. Indeed, to understand the effect of CoeLux[®] lighting on human psychology under stress conditions, several experiments have been

carried out. For example, Canazei *et al.* (2015) assessed the effects on human mood, cognition and physiology by comparing them between the created atmosphere in a standard room and in a CoeLux® room. They found that CoeLux® lighting system might generate positive long-term psychophysiological effects on human beings (Canazei *et al.* 2015). Similarly, it is demonstrate that, while the traditional lighting boxes are characterized by UV that give potential harmful effects, CoeLux® by relying on LEDs (light-emitting diodes) technology provides a better visual sensation and response in people with Seasonal Affective Disorder (www.healingplaces.nl). On the contrary, there are no investigations so far concerning the plant responses to CoeLux® lighting.

The chlorophyll fluorescence is a non-invasive tool that by using a modulated pulse-amplitude is able to assess the efficiency of the photosystem II (PSII) and indirectly the status of photosynthetic apparatus (Misra *et al.*, 2012). For this reason, it is becoming one of the most powerful and popular method to detect changes in plant photosynthetic performance in response to several stress factors (Baker and Rosenqvist, 2004; Chaerle *et al.*, 2007). Once light energy is absorbed by chlorophyll molecules, it can follows three competitive decay pathways: converting the molecule from singlet state to the triplet state driving a photochemical process (photosynthesis), converting the molecule into vibrational energy (heat dissipation) and returning to the ground state with the emission of radiation (fluorescence emission). Thus competitively, while under stress conditions the photochemistry decline, heat dissipation and chlorophyll fluorescence emission increase (Maxwell and Johnson, 2000; Murchie and Lawson, 2013). Among the several chlorophyll fluorescence parameters, F_v/F_m ratio is considered the most useful value reflecting the maximum quantum efficiency of the PSII photochemistry (Genty *et al.*, 1989). It is widely reported that plants in stress conditions show low F_v/F_m due to photoinhibition or down-regulation of PSII, whereas high F_v/F_m values, close to 0.83 indicate photosynthetic tissues in good health status (Woo *et al.*, 2008). For instance, rapid modifications of F_v/F_m are shown from plants stressed by several environmental factors, such as water (Woo *et al.*, 2008; Sperdoui and Moustakas, 2012), temperature (Gray *et al.*, 2003; Ehlert and Hinch, 2008; Janka *et al.*, 2013), wounding (Quilliam *et al.*, 2006), photoinhibition (Gray *et al.*, 2003) or biotic interactions (Rincon *et al.*, 2008; Heidari and Golpayegani, 2012; Rousseau *et al.*, 2013). However, the photosynthetic performance revealed by chlorophyll fluorescence imaging is highly heterogeneous at leaf surface and between leaves. This heterogeneity could be due to changing CO₂ concentration (Genty and Meyer, 1995), light stimuli (Baker *et al.*, 2001), ozone-induced (Leipner *et al.*, 2001), low growth

temperature (Oxborough and Baker, 1997), chilling (Hogewoning and Harbinson, 2007), pathogen attack (Rousseau *et al.*, 2013), drought (Calatayud *et al.*, 2006; Sperdouli and Moustakas 2012) or treatment with abscisic acid (Daley *et al.*, 1989). As well as, Bresson *et al.* (2015) assess the spatial heterogeneity of F_v/F_m values which besides the environmental conditions depends on the developmental stage and genotype of leaf considered for measurements. Although the artificial lighting effects on several plant species are widely studied, the influence of CoeLux[®] lighting system on plant growth is still unknown. Therefore, in the present study for the first time, a study on plant morpho-physiological responses to CoeLux[®] light is dealt by studying the photosynthetic performance from measurements of chlorophyll fluorescence emission, by detecting differences in terms of stomatal conductance and by observing the variation of leaf index.

5.2 Materials and Methods

5.2.1 The CoeLux[®] Lighting System

Thanks to moving nanoparticles that crosses LED light, unlike other artificial lighting systems, CoeLux[®] reproduces Rayleigh scattering effect that occurs when light crosses earth's atmosphere and interacts with gaseous substances (Rayleigh, 1878). Structurally, a Rayleigh scattering panel placed at a specific distance from a light source composes the device. The panel separates the light rays from the source into a transmitted component with Correlated Color Temperature (CCT) lower than that of the source, and into a diffused component with higher CCT. Each single LED characterizing the light source comprises a blue/UV emitter, a phosphor and a collimating dome lens that generate a white light cone with limited divergence, i.e. with a divergence smaller than the divergence of the light scattered by the Rayleigh panel. Furthermore, the embodiment comprises a dichroic optical element able to assure the functionalities of the diffused-light generator and the first emitting surface. (Di Trapani *et al.*, 2014; Di Trapani *et al.*, 2017). Surprisingly, the comparison between solar and CoeLux[®] spectra shows an almost perfect overlapping, except for the region between about 500 and 700 nm of wavelength, which in CoeLux[®] spectrum has less irradiance value (Fig. 5.2).

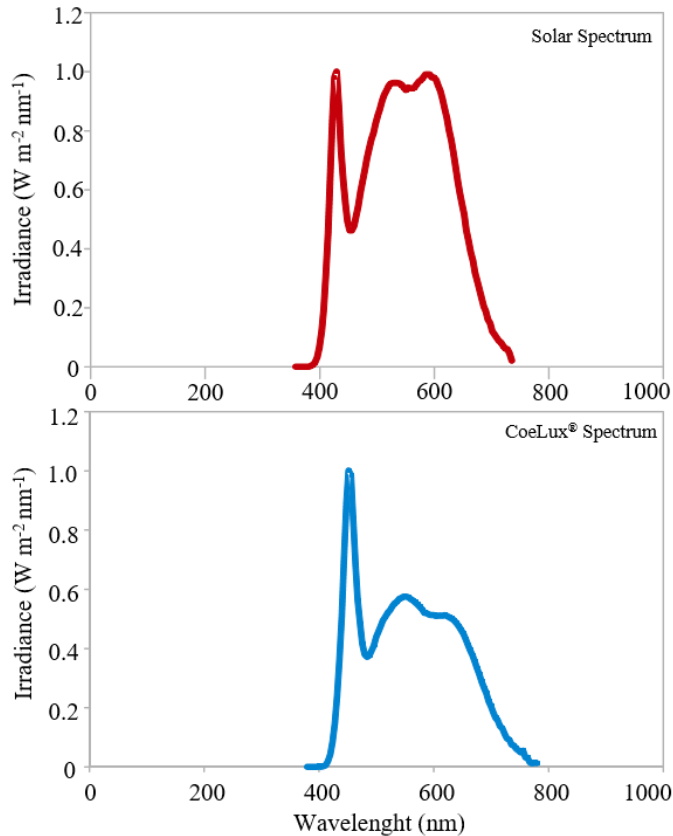


Figure 5.2. Solar and CoeLux[®] spectra. (From Paolo Ragazzi, CoeLux[®]).

5.2.2 Plant material and Experimental Design

Three separate experiments have been carried out in collaboration with the Department of Biotechnology and Life Science of University of Insubria (Varese – Italy) at CoeLux[®] showroom (ComoNExT Science and Technology Park in Lomazzo, CO – Italy). In the showroom there are two distinct rooms illuminated with two different CoeLux[®] sytem: (1) CoeLux 45 HC hereafter named ‘Low’, with a wider and less strong ray (Scheme in Fig. 5.3); (2) CoeLux 45 LC hereafter named ‘High’ with a less wide and stronger ray.

CoeLux® 45 HC

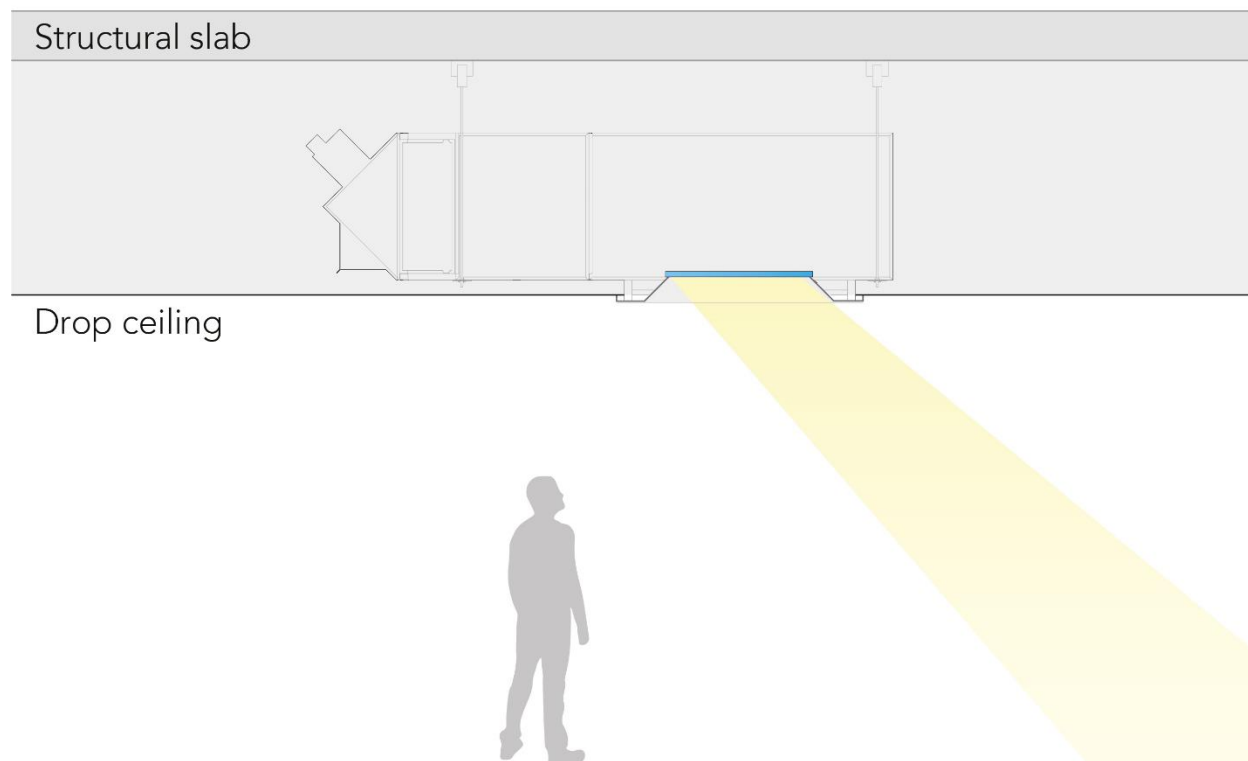


Figure 5.3. A scheme of the CoeLux® 45 HC lighting system. From the upper side: the structural slab for the system housing, the drop ceiling and the light beam.

Short-Term Experiments

A first experiment in both Low and High rooms was performed by using three different plant species, such as two ornamental (*Anthurium andraeanum* Lind. and *Spathiphyllum* Dryand. Ex Sims) and one aromatic (*Ocimum basilicum* L.) in short time exposure. Plants were placed in different position points, each of them characterized by a different PAR (Photosynthetically Active Radiation, $\mu\text{mol m}^{-2} \text{sec}^{-1}$) value. In detail, in Low room six position points were chosen (Fig. 5.4a, b), in correspondence with which plants were placed from shade to full light condition with a corresponding increasing value of PAR (from position point one to six: 2.30, 2.60, 3.20, 16.70, 19.15, 25 $\mu\text{mol m}^{-2} \text{sec}^{-1}$). Similarly, in High room the chosen position points were four (Fig 5.4c, d) and they had the increasing PAR value from one to four as follows: 4.70, 4.85, 11.50, 50.30 $\mu\text{mol m}^{-2} \text{sec}^{-1}$. Starting from the position point with the lowest PAR value, plants were left to

grow for 60 minutes, measurements were carried out and then plants were moved to the next position point with higher PAR value.

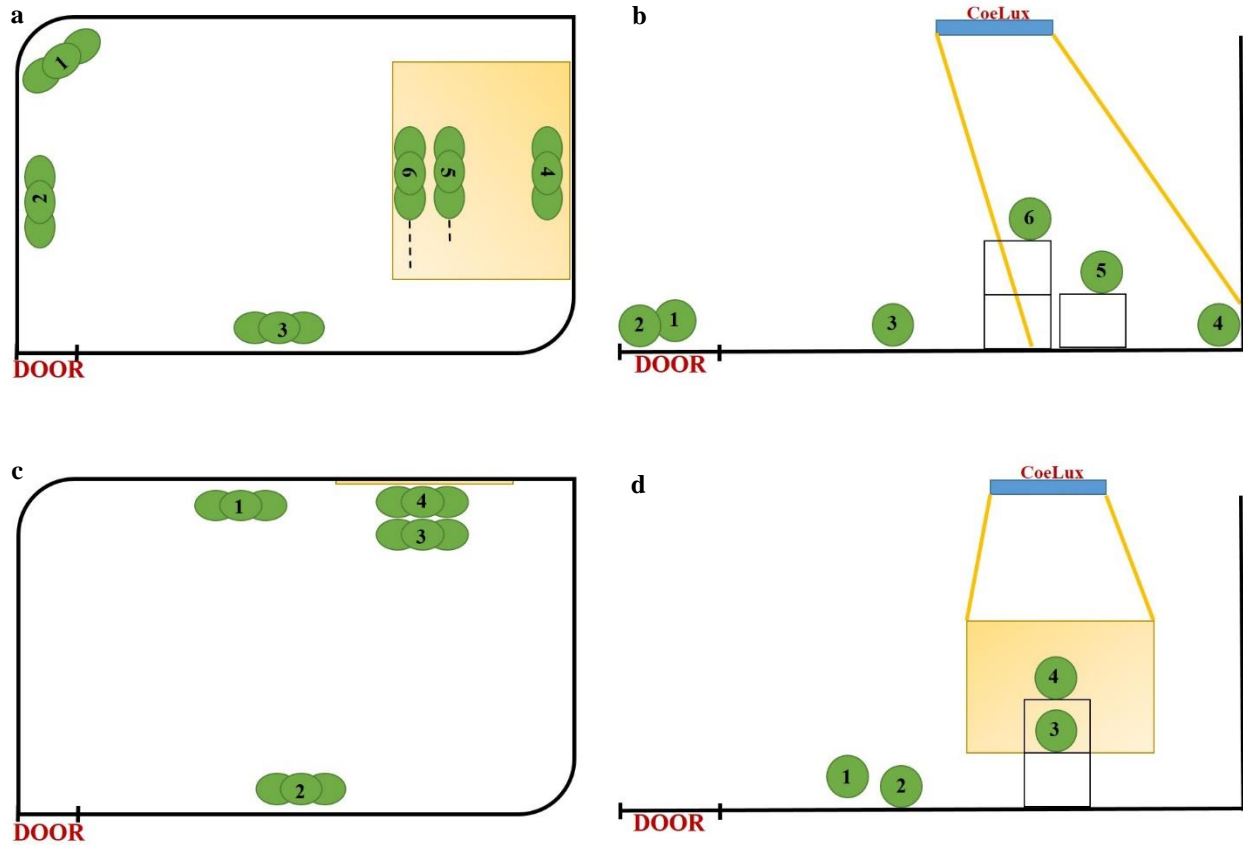


Figure 5.4. View from above (a-c) and side (b-d) of the plant position (green circle) respectively in the Low and the High room. The PAR values in Low room (a, b) are from position point one to six: 2.30, 2.60, 3.20, 16.70, 19.15, 25 $\mu\text{mol m}^{-2} \text{sec}^{-1}$, in High room (c, d) are from position point one to four: 4.70, 4.85, 11.50, 50.30 $\mu\text{mol m}^{-2} \text{sec}^{-1}$.

Long-Term Experiments

Three different plant species were used, two ornamental (*Anthurium* and *Spathiphyllum*) and one aromatic (*Malva sylvestris* L.). Plants were placed in Low room in five position points (5.4a, b) excluding the position point number 2 (2.60 $\mu\text{mol m}^{-2} \text{sec}^{-1}$) that was similar to the PAR value measured from position point number 1 (2.30 $\mu\text{mol m}^{-2} \text{sec}^{-1}$). For each position point, plants were grown for 16 days (16/8 hours light/dark) and successively moved to the next position point characterized by a higher PAR value. From the beginning of each exposure, photosynthetic efficiency in dark-adapted (F_v/F_m), photosystem II yield in light reaction (Φ_{PSII}) and stomatal

conductance (G_s) were measured after 24 hours, 48 hours, 4 days, 8 days and 16 days. Because the obtained results in some position points were similar, in order to facilitate the elaboration of results some of them with a not much different PAR value have been added. Precisely, the data obtained from the measurements in position point 1 ($2.30 \mu\text{mol m}^{-2} \text{sec}^{-1}$) have been added to next one ($3.20 \mu\text{mol m}^{-2} \text{sec}^{-1}$) and that obtained in position point 3 ($16.70 \mu\text{mol m}^{-2} \text{sec}^{-1}$) have been added to the next one ($19.15 \mu\text{mol m}^{-2} \text{sec}^{-1}$).

In the case of High room long term experiment, two potted plant species were used, one agronomic (*Olea europaea* L.) and one forestry (*Quercus ilex* L.). Moreover, three plant species were seeded, one agronomic (*Solanum lycopersicum* L.) and two aromatic (*Ocimum basilicum* and *Coriandrum sativum* L.). The experiment was carried out in three replicates and each replicate (all five plants) was placed in three different growing conditions: a growth chamber, outdoor (at Environmental and Applied Botany Laboratory - University of Insubria, Varese) and the High room. In detail:

- Growth chamber: all five plants were placed under HP Sodium Lamp at $105 \mu\text{mol m}^{-2} \text{sec}^{-1}$.
- Outdoor: all five plants were placed under variable PAR value depending on weather (May-June).
- High room: all five plants were placed in three different position points that were the same of the fig. 5.4b excluding the second position point, for which from position one to three: 4.7 , 11.5 , $50.3 \mu\text{mol m}^{-2} \text{sec}^{-1}$. For each position point, plants were grown for 16 days (16/8 hours light/dark) and successively moved to the next position point, with an increasing PAR value.

5.2.3 Morpho-physiological measurements

The physiological measurements of photosynthetic efficiency (F_v/F_m) and photosystem II yield (Φ_{PSII}) were performed by fluorometer (OS1-FL, Opti-sciences, inc. USA) calculating:

- a) minimal and maximal chlorophyll fluorescence (F_0 and F_m) in dark adapted;
- b) steady state and steady maximal state chlorophyll fluorescence (F_s and F_{ms}) in light reaction;

- c) non-photochemical quenching ($NPQ = (F_m - F_{ms})/F_{ms}$), photochemical quenching ($qP = (F_{ms} - F_s)/F_{ms}$);

Stomatal conductance (H_2O-CO_2 ; G_s) was also measured by the Porometer (PMR 3, PPSsystem, MA, USA).

For each growing condition and from the beginning of each exposure, photosynthetic efficiency in dark-adapted (F_v/F_m), photosystem II yield in light reaction (Φ_{PSII}) and stomatal conductance (G_s) were measured after 24 hours, 4 days, 8 days and 16 days. Moreover, an image of the plants was acquired at the beginning and at the end of the experiment. Afterwards, these images were analyzed by Image J open access software and the leaf area index obtained.

All data were analyzed with a two-tailed T-test with a significance level of 95% ($p < 0.05$).

5.3 Results

5.3.1 Short-Term Experiments

In both rooms, a similar trend of photosynthetic performance and stomatal conductance was observed between the three different plant species (Fig. 5.5, 5.6). Good values of F_v/F_m and Φ_{PSII} , close to the optimal range, were detected in all plants overall the two experiments. In particular, while *Anthurium* in Low room (Fig. 5.5) showed the same NPQ trend between the different position points that are corresponding to the sampling time, in High room (Fig. 5.6) and in the fourth position point, characterized by the highest PAR value, an increased NPQ value was detected. Moreover, *Basilicum* showed higher values of all parameters, except for NPQ that was lower than the other two plant species.

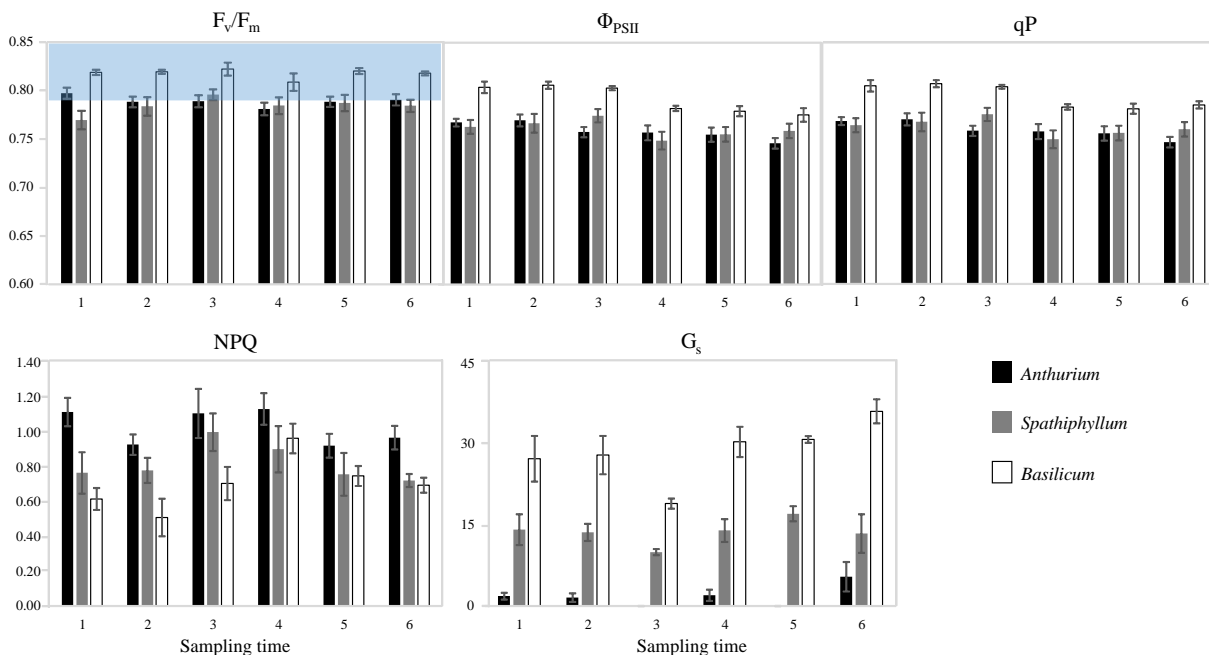


Figure 5.5. Values of F_v/F_m , Φ_{PSII} , qP , NPQ and G_s obtained in Low room. For all graphs, values are in relation to sampling time corresponding to the increasing position points and are the mean value of $n=9$ (\pm SE). *Anthurium*, *Spathiphyllum* and *Basilicum* are indicated with black, grey and white, respectively. The blue horizontal bar in F_v/F_m graph indicates the range of reference values.

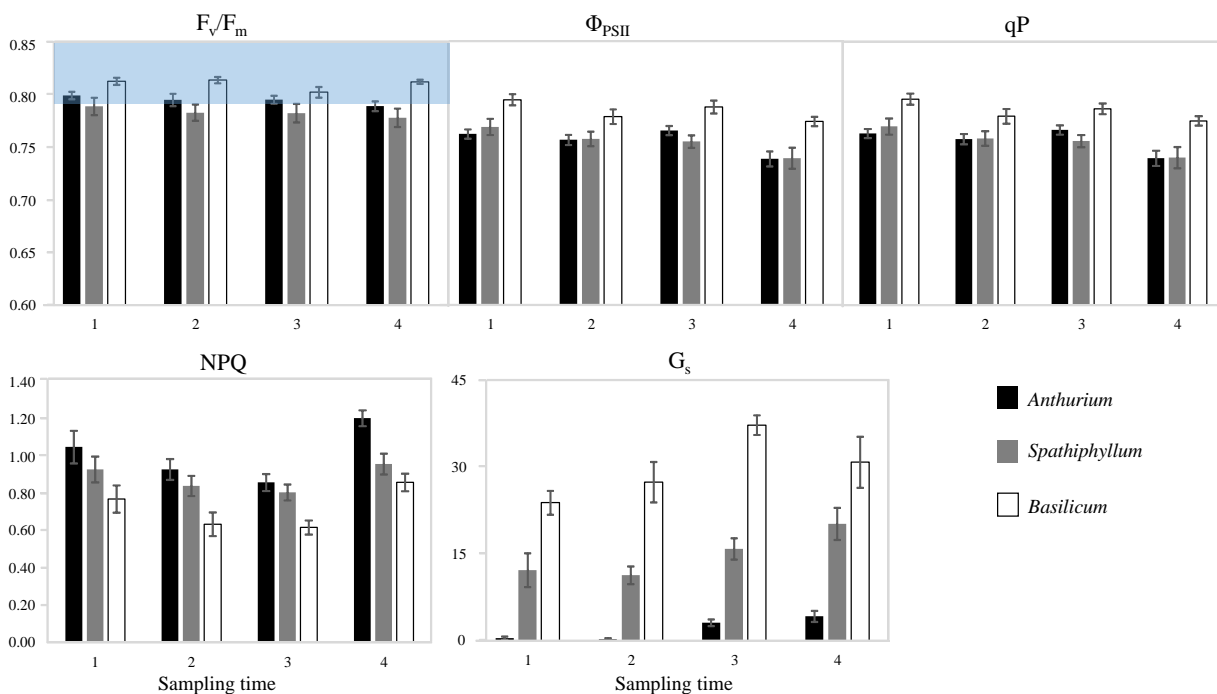


Figure 5.6. Values of F_v/F_m , Φ_{PSII} , qP , NPQ and G_s obtained in Low room. For all graphs, values are in relation to sampling time corresponding to the increasing position points and are the mean value of $n=9$ (\pm SE). *Anthurium*,

Spathiphyllum and *Basilicum* are indicated with black, grey and white, respectively. The blue horizontal bar in F_v/F_m graph indicates the range of reference values.

5.3.2 Long-Term Experiments

Low room

Plants of *Malva sylvestris* did not get to the end of experiment thus not information are showed in graphs. For each position point, similar photosynthetic activity and stomatal conductance were detected between *Anthurium* and *Spathiphyllum* (Fig. 5.7). Both plant species showed a linear Φ_{PSII} trend between the different position points, whereas an increasing F_v/F_m trend was detected as PAR increased when moving to the corresponding position point. Generally, all measured parameters were higher in *Spathiphyllum* than in *Anthurium* in particular for the stomatal conductance (G_s).

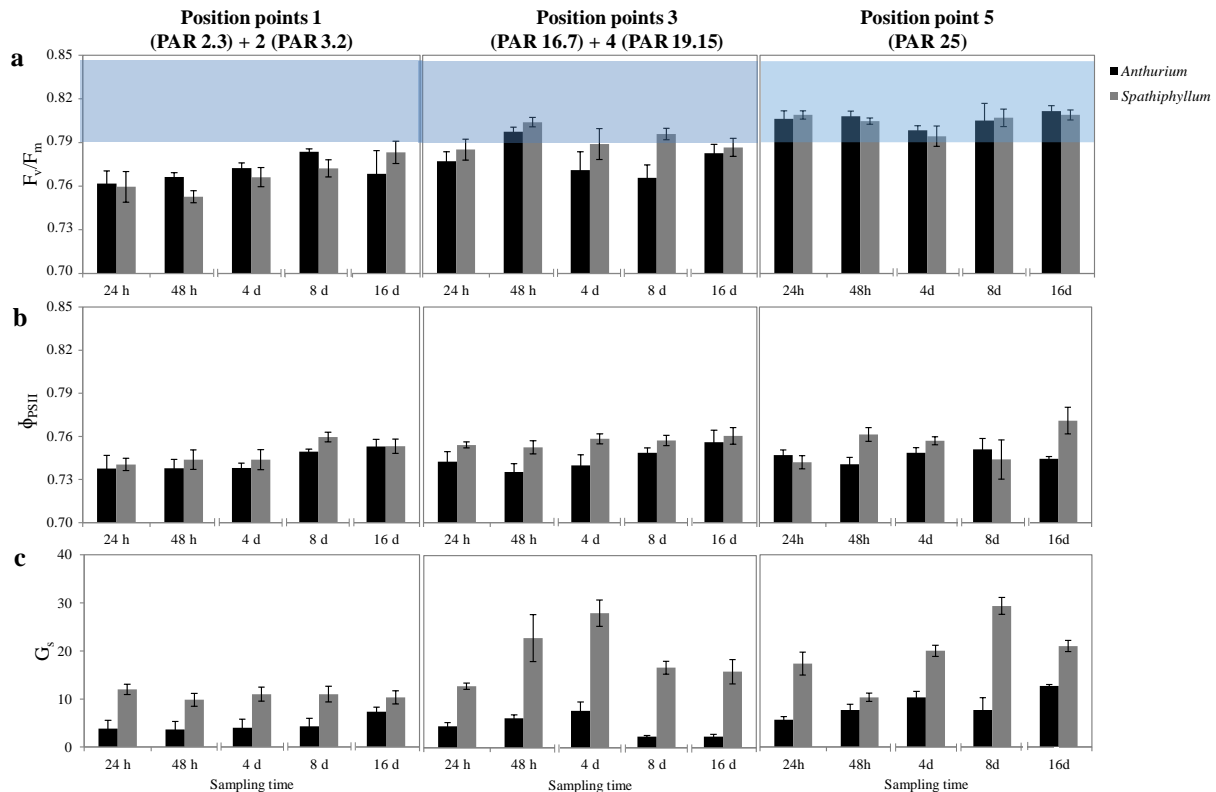


Figure 5.7. For all graphs, values are in relation to sampling time and are the mean value of $n=9$ (\pm SE). First and second position points and third and fourth position points are pooled together and represented in the first and second graph, respectively. *Anthurium* and *Spathiphyllum* are indicated with black and grey, respectively. **a:** Results of F_v/F_m .

The blue horizontal bar graph indicates the range of reference values. **b**: Results of Φ_{PSII} . **c**: Results of stomatal conductance (G_s).

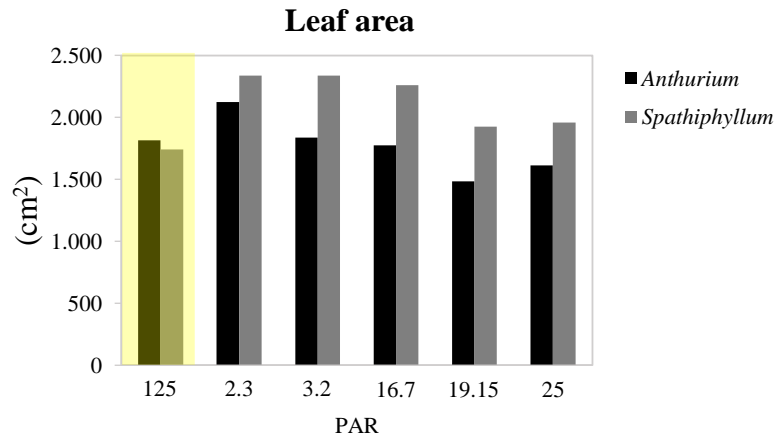


Figure 5.8. Results of leaf area measured at the end of 16 days of each position point. The results highlighted in yellow are relative to the leaf area measured at the beginning of the experiment when plants were in growth chamber at 125 PAR. *Anthurium* and *Spathiphyllum* are indicated with black and grey, respectively.

An increase of leaf index during the first 16 days in the first position point characterized by the lowest PAR value was clearly evident in comparison to the value measured in growth chamber before starting the experiment (Fig. 5.8). However, once plants adapted to that PAR and light conditions, they preferred to extend stalks and to move leaves orienting downwards to the wall light reflection, thus decreasing the leaf area index when measured in the following position points corresponding to the sampling time. Therefore, *Anthurium* (Fig. 5.9a) preferred to grow in expansion, whereas *Spathiphyllum* (Fig. 5.9b) showed a promotion in vertical growth and flowering process.



Figure 5.9. Pictures of (a) *Anthurium* and (b) *Spathiphyllum* taken at the end of the experiment (80th day). The plants of both species outside the red rectangle were grown at the Lab's growth chamber (125 PAR-HP Sodium Lamp), whereas the plant of both species in red rectangle was grown under CoeLux® lighting.

High Room

In each growth condition, a different plant growth was observed in response to many types of variables characterizing overall experiment. For instance, in the first position point in both High room and outdoors, plants showed symptoms of physiological disorders due to the lowest PAR value ($4.7 \mu\text{mol m}^{-2} \text{sec}^{-1}$) and the low temperatures respectively (May with an average temperature of 8°C). Nevertheless, all plants have reached the end of experiment in good morpho-physiological status.

In growth chamber all plants showed a good photosynthetic performance and stomatal conductance in each position point (Fig. 5.10). Basil followed by tomato and coriander seedlings showed a higher G_s in comparison to oak and olive seedlings.

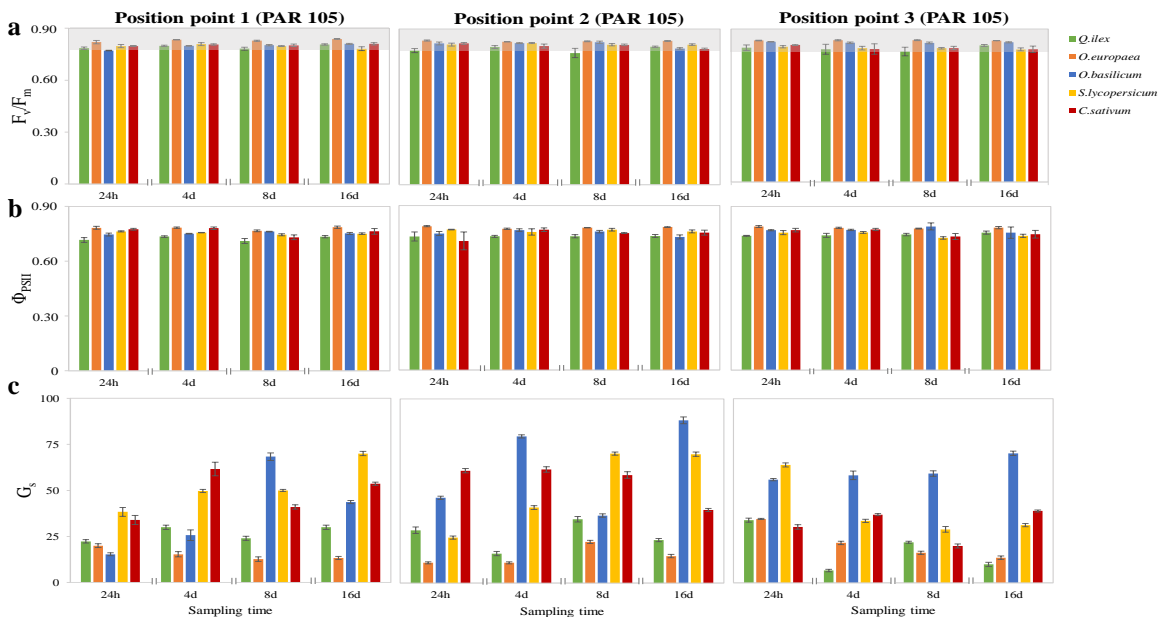


Figure 5.10. Results detected in growth chamber. For all graphs, values are in relation to sampling time and are the mean value of $n=9 (\pm\text{SE})$. *Q. ilex*, *O. europaea*, *O. basilicum*, *S. lycopersicum* and *C. sativum* are indicated with green,

orange, blue, yellow and red, respectively. **a:** Results of F_v/F_m where the grey horizontal bar indicates the range of reference values. **b:** Results of Φ_{PSII} . **c:** Results of stomatal conductance (G_s).

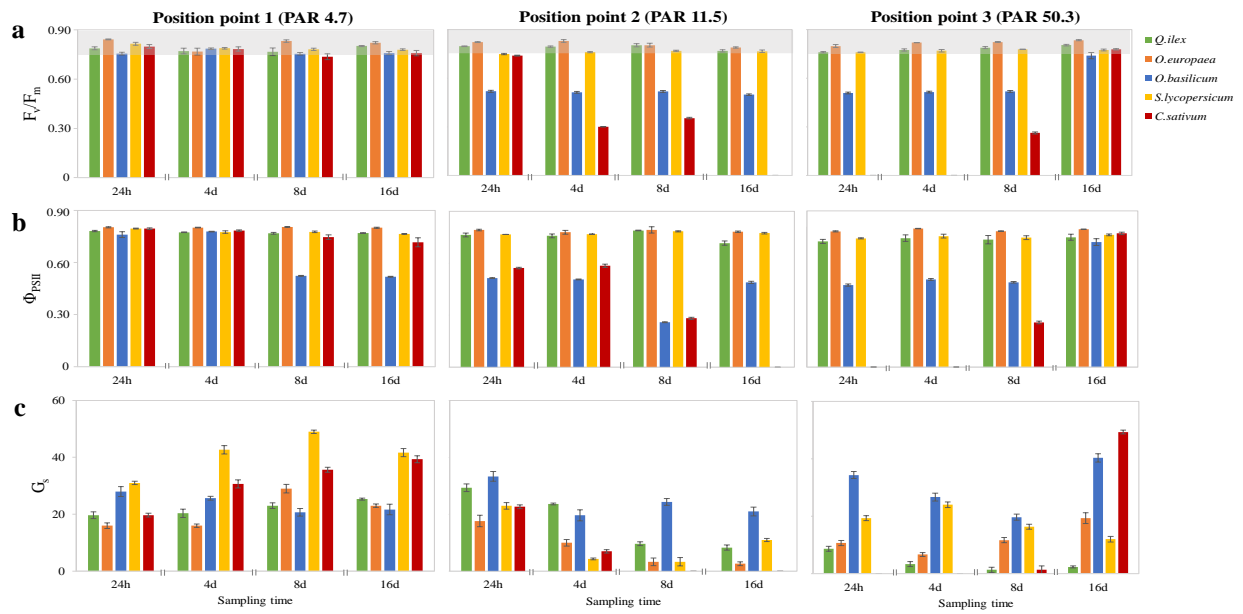


Figure 5.11. Results detected in High room. For all graphs, values are in relation to sampling time and are the mean value of $n=9$ (\pm SE). *Q. ilex*, *O. europaea*, *O. basilicum*, *S. lycopersicum* and *C. sativum* are indicated with green, orange, blue, yellow and red, respectively. **a:** Results of F_v/F_m where the grey horizontal bar indicates the range of reference values. **b:** Results of Φ_{PSII} . **c:** Results of stomatal conductance (G_s).

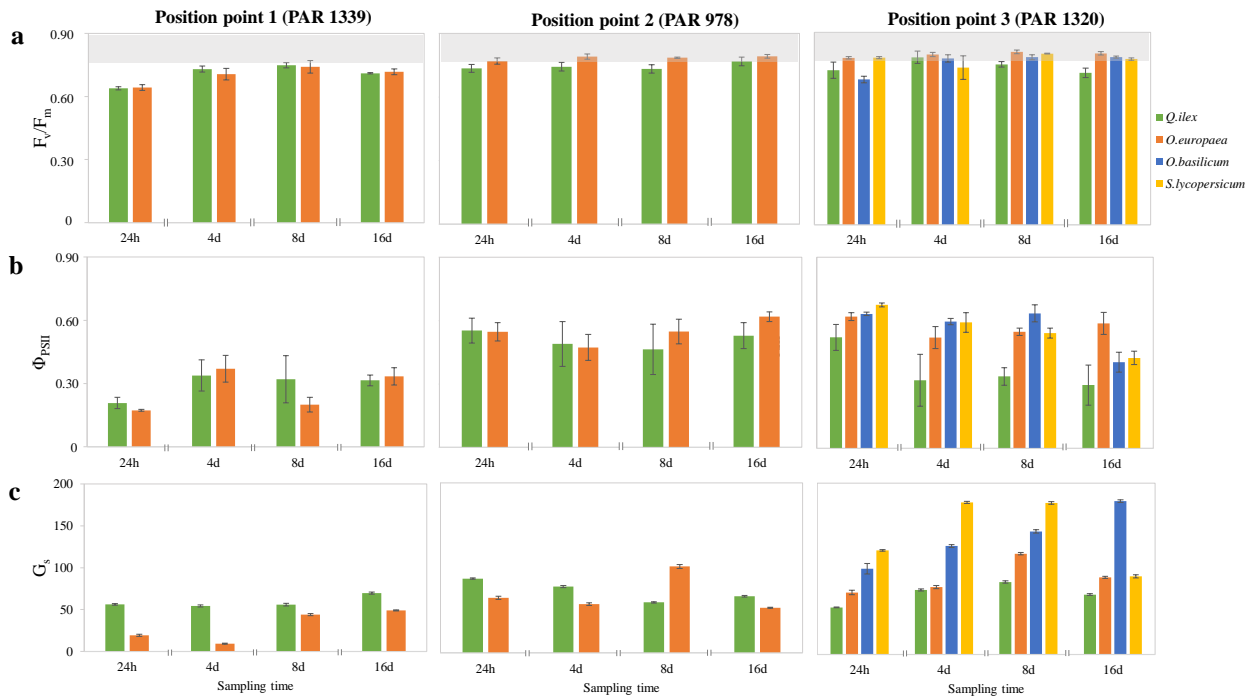


Figure 5.12. Results detected outdoor. For all graphs, values are in relation to sampling time and are the mean value of $n=9$ (\pm SE). *Q. ilex*, *O. europaea*, *O. basilicum*, *S. lycopersicum* and *C. sativum* are indicated with green, orange, blue, yellow and red, respectively. **a:** Results of F_v/F_m where the grey horizontal bar indicates the range of reference values. **b:** Results of Φ_{PSII} . **c:** Results of stomatal conductance (G_s).

Similarly, in High room the F_v/F_m and Φ_{PSII} values were in the optimal range, except for basil and coriander (Fig. 5.11). Indeed for all measured parameters, basil showed only a decrease in the second and third position points, whereas coriander seedlings were not measurable, starting from the last sampling date of the second position point until the third sampling date of the last position point when they recovered their status. Likewise, in outdoor, coriander seedlings have never been measurable because they always showed small leaves and not detected by fluorometer (Fig. 5.12). As well as, tomato and basil seedlings have been measurable only in the third position point when leaves were well expanded, contrarily to oak and olive seedlings that have been measurable from the beginning of the experiment. Besides that, although in outdoor a great variability was recorded, plants showed a good photosynthetic activity and stomatal conductance overall the experiment (Fig. 5.12). Concerning the leaf index, oak and olive seedlings showed the highest leaf area in each position point and in each place (Fig. 5.13). In detail, the leaf area of all plants grown in growth chamber in the three position points was unchanged and it followed a normal growth trend. Similarly, the linear trend in the three position points in High room was detected, however basil and coriander seedlings showed a low growth rate. In outdoor, while oak and olive seedlings followed a linear growth trend, tomato, basil and coriander increased their leaf area starting from the second position point and reaching a very high index in the third position point. Which in turn was characterized by the highest PAR value and high temperatures were recorded for the beginning of summer. However all plants got the end of the experiment and each of them showed a different growth trend in relation to the experimental place (Fig. 5.14).

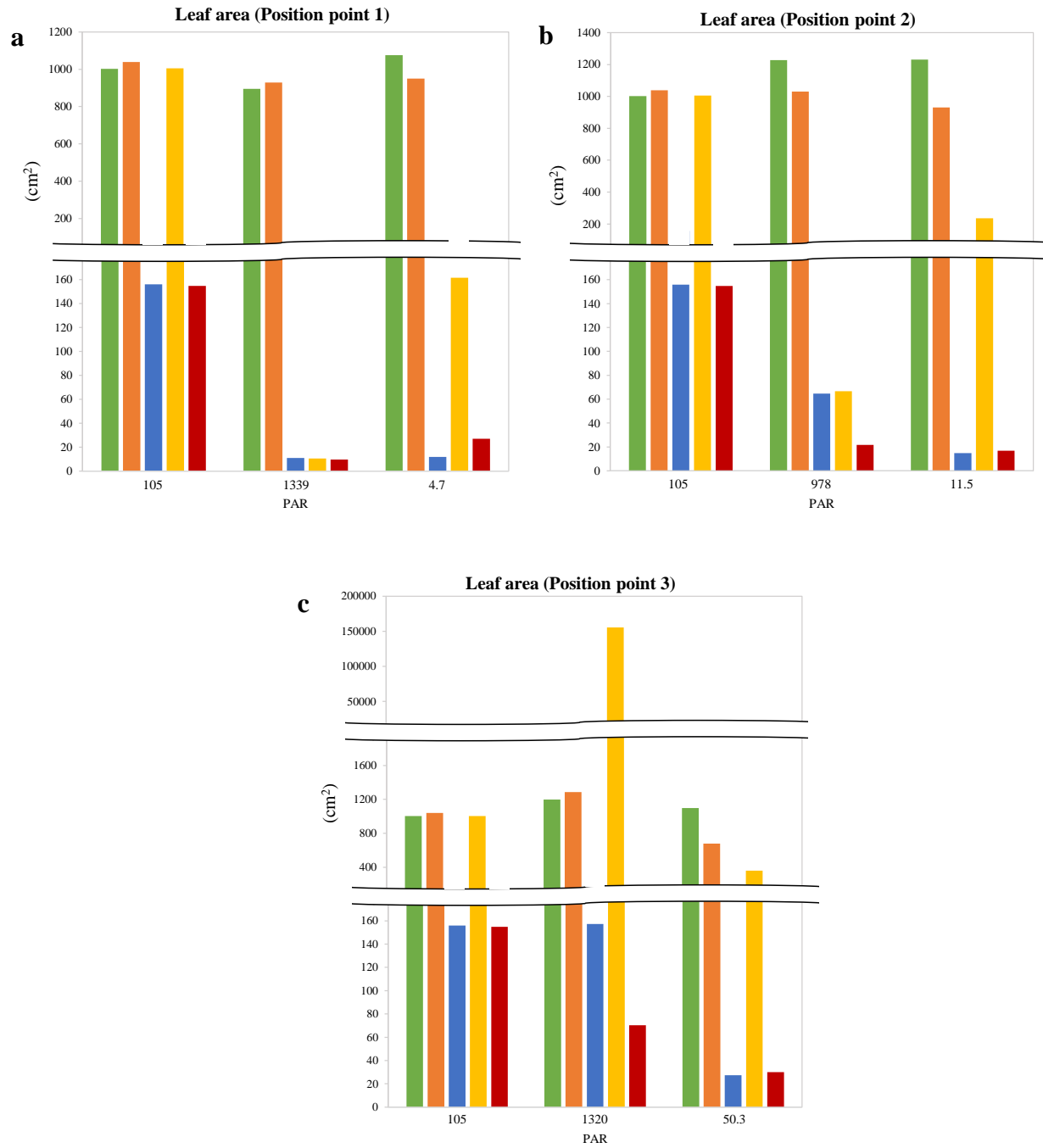


Figure 5.13. Results of leaf area measured at the end of the 16 days of the three position point (a, b, c). Values are in relation to PAR values measured in growth chamber, outdoor and High room. *Q. ilex*, *O. europaea*, *O. basilicum*, *S. lycopersicum* and *C. sativum* are indicated with green, orange, blue, yellow and red, respectively.

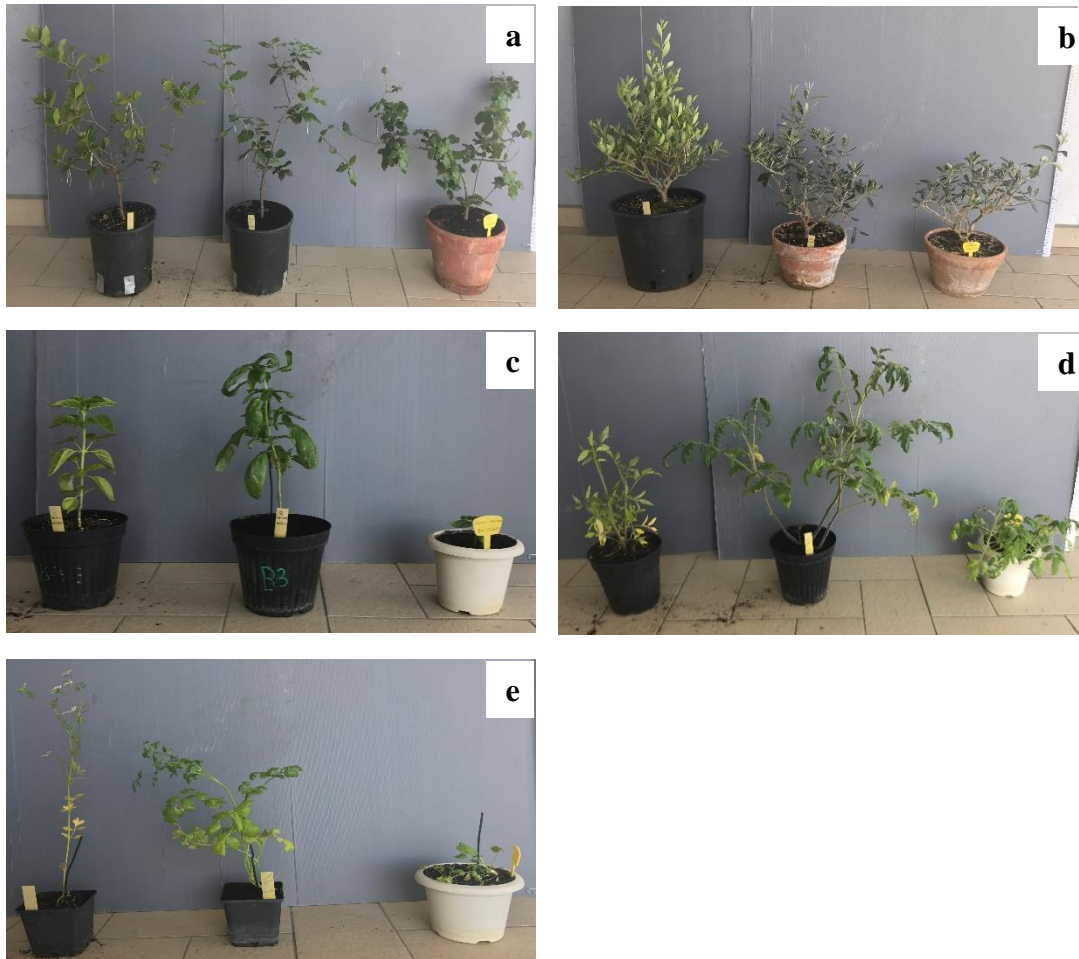


Figure 5.13. Pictures taken at the end of the experiment (after 48th days). The comparisons are among the same plant species: (a) *Q. ilex*, (b) *O. europaea*, (c) *O. basilicum*, (d) *S. lycopersicum* and (e) *C. sativum* grown in growth chamber, outdoor and High room from left to right.

5.4 Discussion and Conclusions

In all performed experiments, the positive plant response to CoeLux® light is demonstrated mainly by the high values of F_v/F_m , close to the reference optimal values as reported in Ritchie *et al.* (2013). However, it is widely reported that plants receiving diffuse light, comprising shadow, show an enhanced photosynthesis compared to plants receiving direct light (Healey *et al.*, 1998; Roderick *et al.*, 2001; Li *et al.*, 2014a). Nevertheless, plants in position points that were in full and direct light characterized by the highest PAR value, showed the highest F_v/F_m values indicating a well-functioning photosynthesis apparatus. Furthermore, in the first short-term experiment low

values of F_v/F_m and high values of NPQ were found in *Anthurium* in comparison to other plant species, suggesting that absorbed energy was not emitted as fluorescence but dissipated as non-photochemical energy. Thus, in according to several reports, this type of response could be a strategy of photoprotection to avoid the damage of photosynthetic proteins and membranes due to excess of absorbed light (Niyogi, 1999; Slattery *et al.*, 2018). Probably, for *Anthurium*, CoeLux[®] irradiance is excessive for both photochemical and fluorescence emission processes such that energy is dissipated as heat. Moreover, the PAR differences characterizing each position point under CoeLux[®] device, seem to promote the leaf expansion only at the beginning of experiment, indeed, a first increase of leaf area index followed by a decrease in the next position points was detected. Supposing that, initially plants under CoeLux[®] light promote leaf expansion to receive more light until an adaptation status for which plants prefer to perform a phototropism orienting leaves toward the diffuse light instead of CoeLux[®] direct light. This response could be attributable to the CoeLux[®] spectral qualities, for instance the less irradiance characterizing the regions between green, yellow, orange and red. Finally, a highly species-specific response is observed. Indeed, each plant species tested had different reaction. Generally, plants characterized by large and thick leaves, such as *Anthurium*, *Spathiphyllum*, *Q. ilex* or *O. europaea* responded in a better way in comparison to plants with thinner and less large leaves like *O. basilicum*, *S. lycopersicum* and *C. sativum*. However the same aromatic and agronomic species performed a better stomatal activity compared to the ornamental and forestry species for their leaf morphology. Besides that, it is well known that plant architectural characteristics, such as the number and geometry of organs, including their shape and position within the plant and the canopy, the leaves elevation angles or the phyllotaxis highly affect the efficiency in light absorption and use (Godin, 2000; Falster and Westoby, 2003; Brites and Valladares, 2005; Sinoquet *et al.*, 2005). Moreover, it is possible to assert that all plant species, especially the agronomic and aromatic ones, a strong growth in controlled growing conditions and in natural environments. Therefore, plants differentially respond to CoeLux[®] light at several PAR values and in different light irradiation, firstly for the CoeLux[®] spectral qualities and then for the intrinsic plant characteristics.

Hence, these first experiments are only the start point to study the plant responses to CoeLux[®] lighting. Our first findings certainly need many further types of investigations to better assess the plant growth under CoeLux[®] device, thus to be able to indicate the lighting device a good source for growing different plant species.

5.5 References

- Baker N. R., Oxborough K., Lawson T., Morison J. I. (2001). High resolution imaging of photosynthetic activities of tissues, cells and chloroplasts in leaves. *Journal of Experimental Botany* 52, 615-21.
- Baker N. R., Rosenqvist E. (2004). Applications of chlorophyll fluorescence can improve crop production strategies: an examination of future possibilities. *Journal of Experimental Botany* 55, 1607-21.
- Bresson J., Vasseur F., Dauzat M., Koch G., Granier C., Vile D. (2015). Quantifying spatial heterogeneity of chlorophyll fluorescence during plant growth and in response to water stress. *Plant Methods* 11, 23.
- Brites D., Valladares F. (2005). Implications of opposite phyllotaxis for light interception efficiency of Mediterranean woody plants. *Trees* 19, 671-679.
- Calatayud A., Roca D., Martínez P. (2006). Spatial-temporal variations in rose leaves under water stress conditions studied by chlorophyll fluorescence imaging. *Plant Physiology and Biochemistry* 44, 564-73.
- Canazei M., Laner M., Staggi S., Pohl W., Ragazzi P., Magatti D., Martinelli E., Di Trapani P. (2015). Room- and illumination-related effects of an artificial skylight. *Lighting Research and Technology*, 0, 1-20.
- Chaerle L., Leinonen I., Jones H. G., Van Der Straeten D. (2007). Monitoring and screening plant populations with combined thermal and chlorophyll fluorescence imaging. *Journal of Experimental Botany* 58, 773-84.
- Daley P. F., Raschke K., Ball J. T., Berry J. A. (1989). Topography of photosynthetic activity of leaves obtained from video images of chlorophyll fluorescence. *Plant Physiology* 90, 1233-8
- Di Trapani P., Magatti D. (2014). Artificial Lighting System for Simulating Natural Lighting. *Patent Application Publication*, US 2014/0133125 A1.

- Di Trapani P., Magatti D. (2017). Artificial Illumination Device. *United States Patent*, US 9,709,245 B2.
- Ehlert B., Hinch D.K. (2008). Chlorophyll fluorescence imaging accurately quantifies freezing damage and cold acclimation responses in *Arabidopsis* leaves. *Plant Methods* 4, 12.
- Falster D. S., Westoby M. (2003). Leaf size and angle vary widely across species: what consequences for light absorption? *New Phytologist* 158, 509-525.
- Genty B., Briantais J.-M., Baker N. R. (1989). The relationship between the quantum yield of photosynthetic electron transport and quenching of chlorophyll fluorescence. *Biochimica et Biophysica Acta (BBA)-General Subjects* 990, 87-92.
- Genty B., Meyer S. (1995). Quantitative mapping of leaf photosynthesis using chlorophyll fluorescence imaging. *Functional Plant Biology* 22, 277-84.
- Godin C. (2000). Representing and encoding plant architecture: a review. *Annals of Forest Science* 57, 413-438.
- Gray G. R., Hope B. J., Qin X. Q., Taylor B. G., Whitehead C. L. (2003). The characterization of photoinhibition and recovery during cold acclimation in *Arabidopsis thaliana* using chlorophyll fluorescence imaging. *Physiologia Plantarum* 119, 365-75.
- Healey K. D., Rickert K. G., Hammer G. L., Bange M. P. (1998). Radiation use efficiency increases when the diffuse component of incident radiation is enhanced under shade. *Australian Journal of Agricultural Research* 49, 665-672.
- Heidari M., Golpayegani A. (2012). Effects of water stress and inoculation with plant growth promoting rhizobacteria (PGPR) on antioxidant status and photosynthetic pigments in basil (*Ocimum basilicum* L.). *Journal of the Saudi Society of Agricultural Sciences* 11, 57-61.
- Hogewoning S. W., Harbinson J. (2007). Insights on the development, kinetics, and variation of photoinhibition using chlorophyll fluorescence imaging of a chilled, variegated leaf. *Journal of Experimental Botany* 58, 453-63.

- Hogewoning S.W., Douwstra P., Trouwborst G., van Ieperen W., Harbinson J. (2010). An artificial solar spectrum substantially alters plant development compared with usual climate room irradiance spectra. *Journal of Experimental Botany*, 61(5), 1267-76.
- Janka E., Körner O., Rosenqvist E., Ottosen C.-O. (2013). High temperature stress monitoring and detection using chlorophyll a fluorescence and infrared thermography in chrysanthemum (*Dendranthema grandiflora*). *Plant Physiology and Biochemistry* 67, 87-94.
- Leipner J., Oxborough K., Baker N. R. (2001). Primary sites of ozone-induced perturbations of photosynthesis in leaves: identification and characterization in *Phaseolus vulgaris* using high resolution chlorophyll fluorescence imaging. *Journal of Experimental Botany* 52, 1689-96.
- Li T., Heuvelink E., Dueck T. A., Janse J., Gort G., Marcelis L. F. M. (2014a). Enhancement of crop photosynthesis by diffuse light: quantifying the contributing factors. *Annals of Botany* 114, 145-156.
- Maxwell K., Johnson G. N. (2000) Chlorophyll fluorescence - a practical guide. *Journal of Experimental Botany* 51, 659-68.
- Mishra Y., Jänkänpää H. J., Kiss A. Z., Funk C., Schröder W. P., Jansson S. (2012). *Arabidopsis* plants grown in the field and climate chambers significantly differ in leaf morphology and photosystem components. *BMC Plant Biology* 12, 6.
- Misra A. N., Misra M., Singh R. (2012). Chlorophyll Fluorescence in Plant Biology. *Biophysics*, Dr. Prof. Dr. A.N. Misra (Ed.), ISBN: 978-953-51-0376-9.
- Murchie E. H., Lawson T. (2013). Chlorophyll fluorescence analysis: a guide to good practice and understanding some new applications. *Journal of Experimental Botany* 64(13), 3983-98.
- Niyogi K. K. (1999). Photoprotection revisited: genetic and molecular approaches. *Annual Review of Plant Physiology and Plant Molecular Biology* 50, 333-359.
- Oxborough K., Baker N. (1997). An instrument capable of imaging chlorophyll a fluorescence from intact leaves at very low irradiance and at cellular and subcellular levels of organization. *Plant Cell and Environment* 20, 1473-83.

- Quilliam R. S., Swarbrick P. J., Scholes J. D., Rolfe S. A. (2006). Imaging photosynthesis in wounded leaves of *Arabidopsis thaliana*. *Journal of Experimental Botany* 57, 55-69.
- Rayleigh L. (1878). On The Instability of Jets. *Proceedings of the London Mathematical Society*, s1-10(1) 4-13.
- Rincon A., Valladares F., Gimeno T. E., Pueyo J. J. (2008). Water stress responses of two Mediterranean tree species influenced by native soil microorganisms and inoculation with a plant growth promoting rhizobacterium. *Tree Physiology* 28, 1693-701.
- Ritchie G. A. (2006). Chlorophyll fluorescence: what is it and what do the numbers mean? USDA Forest Service Proceedings RMRS-P-43.
- Roderick M. L., Farquhar G. D., Berry S. L., Noble I. R. (2001). On the direct effect of clouds and atmospheric particles on the productivity and structure of vegetation. *Oecologia* 129, 21-30.
- Rousseau C., Belin E., Bove E., Rousseau D., Fabre F., Berruyer R., *et al.* (2013). High throughput quantitative phenotyping of plant resistance using chlorophyll fluorescence image analysis. *Plant Methods* 9, 17.
- Sinoquet H., Sonohat G., Phattaralerphong J., Godin C. (2005). Foliage randomness and light absorption in 3-D digitized trees: an analysis from multiscale discretization of the canopy. *Plant, Cell and Environment* 28, 1158-1170.
- Slattery R. A., Walker B. J., Weber A. P. M., Ort D. R. (2018). The impacts of fluctuating light on crop performance. *Plant physiology* 176(2), 990-1003.
- Sperdouli I., Moustakas M. (2012). Spatio-temporal heterogeneity in *Arabidopsis thaliana* leaves under drought stress. *Plant Biology* 14, 118-28.
- Wang J., Lu W., Tong Y., Yang Q. (2016). Leaf morphology, photosynthetic performance, chlorophyll fluorescence, stomatal development of lettuce (*Lactuca sativa* L.) exposed to different ratios of red light to blue light. *Frontiers in Plant Science* 7, 250.
- Woo N. S., Badger M. R., Pogson B. J. (2008). A rapid, non-invasive procedure for quantitative assessment of drought survival using chlorophyll fluorescence. *Plant Methods* 4, 27.

<http://www.healingplaces.nl/single-post/Coelux-Mimics-Daylight-Light-x-Mental-Health>

Chapter VI
Synthesis and Outlook

In the present study, both singular and interplay effects on plant growth of modification of light and nutrient supply have been investigated. The following questions were addressed: 1) How does plants respond to changes in soil quality by using biochar amendment? 2) How does plants respond to the combination of biochar and different light spectra? 3) Does a potential role of plant photoreceptors exist in response to both low levels of nitrogen and light? 4) Does plants survive under artificial lighting system CoeLux[®]?

It is widely reported that biochar, a soil amendment, could promote crop production and reduce the environmental impact of cultivation practices. Nevertheless, given the high heterogeneity of the biochar itself (e.g. parental material and temperature of production), both positive and negative effects on plant performances have been reported. These incoherent findings might be also due to the high variability of soil types where biochar is applied. In the present work, morphology and proteome profiles of tomato plants grown in biochar-amended soil were analyzed. Surprisingly although the effect on plant growth and soil P and N content was considered negligible, both proteomic and molecular analysis showed a misbalance of the photosynthetic machinery and an impairing of the mechanisms recognizing pathogen-derived molecules. Plant traits such as morphology, fluorescence emission and stomatal conductance of *Pisum* and *Arabidopsis* seedlings grown in biochar-amended soil and under different light spectra have been also analyzed. In this case, biochar addition promoting the soil contents of N available and C total improved the soil quality and causing both a decrease and an increase in the growth of *Arabidopsis* and *Pisum* seedlings, respectively. These findings highlight the high species-specificity effect of biochar. However, among the different light spectra tested, the LED light type characterized by the lowest value of R:FR (AP67) had the best influence on the performance of both plant species. In particular, the AP67 light spectra compensated the negative effect of biochar leading to hypothesis a strong interplay of the two factors.

Since biochar is known to enhance N availability in the soil, the biochar effect on N availability in combination to modified light conditions has been reproduced “*in vitro*”. Afterward, the role of plant photoreceptors such as phyB, phyA, and pifs has been studied in seedlings of *Arabidopsis* mutants (*phyB*, *phyAB*, *pifs*). Through these preliminary observations, it is possible to hypothesize that in response to N deprivation and light reduction, phyA has a negative role in plant growth and pigment accumulation. Furthermore, phyB could be involved in the process of N transport and metabolism in order to promote leaf expansion.

Finally, we investigated the effect of a new artificial lighting system (CoeLux[®]) on plant morphology, photosynthetic performance and stomatal activity of different plant species (*Anthurium*, *Spathiphyllum*, *Basilicum*, *Malva*, *Coriandrum*, *S. lycopersicum*, *Q. ilex*, *O. europaea*). Showing that the effect of the CoeLux[®] lighting systems might change according to the plant species analyzed. However, in general, all plant species were able to perform a good photosynthetic and stomatal activity ensuring their survival.

Although the results of this thesis provide important new insights on plant response to nutrient and light, they also opened new questions that require future investigations. As for example the evidence of negative influence of biochar amendment on plant photosynthetic and pathogen defense machinery, raise the question on the defense to other biotic/abiotic stress conditions. Furthermore, by studying the protein pattern and hormonal profiles of *Pisum* and *Arabidopsis*, it could attribute the positive morpho-physiological response to the influence of light or biochar. The first morpho-physiological results of *Arabidopsis* mutants require additional investigations to confirm the assertion on some plant photoreceptor functions. Indeed, it would necessary to study the expression of genes involved in N transport and metabolism in the same mutants and light conditions. Similarly, it could be interesting to test other photoreceptors by using other *Arabidopsis* mutants. Finally, it was demonstrated that CoeLux[®] system is suitable for plant indoor growth. Nevertheless, to better understand the use and efficiency extent of CoeLux[®] light for plant growth, these preliminary results could be confirmed by the study of plant photosynthetic apparatus at molecular level such as the investigation of the photoreceptor expression and functioning.

ORAL/POSTER PRESENTATIONS FROM THIS WORK

Poster presentation “PROTEOMIC AND MOLECULAR ANALYSIS OF BIOCHAR EFFECTS IN TOMATO LEAVES” at the Days of Scientific Research, Department of Biosciences and Territory, University of Molise, Pesche (IS), March 2016.

Oral presentation “NUOVE TECNOLOGIE SOSTENIBILI PER LA CRESCITA DELLE PIANTE: COELUX[®] E BIOCHAR” at the PhD Conference “Sostenibilità e Cambiamento”, University of Molise, Campobasso, December 2016

Poster presentation “EFFECTS OF ARTIFICIAL COELUX[®] ON PLANT GROWTH” at the Days of Scientific Research, Department of Biosciences and Territory, University of Molise, Pesche (IS), March 2017.

Poster presentation “EFFECTS OF ARTIFICIAL LIGHTING SYSTEM (COELUX[®]) ON ORNAMENTAL PLANT GROWTH” at the Global Conference on Plant Science and Molecular Biology, Valencia, Spain, September 2017.

Poster Presentation “THE MORPHOLOGICAL AND PHYSIOLOGICAL RESPONSES OF *ARABIDOPSIS THALIANA* L. MUTANTS TO THE FILTERED LIGHT AND N STARVATION CONDITIONS” at the 113^o Congresso della Società Botanica Italiana – V International Plant Science Conference, University of Fisciano, Fisciano (SA), September 2018.

Oral Presentation “EFFECTS OF LED SPECTRA IN COMBINATION WITH BIOCHAR AMENDMENT ON *PISUM SATIVUM* L. AND *ARABIDOPSIS THALIANA* L. GROWTH” at the 7th Slovenian Symposium on Plant Biology with international participation, Ljubljana, Slovenia, September 2018.

LIST OF ABBREVIATIONS

N	Nitrogen
Pr	Red light
Pfr	Far-red light
R:FR	Red:Far red ratio
LED	Light-emitting diode
C	Non-amended soil
B	Biochar-amended soil
Chl _a	Chlorophyll a
Chl _b	Chlorophyll b
Car	Carotenoid
EC	Electrical conductivity
CEC	Cation exchange capacity
LN	Leaflets number
CLN	Compound leaves
SB	Stem branching
SH	Stem height
LFW	Leaf fresh weight
RFW	Root fresh weight
LDW	Leaf dry weight
RDW	Root dry weight
PAR	Photosynthetically active radiation
SL	Stem length
LBL	Lateral branches length
LBN	Number of lateral branches
TLA	Total leaf area
LRN	Number of leaves per each rosette
FN	Number of flowers
FRL	Total fine root length
FRV	Total fine root volume

FRD	Fine root diameter
LDM	Leaves dry mass
FDM	Fruit dry mass
FRDM	Fine root dry mass
SFRL	Specific fine root length
FRTD	Fine root tissue density
PSII	Photosystem II
F_v/F_m	The maximum quantum efficiency of PSII photochemistry for chlorophyll fluorescence in dark-adapted
Φ_{PSII}	The maximum efficiency of PSII photochemistry in the light
NPQ	Non-photochemical quenching
G_s (or g_s)	Stomatal conductance
das	Days after sowing
Col-0	<i>Arabidopsis columbia</i> wild-type
Phys	Phytochromes
Pifs	Phytochrome-interacting factors
phyB	Phytochrome B
<i>phyB</i>	Phytochrome B mutant
<i>phyAB</i>	Phytochrome AB double mutant
<i>pifs</i>	Phytochrome-interacting factor quadruple mutant
NL	Normal light
LL	Low light

LIST OF TABLES

CHAPTER 1

Table 1.1. Essential macro- and micro- nutrients for plant growth and their functions within plant tissue (Baligar et al., 2007).	4
--	---

CHAPTER 2

Table 2.1. Substrates chemical properties. Data represent the mean (n=4) \pm standard error. Mean values marked with the same letter are not statistically different. One-way ANOVA was applied to weigh the effects biochar treatments ($p \leq 0.05$).	22
---	----

Table 2.2. Differentially-represented proteins in leaves from tomato plants grown in non-amended soils (C) and tomato plants grown in biochar-amended soils (B). The list includes: spot number on the reference gel (see Fig. 2.3), hit and accession number, protein description, Mascot Score, theoretical and experimental protein Mr and pI values, peptides and sequences matched, sequence coverage (%), functional and detail classification, and protein representation levels.	28
---	----

CHAPTER 3

Table 3.1. Spectral distribution and red:far-red of the fluorescent (control) light and the three LED light treatments.	47
--	----

Table 3.2. Biochar chemical-physical characteristics. Each value represents the mean (n = 8) \pm SE.	50
---	----

Table 3.3. Chemical-physical analysis performed on soil samples of control and biochar-treated pots. Each value represents the mean of (n=6) \pm SE. Different letters within sampling time for each species indicate significant differences among light treatments at $p < 0.05$.	51
---	----

Table 3.4. Morphological measurements (means \pm SE) on control (n=6) and biochar treated (n=6) seedlings of <i>Arabidopsis columbia</i> grown under one fluorescent (control) and three LED spectra. Bold values indicate statistically significant differences between control and biochar-treated plants in the same lighting treatment ($p < 0.05$). a, b, c indicate statistically significant differences among lighting type within control plants ($p < 0.05$). x, y, z indicate statistically significant differences among lighting type within biochar-treated plants ($p < 0.05$). SL stem length, LBL lateral branches length, LBN lateral branches number, LRN leaf rosette number,	
--	--

TLA total leaf area, FN flower number, FRL total fine roots length, FRV total fine root volume, FRDM fine root dry mass, SFRL specific fine roots length, FRTD fine roots tissue density. 53

Table 3.5. Morphological measurements (means \pm SE) on control (n=6) and biochar treated (n=6) seedlings of *Pisum sativum* grown under one fluorescent (control) and three LED spectra. Bold values indicate statistically significant differences between control and biochar-treated plants in the same lighting treatment ($p < 0.05$). a, b, c indicate statistically significant differences among lighting type within control plants ($p < 0.05$). x, y, z indicate statistically significant differences among lighting type within biochar-treated plants ($p < 0.05$). SL stem length, LBL lateral branches length, LBN lateral branches number, TLA total leaf area, FRL total fine roots length, FRD fine root diameter, LDM leaf dry mass, FDM fruit dry mass, FRDM fine root dry mass, SFRL specific fine roots length, FRTD fine roots tissue density. 55

LIST OF FIGURES

CHAPTER 1

Figure 1.1. (a) Spectrum of visible light detected with Handheld Spectrometer (UPRtek). (b) Absorption spectra of the two key pigments and β -carotene, the representative of the carotenoid group (OpenStax College, Biology). (c) Absorption regions of main photoreceptors (Modified from Parihar *et al.*, 2016). 5

CHAPTER 2

Figure 2.1. Morphological analysis. The main plant parameters were analyzed, i.e. LN=leaflets number; CLN=compound leaves; SB=stem branching; SH=stem height. Data represent the mean ($n = 6$) \pm standard error. Mean values marked with asterisks are statistically different at $*p \leq 0.05$. C= tomato plants grown in non-amended soils (control); B= tomato plants grown in biochar-amended soils. 23

Figure 2.2. Leaf and root biomass (g of dry tissue weight). Data represent the mean ($n = 6$) \pm standard error. Mean values marked with the same letter are not statistically different ($p \leq 0.05$). C= tomato plants grown in non-amended soils (control); B= tomato plants grown in biochar-amended soils. 24

Figure 2.3. Reproducible 2-DE maps of tomato leaves (control) showing 15 differentially represented proteins. Arrows indicate the position of each protein spot; spot identification information is reported in Table 2.2. 25

Figure 2.4. LeACO1 gene expression level. The LeACO1 expression level in leaves of tomato plant grown on non-amended (C) and biochar-amended (B) soil. Three independent biological replicates were run for each tissue, each with two technical replications. Data were normalized to α -tubulin as a loading control. Bars represent the standard error of mean values. Asterisk indicates significant differences at ($p \leq 0.05$). 29

Figure 2.5. Detection of *P. infestans*. Photos in the upper panel shows representative picture of *P. infestans* infected leaves of tomato plant grown on biochar-amended soil. The lower panel shows the detection of *P. infestans* PiO8-3-3 DNA region in leaves of tomato plant grown on non-amended (C) and biochar-amended (B) soil. Three independent biological replicates were run for each tissue, each with two technical replications. Data were normalized to α -tubulin as a loading control. Bars represent the standard error of mean values. 30

CHAPTER 3

Figure 3.1. The experimental design for physiological and morphological measurements in control (C; solid line □) and biochar treated (B; dashed line ▣) seedlings. Each number corresponds to the sampling date. 46

Figure 3.2. Trends of F_v/F_m , Φ_{PSII} and NPQ (rows) measured in five different days after sowing (das; columns) for seedlings grown in non-(*) and biochar-amended (■) soil and with the fluorescent (control) light and the three LED light spectra. Vertical boxes represent approximately 50% of the observations and lines extending from each box are the upper and lower 25% of the distribution. Outliers are represented as solid dots (•) and extremes are represented as stars. The solid, horizontal line in the center of each box is the median value, whereas the dotted horizontal line is the mean (n=4). The asterisk indicates statistically significant differences between control and biochar-treated plants in the same lighting treatment ($p < 0.05$). a, b, c indicate statistically significant differences among lighting type within control plants ($p < 0.05$). x, y, z indicate statistically significant differences among lighting type within biochar-treated plants ($p < 0.05$). 58

Figure 3.3. g_s pattern (row) detected in five different days after sowing (das; columns) for seedlings grown in non-(*) and biochar-amended (■) soil and with the fluorescent (control) light and the three LED light spectra. Vertical boxes represent approximately 50% of the observations and lines extending from each box are the upper and lower 25% of the distribution. Outliers are represented as solid dots (•) and extremes are represented as stars (*). The solid, horizontal line in the center of each box is the median value, whereas the dotted horizontal line is the mean (n=4). The asterisk indicates statistically significant differences between control and biochar-treated plants in the same lighting treatment ($p < 0.05$). a, b, c indicate statistically significant differences among lighting type within control plants ($p < 0.05$). x, y, z indicate statistically significant differences among lighting type within biochar-treated plants ($p < 0.05$). 59

CHAPTER 4

Figure 4.1. Experimental hydroponic growing system. The experimental design (left) and the real experimental system (right). Modified Eppendorf tubes (a) and a support in which to insert the tubes (b) compose the complete growth system (c). 78

Figure 4.2. Schematic representation of the experimental plan. Sterilized seeds are plated and kept in the dark for 3 days at 4 °C (seed stratification phase). Germination is induced by 3 hours of light treatment and the plates are returned into the darkness at 20–22 °C for 21 hours. The plates are placed into light conditions (full and filtered light) for 12 days. Finally, the solution

is changed applying the N starvation treatment unchanging the light conditions for 7 days before the seedlings are sampled. 79

Figure 4.3. Results of morphological measurements (means \pm SE) of Col-0, *phyB*, *phyAB* and *pifs* (n=12) genotype grown in full nutrition (■) and in N starvation solutions (□). Each measured parameter are reported in two graphs in relation to the light condition: Normal Light (NL, white background) and Low Light (LL, line background). a, b, c, d indicate significant differences between different genotypes in Full nutrition solution and in NL and LL separately ($p < 0.05$). α , β , γ , δ indicate significant differences between different genotypes in N starvation solution and in NL and LL separately ($p < 0.05$). Asterisk (*) indicates significant differences between Full nutrition and N starvation solutions in the same genotype and light conditions ($p < 0.05$). Letters in bold indicate significant differences between NL and LL in the same genotype ($p < 0.05$). 83

Figure 4.4. Overview of the phenotypes of wild-type (Col-0) and mutant (*phyB*, *phyAB*, *pifs*) seedlings. The group of pictures on left and right highlight the comparisons of leaf morphology and emergence respectively. 22-days-old whole seedlings (left) and leaves (right) grown in normal light (NL) and in low light (LL) in each of them in Full nutrition (Full nutr.) and in N starvation (N starv.) conditions. Scale bars are 1 cm. 84

Figure 4.5. Results of photosynthetic pigment level measurements (means \pm SE) of Col-0, *phyB*, *phyAB* and *pifs* (n=3) genotype grown in full nutrition (■) and in N starvation solutions (□). Each measured parameter are reported in two graphs in relation to the light condition: Normal Light (NL, white background) and Low Light (LL, line background). a, b, c, d indicate significant differences between different genotypes in Full nutrition solution and in NL and LL separately ($p < 0.05$). α , β , γ , δ indicate significant differences between different genotypes in N starvation solution and in NL and LL separately ($p < 0.05$). Asterisk (*) indicates significant differences between Full nutrition and N starvation solutions in the same genotype and light conditions ($p < 0.05$). Letters in bold indicate significant differences between NL and LL in the same genotype ($p < 0.05$). 86

CHAPTER 5

Figure 5.1. Pictures of CoeLux[®] system. A view (a) of the sun and (b) of shadows and sky. 96

Figure 5.2. Solar and CoeLux[®] spectra. (From Paolo Ragazzi, CoeLux[®]).

Figure 5.3. A scheme of the CoeLux[®] 45 HC lighting system. From the upper side: the structural slab for the system housing, the drop ceiling and the light beam. 100

Figure 5.4. View from above (a-c) and side (b-d) of the plant position (green circle) respectively in the Low and the High room. The PAR values in Low room (a, b) are from position point one to six: 2.30, 2.60, 3.20, 16.70, 19.15, 25 $\mu\text{mol m}^{-2} \text{sec}^{-1}$, in High room (c, d) are from position point one to four: 4.70, 4.85, 11.50, 50.30 $\mu\text{mol m}^{-2} \text{sec}^{-1}$. 101

Figure 5.5. Values of F_v/F_m , Φ_{PSII} , qP, NPQ and G_s obtained in Low room. For all graphs, values are in relation to sampling time corresponding to the increasing position points and are the mean value of $n=9$ ($\pm\text{SE}$). *Anthurium*, *Spathiphyllum* and *Basilicum* are indicated with black, grey and white, respectively. The blue horizontal bar in F_v/F_m graph indicates the range of reference values. 104

Figure 5.6. Values of F_v/F_m , Φ_{PSII} , qP, NPQ and G_s obtained in Low room. For all graphs, values are in relation to sampling time corresponding to the increasing position points and are the mean value of $n=9$ ($\pm\text{SE}$). *Anthurium*, *Spathiphyllum* and *Basilicum* are indicated with black, grey and white, respectively. The blue horizontal bar in F_v/F_m graph indicates the range of reference values. 104

Figure 5.7. For all graphs, values are in relation to sampling time and are the mean value of $n=9$ ($\pm\text{SE}$). First and second position points and third and fourth position points are pooled together and represented in the first and second graph, respectively. *Anthurium* and *Spathiphyllum* are indicated with black and grey, respectively. a: Results of F_v/F_m . The blue horizontal bar graph indicates the range of reference values. b: Results of Φ_{PSII} . c: Results of stomatal conductance (G_s). 105

Figure 5.8. Results of leaf area measured at the end of 16 days of each position point. The results highlighted in yellow are relative to the leaf area measured at the beginning of the experiment when plants were in growth chamber at 125 PAR. *Anthurium* and *Spathiphyllum* are indicated with black and grey, respectively. 106

Figure 5.9. Pictures of (a) *Anthurium* and (b) *Spathiphyllum* taken at the end of the experiment (80th day). The plants of both species outside the red rectangle were grown at the Lab's growth chamber (125 PAR-HP Sodium Lamp), whereas the plant of both species in red rectangle was grown under CoeLux[®] lighting. 107

Figure 5.10. Results detected in growth chamber. For all graphs, values are in relation to sampling time and are the mean value of $n=9$ ($\pm\text{SE}$). *Q. ilex*, *O. europaea*, *O. basilicum*, *S. lycopersicum* and *C. sativum* are indicated with green, orange, blue, yellow and red, respectively. a: Results of F_v/F_m where the grey horizontal bar indicates the range of reference values. b: Results of Φ_{PSII} . c: Results of stomatal conductance (G_s). 107

108

Figure 5.11. Results detected in High room. For all graphs, values are in relation to sampling time and are the mean value of $n=9$ (\pm SE). *Q. ilex*, *O. europaea*, *O. basilicum*, *S. lycopersicum* and *C. sativum* are indicated with green, orange, blue, yellow and red, respectively. a: Results of F_v/F_m where the grey horizontal bar indicates the range of reference values. b: Results of Φ_{PSII} . c: Results of stomatal conductance (G_s). 108

Figure 5.12. Results detected outdoor. For all graphs, values are in relation to sampling time and are the mean value of $n=9$ (\pm SE). *Q. ilex*, *O. europaea*, *O. basilicum*, *S. lycopersicum* and *C. sativum* are indicated with green, orange, blue, yellow and red, respectively. a: Results of F_v/F_m where the grey horizontal bar indicates the range of reference values. b: Results of Φ_{PSII} . c: Results of stomatal conductance (G_s). 109

Figure 5.13. Results of leaf area measured at the end of the 16 days of the three position point (a, b, c). Values are in relation to PAR values measured in growth chamber, outdoor and High room. *Q. ilex*, *O. europaea*, *O. basilicum*, *S. lycopersicum* and *C. sativum* are indicated with green, orange, blue, yellow and red, respectively. 110

Figure 5.14. Pictures taken at the end of the experiment (after 48th days). The comparisons are among the same plant species: (a) *Q. ilex*, (b) *O. europaea*, (c) *O. basilicum*, (d) *S. lycopersicum* and (e) *C. sativum* grown in growth chamber, outdoor and High room from left to right. 111